

FORWARD DISPLACEMENT ANALYSES
OF IN-PARALLEL PLATFORMS

By

WEI LIN

A DISSERTATION PRESENTED TO THE GRADUATE SCHOOL
OF THE UNIVERSITY OF FLORIDA IN PARTIAL FULFILLMENT
OF THE REQUIREMENTS FOR THE DEGREE OF
DOCTOR OF PHILOSOPHY

UNIVERSITY OF FLORIDA

1992

ACKNOWLEDGEMENTS

The author wishes to express his sincere appreciation and gratitude to his supervisory committee chairman, Dr. Joseph Duffy, for his initial suggestion of this research topic and for all of his subsequent guidance, advice, and enthusiasm. He would also like to thank his committee members, Dr. Ralph G. Selfridge, Dr. Gary K. Matthew, Dr. Carl D. Crane, and Dr. Neil L. White, for their discussions and comments.

The author is grateful to many of his colleagues in CIMAR (Center for Intelligent Machines and Robotics) for their friendship and sharing of knowledge. Special thanks are due to Dr. Michael W. Griffis for his support, and Dr. Hongyou Lee for his valuable suggestions.

The financial support from the State of Florida Center of Excellence is acknowledged.

Finally, the author would like to thank his parents, his friend Ms. Wan Yu Lam, and his entire family for their encouragement and patience throughout his study.

TABLE OF CONTENTS

ACKNOWLEDGEMENTS	ii
ABSTRACT	v
1 INTRODUCTION	1
1.1 Background	1
1.2 Literature Survey	4
1.3 Scope of Study	6
2 SOME RELATIONS BETWEEN DIHEDRAL ANGLES IN SOME POLYHEDRA	8
2.1 Introduction	8
2.2 Relation between Two Dihedral Angles in a Skew-Quadrangular Pyramid	10
2.3 Relations among Three Dihedral Angles in a Skew-Hexahedron ..	13
2.4 Some Relations between Some Angles	16
3 THE ANALYSES OF THE 4-4 PLATFORMS	19
3.1 Introduction	19
3.2 Formulation of the Forward Analyses	21
3.2.1 Case 4-4-A, a T-T-Q-T-T-Q Platform	21
3.2.2 Case 4-4-B, a T-T-T-Q-T-Q Platform	24
3.2.3 Case 4-4-C, a T-T-T-T-Q-Q Platform	28
3.3 The Eliminants of the Equation Sets	32
3.3.1 Cases 4-4-A and 4-4-C	33
3.3.2 Case 4-4-B	34
3.4 Numerical Verifications	35
3.4.1 Case 4-4-B	35
3.4.2 Case 4-4-C	38
4 THE ANALYSES OF THE 4-5 PLATFORMS	40
4.1 Introduction	40
4.2 Formulation of the Analyses	42
4.2.1 Case 4-5-A, a T-Q-T-Q-T-Q Platform	43
4.2.2 Case 4-5-B, a T-T-Q-T-Q-Q Platform	44

4.2.3 Case 4-5-C, a T-T-T-Q-Q-Q Platform	56
4.3 The Eliminants of the Equation Sets	60
4.4 Numerical Verifications	64
4.4.1 Case 4-5-Ba	65
4.4.2 Case 4-5-C	72
5 A SURVEY OF OTHER CLASSES OF IN-PARALLEL PLATFORMS ..	77
5.1 Introduction	77
5.2 The 3-4 and 3-5 Platforms	78
5.3 The 4-6 Platforms	80
5.3.1 Case 4-6-A, a T-Q-T-Q-Q-Q Platform	80
5.3.2 Case 4-6-B, a T-Q-Q-T-Q-Q Platform	82
5.4 The 5-5 Platforms	84
5.5 The 5-6 and 6-6 Platforms	95
6 SUMMARY AND DISCUSSION	97
REFERENCES	102
BIOGRAPHICAL SKETCH	106

Abstract of Dissertation Presented to the Graduate School
of the University of Florida in Partial Fulfillment of the
Requirements for the Degree of Doctor of Philosophy

FORWARD DISPLACEMENT ANALYSES
OF IN-PARALLEL PLATFORMS

By

WEI LIN

MAY 1992

Chairman: Dr. Joseph Duffy
Major Department: Mechanical Engineering

The device which is called the In-parallel Platform in this study is a six-degrees-of-freedom, fully in-parallel mechanism. The In-parallel Platform consists of a top platform which is connected to a base by six spherical joint-ended-legs. The legs are connected either singly or in a pair-wise fashion at the vertices of the top platform and base.

The forward displacement analysis problem is stated as follows: Given the lengths of the six legs, together with the dimensions of the top and base platforms, find all possible locations (positions and orientations) of the top platform measured relative to the base. This study succeeds in solving this problem for many forms of In-parallel Platforms.

The In-parallel Platforms are classified into many cases according to the numbers of vertices in the top and base platforms. The closed-form forward displacement analysis is performed for the Platforms by using geometrical constructions and serial chain models. A polynomial in a tan-half-angle that measures the angle between two planar faces of a polyhedron embedded within the Platform is derived for each distinct case. The degrees of the polynomials for some cases that contain zero, one, and two legs which are singly connected at the vertices of both the top platform and base are found to be respectively sixteenth, twenty-fourth, and thirty-second. All the results are verified numerically by performing a reverse displacement analysis.

CHAPTER 1 INTRODUCTION

1.1 Background

Most of the robot manipulators used today are serial kinematic devices that resemble more or less the human arm. A serial manipulator is essentially a combination of lower kinematic pairs and links alternately connected along an open kinematic chain. Each kinematic pair is a single-degree-of freedom joint which is driven by an actuator. This type of manipulator offers the advantages of large workspace and dexterity. However, serial manipulators are intrinsically lacking in precision positioning and orientating the end-effector. As the actuator errors accumulate from the base outwards, the error at the end-effector is magnified. Also, loads are poorly distributed throughout the serial system and hence each actuator must carry the loads associated with all bodies attached to its corresponding joint. Moreover, due to their open chain structural arrangement, serial manipulators suffer from insufficient rigidity.

On the other hand, parallel manipulators where two or more serially connected chains join a platform or end-effector to ground provide many advantages over serial ones. These manipulators are capable of high precision operations because position errors in actuators are not cumulative and in fact the errors often

average out. In addition, they are structurally more rigid and are able to distribute the loads throughout the system. A comparison in terms of performance characteristics between serial and parallel mechanisms was presented in great detail by Cox (1981) and later by Mohamed (1983).

Parallel mechanisms have been proposed in many robotic applications. In 1965, Stewart wrote his paper describing a parallel mechanism device that his name has been associated with (Stewart, 1965). Hunt in 1983 indicated that the flight simulator was the only modern application of the Stewart Platform (Hunt, 1983). The flight simulator is a high payload device for pilot training. Fichter and McDowell (1980) described the advantages and disadvantages of the Stewart Platform as a manipulator. Recently, parallel mechanisms have been suggested to be used as a micromanipulator (Hara and Sugimoto, 1989), force-torque and position-orientation sensors (Kerr, 1989; Yangsheng and Paul, 1988), and for the purposes of simulating the mating of mechanical parts in space (Premack, etc., 1984). Griffis and Duffy (1990) implemented a parallel mechanism at the wrist of a robot to model spatial stiffness of a compliant coupling for simultaneously regulating force and displacement. Most of these applications require high speed and precision performance. Due to the fact that there is no closed-form forward displacement analysis for many parallel mechanisms, the implementation of control systems is very complicated. As a result, there is limited use of parallel mechanisms in industry.

In this study, the mechanism consists of two platforms which are connected

by six SPS¹ serial chains (or legs). The legs which act in-parallel meet either singly or in a pair-wise fashion at the vertices of the two platforms. One of the platforms, which is called the "top platform" has six degrees-of-freedom relative to the other platform, which is called the "base." This type of parallel mechanism is called the "In-parallel Platform."

The most important step in mechanism analysis is to obtain displacement solutions for the links in the mechanism. The displacement analysis of a mechanism includes the reverse analysis (viz., it requires finding a set of angular displacements or leg lengths with given position and orientation of the end-effector) and the forward analysis (viz., with given angular displacements or leg lengths, the position and orientation of the end-effector are computed). In the case of the forward displacement analysis of the In-parallel Platforms, the precise statement of the problem is

Given the six lengths of legs, together with the dimensions of the top and base platforms, what are all the possible ways to assemble the legs, such that some criteria of leg arrangements remain the same?

Parallel and serial mechanisms have inverse characteristics in displacement analysis. For serial mechanisms, the forward displacement analysis is straightforward; however the forward analysis for parallel mechanisms is very complicated and it

¹Here and throughout, the capital letters R, S, and P denote respectively, revolute, spherical, and prismatic kinematic pairs.

In an SPS serial chain, an extra degree-of-freedom produced by the two spherical pairs (S) in terms of rotation about the axis of its prismatic pair does not affect the gross motion of the top platform.

involves highly nonlinear equations. On the contrary, the reverse displacement analysis for parallel is generally an easier problem than for serial devices.

1.2 Literature Survey

Much of the early research in the literature has put a great deal of emphasis on the reverse displacement analysis (Cox, 1981; Fichter, 1986; Mohamed, 1983; Weng, 1988). Numerical solutions were used for the forward displacement analysis. An earlier NASA paper by Dieudonne et al. (1972) gave an iterative solution of the forward analysis of the Stewart Platform. Behi (1988) formulated a forward displacement analysis for a parallel mechanism which was solved numerically. Reinholz and Gokhale (1987) used the Newton-Raphson Method to obtain an iterative solution for the forward displacement analysis of a Stewart Platform. Recently, Hunt and Primrose (1991) determined the number of assembly configurations of some parallel manipulators by using methods of synthetic geometry. Some of the mechanisms they examined were very similar to those in this study.

A closed-form forward displacement analysis will provide more information about the geometry and kinematic behavior of a parallel mechanism. This information is also extremely useful in practice for the control of parallel mechanisms. The importance of obtaining a forward displacement analysis in closed-form was discussed in detail by Griffis and Duffy (1989).

As far as the author is aware, the paper published by Griffis and Duffy in 1989 was the first correct closed-form forward displacement analysis of in-parallel

mechanism and specifically the Stewart Platform. This mechanism, which is called the "3-3 Platform", contained six legs which met in a pair-wise fashion at three points in the top platform and base (Fig. 1.1). An eighth degree polynomial in the square of the tan-half-angle that measured the elevation of a triangular face in the mechanism relative to the base triangle was derived. It indicated that there were sixteen locations (positions and orientations) for the top platform for a given set of leg lengths. Their solution was easily extended for the case where the legs met at six distinct points in a planar base. This case will be called the "3-6 Platform" in this study. A paper by Nanua and Waldron (1989) presented a closed-form solution for the 3-6 Platform which resulted in a 24th degree polynomial. The solutions contained extraneous roots. Charentus and Renaud (1989) obtained a closed-form solution for a similar case whose platform and base were equilateral triangles. In a later paper, Nanua, Waldron, and Murthy (1990) solved the 3-6 Platform with a planar base. The degree of polynomial from their result was the same as that in Griffis and Duffy (1989), although the formulation was much more complicated.

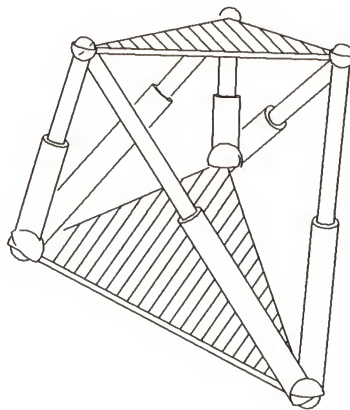


Fig. 1.1 The 3-3 Platform

A case of the 3-6 Platform with a nonplanar base was analyzed by Innocenti and Parenti-Castelli (1989). In their method, the three points in the top platform were disconnected so that each end of the leg described a circle about each side of the base. Then the closure vector equations were introduced, from which a 16th degree polynomial was obtained. Murthy and Waldron (1990) also investigated the same case using a vector approach. Parenti-Castelli and Innocenti (1990) analyzed some other types of parallel mechanisms.

1.3 Scope of Study

The most general form of the In-parallel Platform has its six legs meet at six distinct points in the top platform as well as the base (Fichter,1986). (See Figure 1.2.) Its closed-form displacement analysis is considered to be the most challenging task in analysis of the In-parallel Platform. Many highly nonlinear equations can be involved and they are extremely difficult to solve. There is no idea how many assembly configurations can be obtained. To achieve the goal of solving the general case, it is instructive to solve some simplified cases, in which there are some concentric spherical joints in the top and base platforms. This may provide an insight into solving the general case.

The objective of this research is to obtain the closed-form forward displacement analysis for the In-parallel Platforms which contain one, two, or three pairs of concentric and independent spherical joints in the top or base platforms.

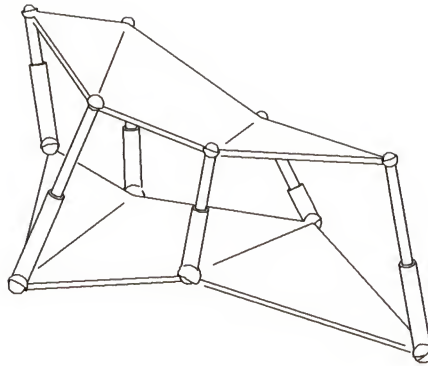


Fig. 1.2 The 6-6 Platform

In order to simplify the analysis, the top or base platforms in some cases are assumed to be planar. According to Hunt and Primrose (1991), the number of assembly configurations obtained from the analysis is unchanged when the planar platforms are generalized to nonplanar ones. Since the mechanisms are analyzed from a theoretical standpoint, some practical problems such as the limitations on the lengths of the legs and angular displacements of the spherical joints, and interference between either the legs themselves or the top or base platforms are ignored.

It should be noted that all the mechanisms depicted in this study are three-dimensional. Moreover, the six legs, which are linear actuators in practice, are represented by line segments in most of the figures for the purpose of clarity. Also, in this study, the platforms which have equal or less numbers of vertices than the other ones are always considered to be the top platforms. This consideration does not affect the results of the analysis. In other words, if the Platforms are turned up side down so that the bases become the top platforms, the formulation of the analyses can still be applied.

CHAPTER 2

SOME RELATIONS BETWEEN DIHEDRAL ANGLES IN SOME POLYHEDRA

2.1 Introduction

In the forward displacement analysis, it is necessary to derive some relations between the angles of a pair of planar faces of a polyhedron embedded within the parallel mechanisms. Each of the mechanisms in this study has six legs met either in single or pair-wise fashion at three, four, five or six points in the top or base platforms. These type of mechanisms can be analyzed in term of solid geometry.

The edges of the top and base platforms together with the six legs form a "wire-frame" of a "skew-polyhedron." The faces of this "skew-polyhedron" consist of "triangles," "skew-quadrilaterals," and "skew-polygons." A "triangle" is formed by two adjacent legs and one edge either from the top or base platform, and a "skew-quadrilateral" by two adjacent legs, an edge from the top, and an edge from the base. It is called a "skew-quadrilateral" because, in general, it does not lie in a plane. A "skew-polygon" represents either the top or base platform of a mechanism. A "3-3 Platform" has a total of eight triangles. In terms of solid geometry, this structure is an octahedron. For In-parallel Platforms which have a singly connected leg in the platforms, some of the faces of the polyhedra become skew-quadrilaterals. This kind

of polyhedra will be called "skew-octahedra."

Most of the skew-octahedra of the mechanisms in this study can be subdivided into some basic "structures." The most common structure is a skew-polyhedron which has a skew-quadrilateral base and four triangles which have a common vertex. (See Fig. 2.1.) This structure is called the "skew-quadrangular pyramid." Section 2.1 presents a relation between two dihedral angles² about a common face in the skew-quadrangular pyramid. Another structure which is quite common in the skew-octahedron is a kind of skew-hexahedron shown in Fig. 2.2. It is formed by four triangles T_1 , T_2 , T_3 , and T_4 which join serially at their edges, and two skew-quadrilaterals which join along a common edge p_1p_2 . A relationship among the three dihedral angles formed by the four triangles is derived in Section 2.3. Section 2.4 presents some other fundamental relations between some angles which will see applications in later chapters.

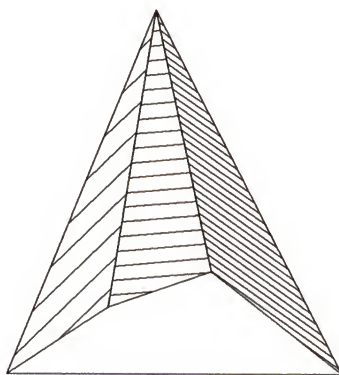


Fig. 2.1 A Skew-Quadrangular Pyramid

²Two nonparallel planes passing across each other have four distinct angles between them. Any one of these angles is called a dihedral angle.

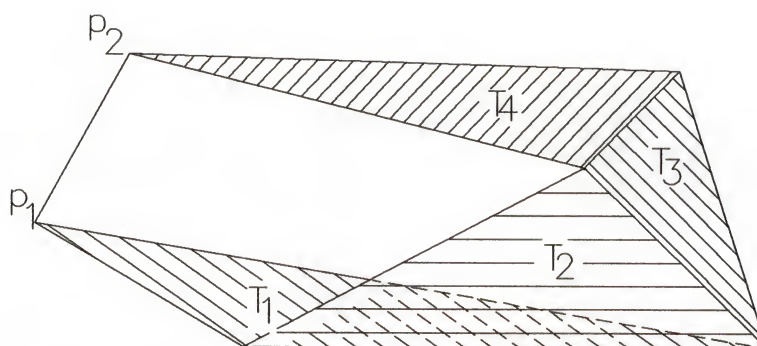


Fig. 2.2 A Skew-Hexahedron

2.2 Relation between Two Dihedral Angles in a Skew-Quadrangular Pyramid

Two dihedral angles, θ_1 and θ_4 , in a quadrangular pyramid are designated in Fig. 2.3. The dihedral angle θ_1 is between triangles Δcob and Δboa , and θ_4 between triangles Δdoa and Δboa . A relation between these two dihedral angles can be most easily derived by using a model of a spherical mechanism.

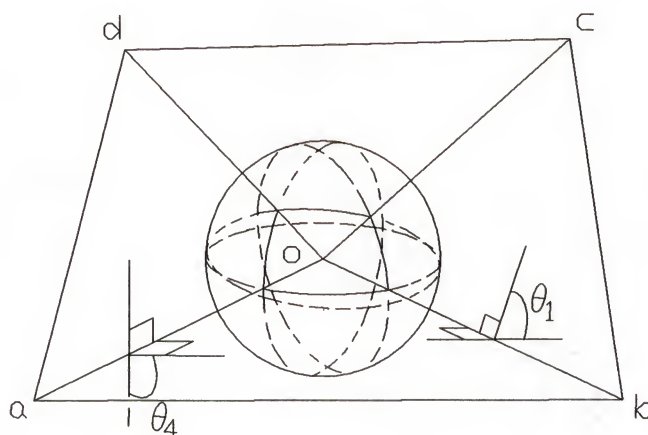


Fig. 2.3 A Skew-Quadrangular Pyramid with
a Unit Sphere Located at Vertex o

At vertex o , a unit sphere is cut in four arcs of great circles by the four triangles. These four arcs of great circles form a spherical quadrilateral. In terms of mechanisms, it can be represented by a skeletal model of a 4R spherical mechanism with mobility one (Duffy, 1980).

A single, generalized spherical four-bar linkage is illustrated in Fig. 2.4. The four links, the output, coupler, input, and grounded links are represented, respectively, by angles α_{12} , α_{23} , α_{34} , and α_{41} . The input angle is denoted by θ_4 , and the output angle by θ_1 . The relationship between these two angles is dependent on the four link angles, and this relationship is

$$(s_{12}c_{41}s_{34})c_4c_1 + (s_{12}s_{41}c_{34})c_1 + (s_{41}s_{34}c_{12})c_4 - (s_{12}s_{34})s_4s_1 + c_{23} - c_{12}c_{41}c_{34} = 0. \quad (2.1)$$

Here and throughout this study, the abbreviations $s_{ij} = \sin\alpha_{ij}$, $c_{ij} = \cos\alpha_{ij}$, $s_i = \sin\theta_i$, and $c_i = \cos\theta_i$, are used.

The derivation of this relationship can be found in Duffy, 1980.

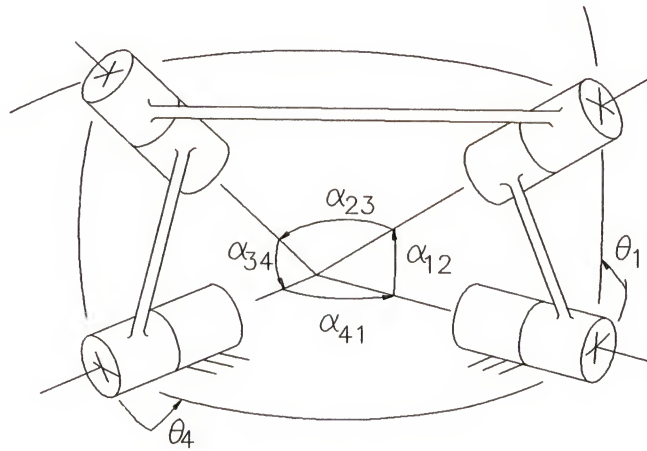


Fig. 2.4 The Generalized Spherical Four-Bar Mechanism

Introducing the tan-half-angle relationships for θ_4 and θ_1 gives

$$c_i = \frac{1 - \tau_i^2}{1 + \tau_i^2} \quad \text{and} \quad s_i = \frac{2\tau_i}{1 + \tau_i^2}, \quad \text{where } \tau_i = \tan\left(\frac{\theta_i}{2}\right)$$

for $i = 1$ and 4 .

Substituting c_i and s_i into (2.1) yields

$$A\tau_1^2\tau_4^2 + B\tau_1^2 + C\tau_4^2 + D\tau_1\tau_4 + E = 0, \quad (2.2)$$

where the five coefficients for the input-output relation are

$$A = s_{12}c_{41}s_{34} - s_{12}s_{41}c_{34} - s_{41}s_{34}c_{12} + c_{23} - c_{12}c_{41}c_{34},$$

$$B = -s_{12}c_{41}s_{34} - s_{12}s_{41}c_{34} + s_{41}s_{34}c_{12} + c_{23} - c_{12}c_{41}c_{34},$$

$$C = -s_{12}c_{41}s_{34} + s_{12}s_{41}c_{34} - s_{41}s_{34}c_{12} + c_{23} - c_{12}c_{41}c_{34},$$

$$D = -4s_{12}s_{34},$$

$$E = s_{12}c_{41}s_{34} + s_{12}s_{41}c_{34} + s_{41}s_{34}c_{12} + c_{23} - c_{12}c_{41}c_{34}.$$

To determine the link angles, α_{12} , α_{23} , α_{34} , and α_{41} , it is necessary to obtain the cosines and sines of these angles. The cosines of the link angles are obtained through the cosine law for an interior angle of a planar triangle. For example, c_{34} is calculated in terms of the lengths of the triangle Δaod using the cosine law. In order to determine the sines of the link angles, proper signs must be chosen. The signs of the sines of the grounded link α_{41} are known, since the locations of the points a , o , and b are known. For the coupler link α_{23} , it can be seen that the relationship (Equation 2.1) is independent of the sine of this angle, therefore it is not necessary to consider the signs of the sines of the coupler link. Finally, the signs of the sines of the pairs of input and output links are not known. According to Gilmartin and Duffy (1972),

this does not give any problem for a single four-bar spherical mechanism. For the sake of consistency, when the signs of the sines of the link angles are unknown, they are simply given as positive.

2.3 Relations among Three Dihedral Angles in a Skew-Hexahedron

Figure 2.5 shows three dihedral angles which are designated in a skew-hexahedron. The dihedral angles θ_2 , θ_3 , θ_4 are, respectively, angles between triangles Δp_2ab and Δcab , Δcab and Δcbd , Δcbd and Δp_1cd . To obtain a relation among these three dihedral angles, the skew-hexahedron is modeled by a kinematic chain as illustrated in Fig. 2.6.

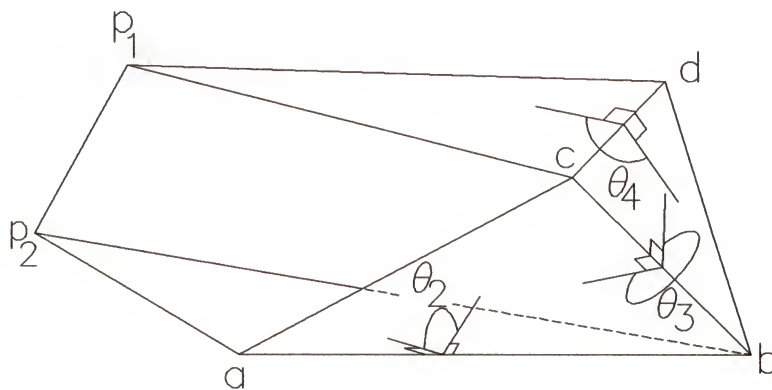


Fig. 2.5 A Skew-Hexahedron

The kinematic chain consists of three serially connected revolute joints whose axes are defined by unit vectors \underline{S}_2 , \underline{S}_3 , and \underline{S}_4 and whose offsets are denoted by S_{22} , S_{33} , and S_{44} . The vectors $S_{11}\underline{S}_1$ and $S_{55}\underline{S}_5$ represent, respectively, the first and last links in the open serial chain. The twist angles, viz. α_{ij} , ($ij = 12, 23, 34$, and 45) are measured by a right-handed rotation of \underline{S}_i into \underline{S}_j about \underline{a}_{ij} . These twist angles are

constants. The relative angular joint displacements θ_j are measured by a right-handed rotation of \underline{a}_{ij} into \underline{a}_{jk} about \underline{S}_j . Now, a vector $\underline{\ell}$ is introduced to close the open serial chain. A vector loop equation for the closed loop chain can be expressed as follows,

$$\underline{S}_{11}\underline{S}_1 + \underline{S}_{22}\underline{S}_2 + \underline{S}_{33}\underline{S}_3 + \underline{S}_{44}\underline{S}_4 + \underline{S}_{55}\underline{S}_5 = \underline{\ell}\underline{\ell}. \quad (2.3)$$

Taking self-scalar products for both sides of (2.3) yields

$$\begin{aligned} k + \underline{S}_{11}\underline{S}_1 \cdot (\underline{S}_{22}\underline{S}_2 + \underline{S}_{33}\underline{S}_3 + \underline{S}_{44}\underline{S}_4 + \underline{S}_{55}\underline{S}_5) \\ + \underline{S}_{22}\underline{S}_2 \cdot (\underline{S}_{33}\underline{S}_3 + \underline{S}_{44}\underline{S}_4 + \underline{S}_{55}\underline{S}_5) \\ + \underline{S}_{33}\underline{S}_3 \cdot (\underline{S}_{44}\underline{S}_4 + \underline{S}_{55}\underline{S}_5) \\ + \underline{S}_{44}\underline{S}_4 \cdot \underline{S}_{55}\underline{S}_5 = 0, \end{aligned} \quad (2.4)$$

where $k = (\underline{S}_{11}^2 + \underline{S}_{22}^2 + \underline{S}_{33}^2 + \underline{S}_{44}^2 + \underline{S}_{55}^2 - \underline{\ell}^2)/2$.

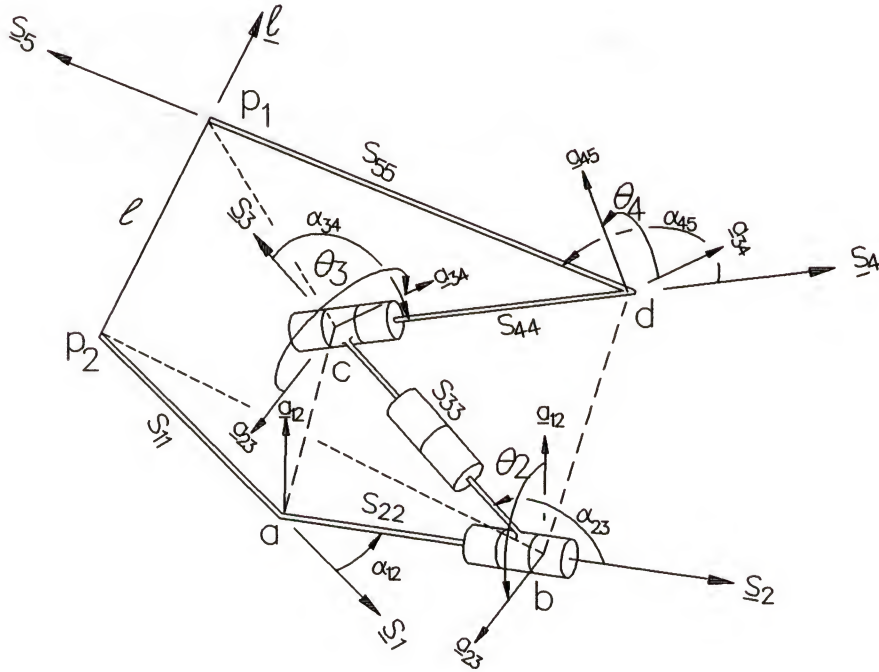


Fig. 2.6 A Model for the Serially Connected Triangles

Expressions for the scalar products in (2.4) can be obtained from direction cosines Table 2.13 in Duffy (1980), and the equation can be expressed in the following form:

$$\begin{aligned} K + S_{11}S_{22}c_{12} + S_{11}S_{33}Z_2 + S_{11}S_{44}Z_{32} + S_{11}S_{55}Z_{432} + S_{22}S_{33}c_{23} \\ + S_{22}S_{44}Z_3 + S_{22}S_{55}Z_{43} + S_{33}S_{44}c_{34} + S_{33}S_{55}Z_4 + S_{44}S_{55}c_{45} = 0, \end{aligned} \quad (2.5)$$

where the expanded forms of the direction cosines Z with one or more subscripts can be found in Duffy (1980). This notation results in expressions that are linear in the sines and cosines of joint angles.

The sines and cosines of the joint angles in (2.5) can be expressed in terms of the tan-half-angles where $x = \tan(\theta_3/2)$, and $y = \tan(\theta_4/2)$. Introducing these tan-half-angles and re-grouping terms, (2.5) is expressed as

$$(a_i x^2 + b_i x + c_i) y^2 + (d_i x^2 + e_i x + f_i) y + g_i x^2 + h_i x + j_i = 0, \quad (2.6)$$

where

$$\begin{aligned} a_i &= a_{i0} c_2 + a_{i2}, & b_i &= b_{i1} s_2, & c_i &= c_{i0} c_2 + c_{i2}, \\ d_i &= d_{i1} s_2, & e_i &= e_{i0} c_2 + e_{i2}, & f_i &= f_{i1} s_2, \\ g_i &= g_{i0} c_2 + g_{i2}, & h_i &= h_{i1} s_2, & j_i &= j_{i0} c_2 + j_{i2}. \end{aligned}$$

Further, the expressions of the coefficients a_{i0} , a_{i2} , b_{i1} , c_{i0} , ..., j_{i2} of c_2 and s_2 are listed in Table 2.1. The subscript i will see its usage in later chapters.

Equation 2.6 contains all the cosines and sines of the twist angles α_{ij} ($ij = 12, 23, 34, \text{ and } 45$). The cosines of the twist angles are obtained by using the cosine law for an angle of a planar triangle in the skew-hexahedron. The twist angles in the serial chain are defined as the exterior angles of the triangle. For example, α_{12} is the supplementary angle with $\angle p_2ab$ in the triangle Δp_2ab . The sines of the twist angles

are obtained from the cosines of the angles. All the signs of the sines are taken as positive. This does not give any problem in determining the relationship of the joint angles in the analysis.

2.4 Some Relations between Some Angles

The Relationship Between Two Opposite Angles in a Skew-Quadrilateral.

The skew-quadrilateral shown in Fig. 2.7 is formed by two triangles Δacb and Δacd .

Applying the cosine law for the two planar triangles gives,

$$ca^2 = ad^2 + dc^2 - 2 ad dc \cos\omega_2,$$

$$ca^2 = ab^2 + bc^2 - 2 ab bc \cos\omega_1.$$

Combining the above two equations, the following relationship between ω_1 and ω_2 can be obtained:

$$\cos\omega_1 = K_1 + K_2\cos\omega_2, \quad (2.7)$$

where

$$K_1 = \frac{ab^2 + bc^2 - ad^2 - dc^2}{2 ab bc} \quad \text{and} \quad K_2 = \frac{ad dc}{ab bc}.$$

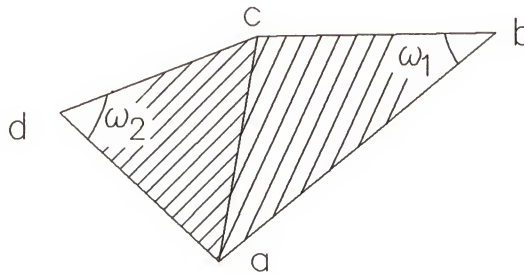


Fig. 2.7 A Skew-Quadrilateral

Cosine Law for the Spherical Triangle. Figure 2.8 shows a unit sphere center at vertex o of a tetrahedron. This sphere is cut in three great circles by three planes. The three arcs of the circles form a spherical triangle. The lengths of the arcs are denoted by central angles ν_1 , δ_0 , and δ_1 . The cosine law gives the relationship between ν_1 and the dihedral angle ϕ . (See Duffy, 1980.) This relationship is

$$\cos \nu_1 = K_3 + K_4 \cos \phi, \quad (2.8)$$

where

$$K_3 = \cos \delta_0 \cos \delta_1,$$

$$K_4 = -\sin \delta_0 \sin \delta_1.$$

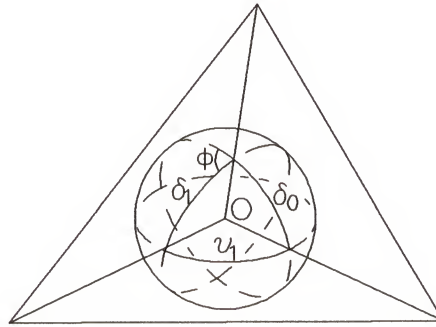


Fig. 2.8 A Spherical Triangle Formed by Three Arcs of Great Circles

Table 2.1 Coefficients of the Serial Chain Model

$a_{i0} = A + B + C + D + E + F$	$a_{i2} = G + H + I + J + K + L + M + N$
$b_{i1} = P + Q$	
$c_{i0} = A - B + C - D - E + F$	$c_{i2} = G - H + I + J - K + L - M + N$
$d_{i1} = R$	$e_{i0} = U$
	$e_{i2} = V$
	$f_{i1} = -R$

$$g_{i0} = A + B + C + D - E - F$$

$$g_{i2} = G + H + I + J + K + L - M - N$$

$$h_{i1} = P - Q$$

$$j_{i0} = A - B + C - D + E - F$$

$$j_{i2} = G - H + I + J - K + L + M - N$$

$$A = -s_{12}s_{23}s_{11}s_{33} - c_{34}s_{12}s_{23}s_{11}s_{44}$$

$$D = c_{23}c_{45}s_{12}s_{34}s_{11}s_{55}$$

$$B = c_{23}s_{12}s_{34}s_{11}s_{44}$$

$$E = -c_{23}c_{34}s_{12}s_{45}s_{11}s_{55}$$

$$C = -c_{34}c_{45}s_{12}s_{23}s_{11}s_{55}$$

$$F = -s_{12}s_{23}s_{34}s_{45}s_{11}s_{55}$$

$$G = k + c_{12}s_{11}s_{22} + c_{12}c_{23}s_{11}s_{33} + c_{23}s_{22}s_{33} + c_{12}c_{23}c_{34}s_{11}s_{44} + c_{23}c_{34}s_{22}s_{44} + c_{34}s_{33}s_{44}$$

$$H = c_{12}s_{23}s_{34}s_{11}s_{44} + s_{23}s_{34}s_{22}s_{44}$$

$$I = c_{12}c_{23}c_{34}c_{45}s_{11}s_{55} + c_{23}c_{34}c_{45}s_{22}s_{55}$$

$$J = c_{34}c_{45}s_{33}s_{55}$$

$$K = c_{12}c_{45}s_{23}s_{34}s_{11}s_{55} + c_{45}s_{23}s_{34}s_{22}s_{55}$$

$$L = c_{45}s_{44}s_{55}$$

$$M = -c_{12}c_{34}s_{45}s_{11}s_{55} - c_{34}s_{23}s_{45}s_{22}s_{55}$$

$$N = c_{12}c_{23}s_{34}s_{45}s_{11}s_{55} + c_{23}s_{34}s_{45}s_{22}s_{55} + s_{34}s_{45}s_{33}s_{55}$$

$$P = 2s_{12}s_{34}s_{11}s_{44} + 2c_{45}s_{12}s_{34}s_{11}s_{55}$$

$$Q = -2c_{34}s_{12}s_{45}s_{11}s_{55}$$

$$R = -2s_{12}s_{45}s_{11}s_{55}$$

$$U = 4c_{23}s_{12}s_{45}s_{11}s_{55}$$

$$V = 4c_{12}s_{23}s_{45}s_{11}s_{55} + 4s_{23}s_{45}s_{22}s_{55}$$

CHAPTER 3 THE ANALYSES OF THE 4-4 PLATFORMS

3.1 Introduction

Most of the parallel mechanisms proposed by researchers (Behi, 1988; Charentus and Renaud, 1989; Fichter, 1986; Griffis and Duffy, 1989; Innocenti and Parenti-Castelli, 1989; Parenti-Castelli and Innocenti, 1990; Murthy and Waldron, 1990) have a general feature that the top platform is always connected by three pairs of concentric spherical joints at three points. Whilst this type of parallel mechanism arrangement is the easiest to analyze, it is far simpler geometrically than a more general arrangement where six legs connected at six distinct points in both the top and base platforms (Fichter, 1986, also see Fig. 1.2).

As mentioned in Griffis and Duffy (1989) on the 3-3 Platform, pairs of concentric spherical joints may cause design problems. It is most important to eliminate, as far as possible, the use of concentric spherical joints. In this respect, this chapter (Lin, Griffis, and Duffy, 1990) presents another class of In-parallel Platforms, in which the number of connection points of the six legs in the top and base platforms is four. The resulting In-parallel Platform arrangement is called the "4-4 Platform."

The top platform of the 4-4 Platform is supported by six SPS serial chains

(legs) that act in-parallel. The ends of the six legs in the base are coplanar, and the ends of the six legs where they join the platform are also coplanar. An example of the mechanism is illustrated in Fig. 3.1. The platforms and bases of the 4-4 Platforms in this study are quadrilaterals whose sides are not parallel. No more than two legs can meet at one point. In term of geometry, the 4-4 Platforms can be classified into three cases according to the arrangements of the "triangles" and "skew-quadrilaterals," which are seen in top views. Fig. 3.2 illustrates the top views of the three main cases. The letter "T" represents a triangle formed by two adjacent legs and one edge either from the top or base platform. The letter "Q" represents a skew-quadrilateral formed by two adjacent legs, an edge from the top, and an edge from the base. Each case has a different sequence of the T's and Q's around the top platform. For Cases 4-4-A, 4-4-B, and 4-4-C, the leg arrangements are, respectively, represented by T-T-Q-T-T-Q, T-T-T-Q-T-Q, and T-T-T-T-Q-Q. Case 4-4-A has two variations of T-T-Q-T-T-Q sequences as shown in Figs. 3.2(a) and 3.2(b).

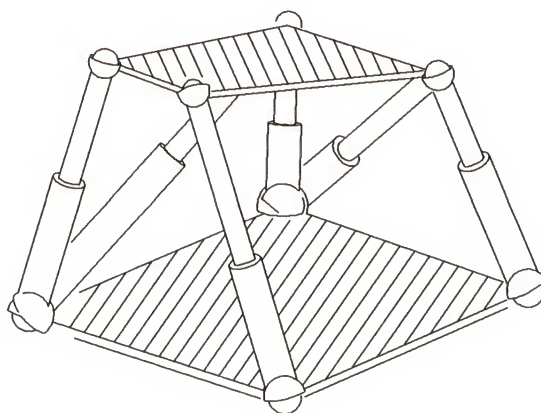


Fig. 3.1 Case 4-4-C Platform

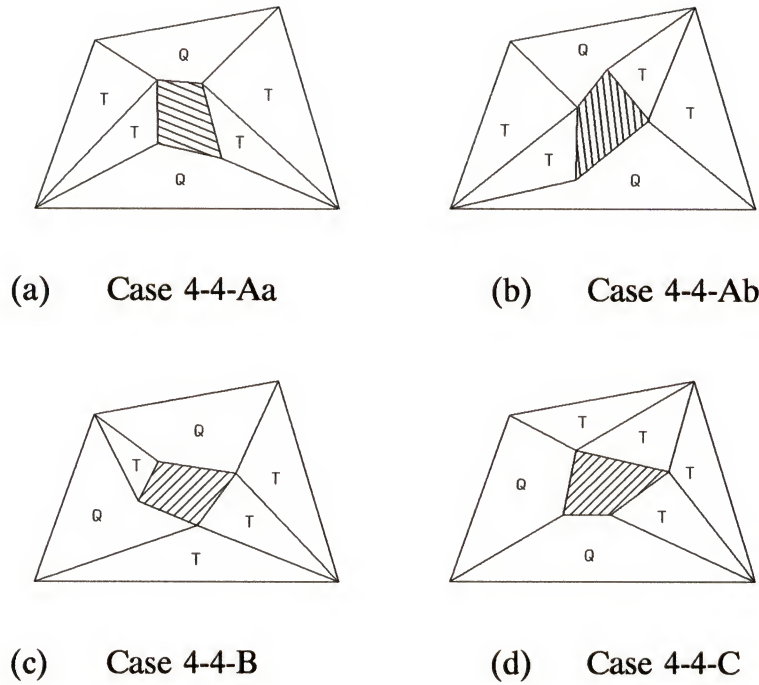


Fig. 3.2 The Four Cases of 4-4 Platforms (Top Views)

3.2 Formulation of the Forward Analyses

The procedure to obtain the forward displacement analysis for all the four cases of the 4-4 Platforms is the same: it is necessary to obtain three simultaneous equations which contain three tan-half-angles. Then, an eliminant for these equations is derived. The derivations of the three equations for each case of the 4-4 Platforms are performed separately.

3.2.1 Case 4-4-A, a T-T-Q-T-T-Q Platform

There are two variations of leg arrangements for Case 4-4-A as shown in Figs. 3.2(a) and 3.2(b). The formulations for Cases 4-4-Aa and 4-4-Ab are quite similar as

both of them can be modeled by 3-3 Platforms by constructions. Griffis and Duffy (1989) used constructions to model a 6-3 Platform by a 3-3 Platform. It should be noted that for both Cases 4-4-Aa and 4-4-Ab, the sides ad^3 and bc of the top platform are not parallel and the sides AD and BC of the base are not parallel.

Case 4-4-Aa can be modeled by an equivalent 3-3 Platform by extending the sides of the quadrilateral base AD and CB and the sides of the top platform ad and bc as shown in Fig. 3.3. Knowing the lengths of these extension lines, the four "virtual" connecting leg lengths (Ec , Ed , Ae , and Be) can be uniquely determined. Thus a "virtual" 3-3 Platform with the triangular top platform (d , c , and e) and the triangular base (A , B , and E) is created. The dihedral angles θ_1 , θ_2 , and θ_3 measure, respectively, the elevations of the triangles $\triangle ABe$, $\triangle BCc$, and $\triangle DAd$ relative to the base $ABCD$. The solution of the forward analysis problem for the 3-3 Platform is presented by Griffis and Duffy (1989) and will not be repeated here.

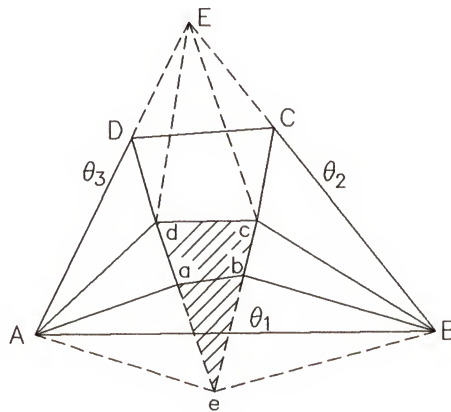


Fig. 3.3 A "Virtual" 3-3 Platform of Case 4-4-Aa

³Here and throughout, the pair of letters, XY , (where X or Y can be A , ..., G , a , ..., or e) denotes either a leg, leg length, or an edge length of the top or base platform.

For Case 4-4-Ab, the sides of the base are extended to meet at point E as shown in Fig. 3.4(a). Then the lengths of the "virtual" legs Ed and Eb, which connect to the top platform at vertices d and b, can be uniquely calculated. Specifically, the leg Eb is determined from the angle $\angle CBB$, the new side length of the base EB, and the leg length Bb by using cosine law of a planar triangle. As a result, it can be considered that the "virtual" leg Eb replaces the leg bB which becomes redundant. Therefore, the triangle with vertices A, C, and E forms the base of an equivalent 3-3 mechanism as shown in Fig. 3.4(b). Again, the sides of the top platform are extended to form a triangular face. Thus, a "virtual" 3-3 Platform with the top platform having the vertices e, b, and d and the base A, C, and E is created. The dihedral angles θ_1 , θ_2 , and θ_3 are, respectively, defined as the angles between the base and the triangular faces $\triangle EAd$, $\triangle ACe$, and $\triangle CEb$.

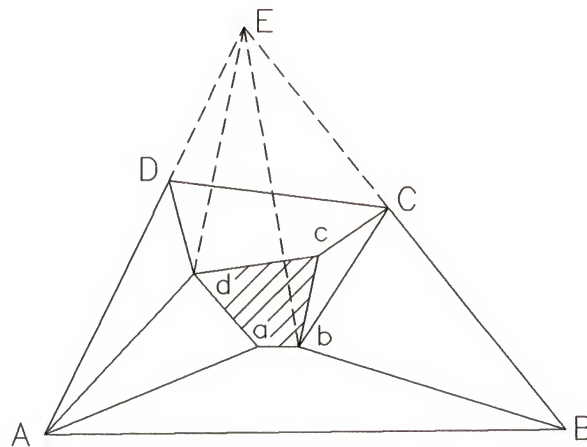


Fig. 3.4(a) Case 4-4-Ab with a "Virtual" Triangular Base

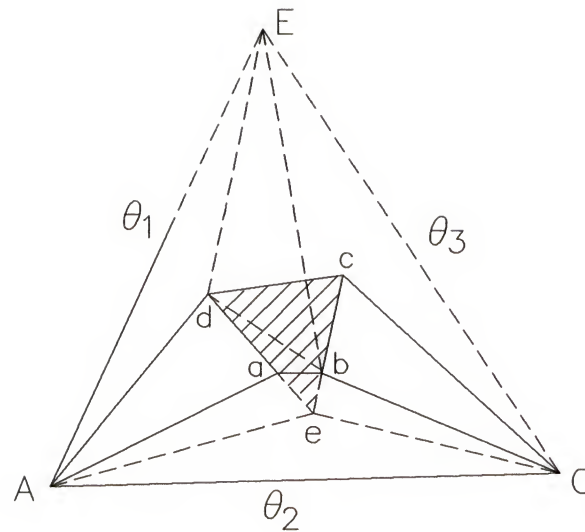


Fig. 3.4(b) A "Virtual" 3-3 Platform of Case 4-4-Ab

The dihedral angles [θ_1 , θ_2 , and θ_3 in Figs. 3.3 and 3.4(b)] in the form of tan-half-angles are the three variables in three quadratic equations. From these equations, the polynomial in one of the tan-half-angles can be derived, and the locations of the vertices a, b, c, and d can then be determined.

3.2.2 Case 4-4-B, a T-T-T-Q-T-Q Platform

The three variables defined for computing the position and orientation of the top platform relative to the base platform are the dihedral angles θ_2 , θ_3 , and θ_4 as shown in Fig. 3.7. The dihedral angle θ_2 measures the elevation of the triangular face ΔABa relative to the base, θ_3 measures ΔABa relative to ΔaBb , and θ_4 measures ΔaBb relative to the top platform.

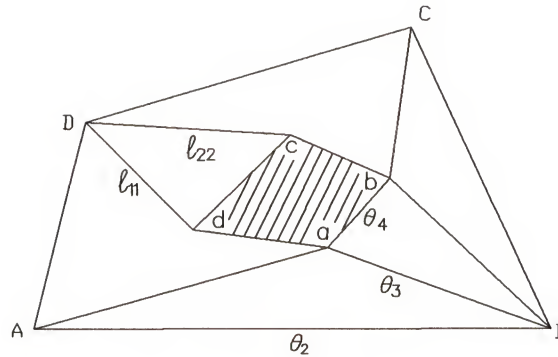


Fig. 3.5 Case 4-4-B Platform

The top platform is connected to the base by two triangles in serial fashion at the edges of the three dihedral angles. A relationship between these three angles can be obtained by introducing a skew-hexahedron as illustrated in Fig. 2.2. The skew-hexahedron consists of four triangles denoted by T_1 , T_2 , T_3 , and T_4 , and two skew quadrilaterals. There are two skew-hexahedra exist in the skew-octahedron of the Case 4-4-B mechanism and they share the three triangles, T_1 , T_2 , and T_3 , which are defined, respectively, by ΔDAB , ΔABa , and ΔaBb (see Fig. 3.5). The triangle T_4 represents a triangle in the top platform. In one of the skew-hexahedra, T_4 is defined by Δdab , and in other by Δcab .

Two of the necessary three equations contain the three dihedral angles θ_2 , θ_3 , and θ_4 and the third one contains θ_2 and θ_3 only. All three equations are obtained by using a serial chain which models the skew-hexahedra and the derivation of the equations is presented in Section 2.3. Equation 2.5 which resulted from a vector loop equation for the closed loop chain is again expressed as in the form

$$\begin{aligned}
& k^{(i)} + S_{11}S_{22}c_{12} + S_{11}S_{33}Z_2 + S_{11}S_{44}Z_{32} + S_{11}S_{55}^{(i)}Z_{432}^{(i)} \\
& + S_{22}S_{33}c_{23} + S_{22}S_{44}Z_3 + S_{22}S_{55}^{(i)}Z_{43}^{(i)} + S_{33}S_{44}c_{34} \\
& + S_{33}S_{55}^{(i)}Z_4^{(i)} + S_{44}S_{55}^{(i)}c_{45}^{(i)} = 0,
\end{aligned} \tag{3.1}$$

where

$$k^{(i)} = (S_{11}^2 + S_{22}^2 + S_{33}^2 + S_{44}^2 + S_{55}^{(i)2} - \ell_{ii}^2)/2.$$

The first two equations ($i = 1$ and 2) respectively for legs $\ell_{11} = Dd$ and $\ell_{22} = Dc$ (see Fig. 3.5) are expressed as

$$S_{55}^{(i)}s_{45}^{(i)}(A_{23}c_4 + B_{23}s_4) + D_{23}^{(i)} = 0, \tag{3.2}$$

where the coefficients A_{23} , B_{23} , and $D_{23}^{(i)}$ are presented in Table 3.1.

Table 3.1 Coefficients A_{23} , B_{23} , and $D_{23}^{(i)}$ in (3.2)

$A_{23} = p_1c_3 + q_1s_3 + r_1$	$B_{23} = (q_1c_3 - p_1s_3)/c_{34}$	$D_{23}^{(i)} = p_2^{(i)}c_3 + q_2^{(i)}s_3 + r_2^{(i)}$
$p_1 = p_{11}c_2 + p_{12}$	$q_1 = q_{11}s_2$	$r_1 = r_{11}c_2 + r_{12}$
$p_{11} = -c_{34}c_{23}s_{12}S_{11}$	$p_{12} = -c_{34}s_{23}(c_{12}S_{11} + S_{22})$	
$q_{11} = c_{34}s_{12}S_{11}$		
$r_{11} = s_{34}s_{12}s_{23}S_{11}$	$r_{12} = -s_{34}(c_{12}c_{23}S_{11} + c_{23}S_{22} + S_{33})$	
$p_2^{(i)} = p_{21}^{(i)}c_2 + p_{22}^{(i)}$	$q_2^{(i)} = q_{21}^{(i)}s_2$	$r_2^{(i)} = r_{21}^{(i)}c_2 + r_{22}^{(i)}$
$p_{21}^{(i)} = s_{34}(c_{45}^{(i)}S_{55}^{(i)} + S_{44})p_{11}/c_{34}$	$p_{22}^{(i)} = s_{34}(c_{45}^{(i)}S_{55}^{(i)} + S_{44})p_{12}/c_{34}$	
$q_{21}^{(i)} = s_{12}s_{34}S_{11}(c_{45}^{(i)}S_{55}^{(i)} + S_{44})$		
$r_{21}^{(i)} = -s_{12}s_{23}S_{11}m_1^{(i)}$		
$r_{22}^{(i)} = c_{12}S_{11}(c_{23}m_1^{(i)} + S_{22}) + c_{23}S_{22}m_1^{(i)} + c_{34}S_{33}(c_{45}^{(i)}S_{55}^{(i)} + S_{44}) + c_{45}^{(i)}S_{44}S_{55}^{(i)} + k^{(i)}$		
$m_1^{(i)} = c_{34}(c_{45}^{(i)}S_{55}^{(i)} + S_{44}) + S_{33}$		

For $i = 1$,

$$S_{55}^{(1)} = bd, \quad s_{45}^{(1)} = \sin(\angle dba), \quad \text{and} \quad c_{45}^{(1)} = -\cos(\angle dba).$$

For $i = 2$,

$$S_{55}^{(2)} = bc, \quad s_{45}^{(2)} = \sin(\angle cba), \quad \text{and} \quad c_{45}^{(2)} = -\cos(\angle cba).$$

The third equation is derived from (3.1) with $S_{55}^{(i)} = 0$, $\ell_{ii} = Cb$, and $S_{11} = CA$.

It contains the dihedral angles θ_2 and θ_3 only and can be expressed in the form

$$p_3 c_3 + q_3 s_3 + r_3 = 0, \quad (3.3)$$

where

$$p_3 = p_{31} c_2 + p_{32}, \quad q_3 = q_{31} s_2, \quad r_3 = r_{31} c_2 + r_{32}.$$

Further,

$$p_{31} = -c_{23}s_{12}s_{34}S_{11}S_{44}, \quad p_{32} = -s_{23}s_{34}S_{44}(c_{12}S_{11} + S_{22}),$$

$$q_{31} = s_{12}s_{34}S_{11}S_{44}, \quad r_{31} = -s_{12}s_{23}S_{11}m_2,$$

$$r_{32} = c_{12}S_{11}(c_{23}m_2 + S_{22}) + c_{23}S_{22}m_2 + c_{34}S_{33}S_{44} + k^{(i)},$$

$$m_2 = c_{34}S_{44} + S_{33}.$$

The two equations in (3.2) together with (3.3) are the three equations that are used to obtain a polynomial in tan-half-angle $x = \tan(\theta_2/2)$ by an elimination process detailed in Section 3.5. The degree of the polynomial obtained for this case is four in x^2 which yields eight values of θ_2 . Linear elimination of θ_4 from the two equations in (3.2) yields an equation that together with (3.3) provides the two relations necessary to obtain one θ_3 for each θ_2 . Finally, by using either equation in (3.2), each pair of θ_2 and θ_3 yields two values of θ_4 which results in 16 solution sets of the angles θ_2 , θ_3 , and θ_4 .

3.2.3 Case 4-4-C, a T-T-T-T-Q-Q Platform

Figure 3.2(d) shows a Case 4-4-C Platform. The top platform has vertices a, b, c, d, and the base has vertices A, B, C, D. The dihedral angle θ_1 is defined as the angle between the triangles ΔCcB and ΔCcd , θ_2 between ΔcBC and ΔcBb , and θ_3 between ΔCcB and the base. (See Fig. 3.6.)

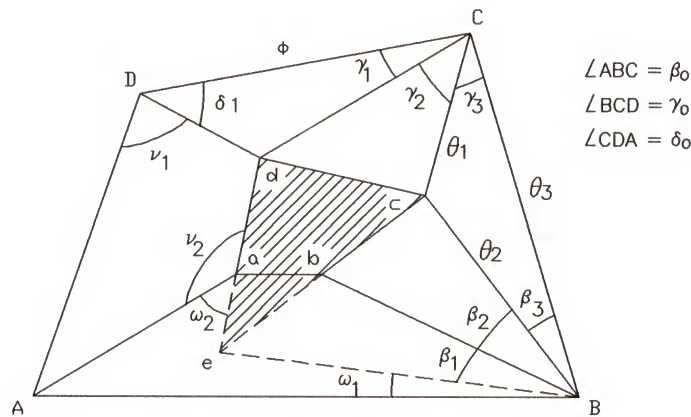


Fig. 3.6 Case 4-4-C Platform
with a "Virtual" Triangular Platform

The formulations for the first two equations are the same. The vertices c and C respectively in the top and base platforms are considered to be the centers of two concentric spherical joints which are modeled by four-bar linkages. By an exchange of variables, (2.2) can be used to obtain the input-output equations for the two spherical four-bar at vertices c and C. These equations are expressed in the form

$$A_{31}x^2y^2 + B_{31}x^2 + C_{31}y^2 + D_{31}xy + E_{31} = 0, \quad (3.4)$$

$$A_{32}z^2x^2 + B_{32}z^2 + C_{32}x^2 + D_{32}zx + E_{32} = 0. \quad (3.5)$$

Here, the five coefficients A_{31}, \dots, E_{31} replace A, \dots, E of (2.2) where the link angles

$\alpha_{12}, \dots, \alpha_{41}$ are given by $\angle Ccd, \angle dcb, \angle bcB, \angle BcC$. Also, the relations $x = \tan(\theta_1/2)$ and $y = \tan(\theta_2/2)$ replace τ_1 and τ_4 . Similarly for (2.10), the five coefficients A_{32}, \dots, E_{32} replace A, \dots, E of (2.2), where $\alpha_{12}, \dots, \alpha_{41}$ are given by $\angle BCD, \angle DCd, \angle dCc, \angle BCc$ and $z = \tan(\theta_3/2)$ and x replace τ_1 and τ_4 . To adequately determine the link angles from the edge lengths, the signs of the sines of these angles must be consistent. In the formulation, the signs of the sines of all the link angles $\alpha_{12}, \dots, \alpha_{41}$ are taken as positive.

While the first two equations are in the same form as that in the other two cases, the third equation contains all three variables x, y , and z . Its derivation is more complicated. A construction is used on the Case 4-4-C Platform to obtain the relationship between the dihedral angles θ_2 and θ_3 and the third dihedral angle θ_1 . Figure 3.6 shows the extension lines ae, be in the top platform and the "virtual" leg Be added to the Case 4-4-C Platform. The lengths of the extension lines can be determined by using the cosine law for a planar triangle.

Vertex B is now considered to be the location of a spherical four-bar linkage. (See Section 2.2.) Instead of the leg Bb being one of the axes of the four-bar linkage, the "virtual" leg Be is used so that the following equation can be used:

$$Z_{23} = \cos \omega_1. \quad (3.6)$$

Equation (3.6) results in the form of (2.1). The link angles α_{12}, α_{34} , and α_{41} in (2.1) are replaced, respectively, by $(\beta_1 + \beta_2), \beta_0$, and β_3 , and ω_1 replaces α_{23} . The input and output angles are θ_3 and θ_2 .

Applying (2.7) to the skew-quadrilateral $AaeB$, the following relation between

ω_1 and ω_2 can be obtained:

$$\cos\omega_1 = K_1 + K_2\cos\omega_2, \quad (3.7)$$

where

$$K_1 = \frac{eB^2 + AB^2 - aA^2 - ae^2}{2 eB AB} \quad \text{and} \quad K_2 = \frac{aA ae}{eB AB}.$$

Similarly, the relationship between v_1 and v_2 in the skew-quadrilateral DdaA is given by

$$\cos v_2 = K_3 + K_4 \cos v_1, \quad (3.8)$$

where

$$K_3 = \frac{ad^2 + aA^2 - dD^2 - DA^2}{2 ad aA} \quad \text{and} \quad K_4 = \frac{dD DA}{ad aA}.$$

Since v_2 and ω_2 are supplementary,

$$\cos v_2 = -\cos\omega_2. \quad (3.9)$$

Combining (3.7), (3.8), and (3.9) gives

$$\cos\omega_1 = K_1 - K_2K_3 - K_2K_4\cos v_1. \quad (3.10)$$

The vertex at D is connected by a single leg. The spherical trigonometric cosine law (2.8) can then be applied to obtain the following relationship between v_1 and ϕ :

$$\cos v_1 = K_5 + K_6\cos\phi, \quad (3.11)$$

where

$$K_5 = \cos\delta_1\cos\delta_0,$$

$$K_6 = -\sin\delta_1\sin\delta_0.$$

The dihedral angle ϕ measures the elevation of the triangle ΔCDd relative to the

base platform.

For the spherical four-bar linkage at vertex C, there is a relationship between $\cos\phi$ and $\cos\theta_1$ and it is given by

$$\cos\phi = K_7 + K_8\cos\theta_1, \quad (3.12)$$

where

$$K_7 = \frac{\cos\gamma_1\cos\gamma_0 - \cos\gamma_2\cos\gamma_3}{\sin\gamma_1\sin\gamma_0} \quad \text{and} \quad K_8 = \frac{\sin\gamma_2\sin\gamma_3}{\sin\gamma_1\sin\gamma_0}.$$

Equation (3.12) is derived from the sine, sine-cosine, and cosine laws for a spherical quadrilateral (Duffy, 1980).

Combining (3.6), (3.10), (3.11), and (3.12), the equation which contains θ_2 , θ_3 , and θ_1 is obtained in the form

$$Z_{23} = \xi_6 + \xi_7\cos\theta_1, \quad (3.13)$$

where

$$\xi_6 = K_1 - K_2K_3 - K_2K_4K_5 - K_2K_4K_6K_7,$$

$$\xi_7 = K_2K_4K_6.$$

By introducing the tan-half-angles for θ_1 , θ_2 and θ_3 and re-grouping, (3.13) can be expressed in the form

$$\begin{aligned} y^2z^2(A_{33}x^2 + C_{33}) + y^2(B_{33}x^2 + F_{33}) + z^2(D_{33}x^2 + G_{33}) \\ + yz(H_{33}x^2 + I_{33}) + E_{33}x^2 + J_{33} = 0, \end{aligned} \quad (3.14)$$

where

$$A_{33} = \xi_1 - \xi_2 - \xi_3 + \xi_5 - \xi_6 + \xi_7,$$

$$B_{33} = -\xi_1 - \xi_2 + \xi_3 + \xi_5 - \xi_6 + \xi_7,$$

$$C_{33} = \xi_1 - \xi_2 - \xi_3 + \xi_5 - \xi_6 - \xi_7,$$

$$D_{33} = -\xi_1 + \xi_2 - \xi_3 + \xi_5 - \xi_6 + \xi_7,$$

$$E_{33} = \xi_1 + \xi_2 + \xi_3 + \xi_5 - \xi_6 + \xi_7,$$

$$F_{33} = -\xi_1 - \xi_2 + \xi_3 + \xi_5 - \xi_6 - \xi_7,$$

$$G_{33} = -\xi_1 + \xi_2 - \xi_3 + \xi_5 - \xi_6 - \xi_7,$$

$$H_{33} = I_{33} = 4\xi_4,$$

$$J_{33} = \xi_1 + \xi_2 + \xi_3 + \xi_5 - \xi_6 - \xi_7.$$

Further,

$$\xi_1 = \sin(\beta_1 + \beta_2)\cos\beta_3\sin\beta_0,$$

$$\xi_2 = \sin(\beta_1 + \beta_2)\sin\beta_3\cos\beta_0,$$

$$\xi_3 = \sin\beta_3\sin\beta_0\cos(\beta_1 + \beta_2),$$

$$\xi_4 = -\sin(\beta_1 + \beta_2)\sin\beta_0,$$

$$\xi_5 = -\cos(\beta_1 + \beta_2)\cos\beta_3\cos\beta_0.$$

Equations (3.4), (3.5), and (3.14) are the three simultaneous equations which are used to derive the polynomial in the tan-half-angle x .

3.3 The Eliminants of the Equation Sets

The eliminants of the equation sets can be expressed in the form of polynomials equations in one variable. To obtain the eliminants, it is necessary to eliminate two unwanted variables in the equation sets. The elimination process for each case is described below.

3.3.1 Cases 4-4-A and 4-4-C

The formulation of the forward analyses for each of Cases 4-4-A and 4-4-C generates three equations in the following forms:

$$A_1x^2y^2 + B_1x^2 + C_1y^2 + D_1xy + E_1 = 0, \quad (3.15)$$

$$A_2z^2x^2 + B_2z^2 + C_2x^2 + D_2zx + E_2 = 0, \quad (3.16)$$

$$A_3y^2z^2 + B_3y^2 + C_3z^2 + D_3yz + E_3 = 0. \quad (3.17)$$

Note that for Case 4-4-C, the coefficients A_3, \dots, E_3 in the third equation are quadratic in x . It is necessary to eliminate y and z from these equations to obtain a polynomial equation in x for each case. The procedure for the elimination is the same as that developed by Griffis and Duffy (1989). The eliminant is expressed as

$$\Delta = \alpha^2 - 4\beta^2\rho_1\rho_2, \quad (3.18)$$

where

$$\begin{aligned} \alpha = & 2A_3B_3a_2c_1^2c_2 - 4A_3B_3c_1^2b_2^2 + 2A_3C_3a_1c_1c_2^2 - 4A_3C_3c_2^2b_1^2 - 2A_3E_3a_1a_2c_1c_2 \\ & + 4A_3E_3a_1c_1b_2^2 + 4A_3E_3a_2c_2b_1^2 - 8A_3E_3b_1^2b_2^2 - 2A_3D_3c_1c_2b_1b_2 \\ & - 2B_3C_3a_1a_2c_1c_2 + 4B_3C_3a_1c_1b_2^2 + 4B_3C_3a_2c_2b_1^2 - 8B_3C_3b_1^2b_2^2 \\ & + 2B_3E_3a_1a_2^2c_1 - 4B_3E_3a_2^2b_1^2 - 2B_3D_3a_2c_1b_1b_2 + 2C_3E_3a_1^2a_2c_2 \\ & - 4C_3E_3a_1^2b_2^2 - 2C_3D_3a_1c_2b_1b_2 - 2D_3E_3a_1a_2b_1b_2 - D_3^2a_1a_2c_1c_2 \\ & - A_3^2c_1^2c_2^2 - B_3^2a_2^2c_1^2 - C_3^2a_1^2c_2^2 - E_3^2a_1^2a_2^2, \end{aligned}$$

$$\beta = 4A_3E_3b_1b_2 + A_3D_3c_1c_2 + D_3E_3a_1a_2 - 4B_3C_3b_1b_2 - B_3D_3a_2c_1 - C_3D_3a_1c_2,$$

$$\rho_1 = b_1^2 - a_1c_1,$$

$$\rho_2 = b_2^2 - a_2c_2.$$

Further,

$$\begin{aligned}
a_1 &= A_1 x^2 + C_1, & b_1 &= 0.5 D_1 x, & c_1 &= B_1 x^2 + E_1, \\
a_2 &= A_2 x^2 + B_2, & b_2 &= 0.5 D_2 x, & c_2 &= C_2 x^2 + E_2.
\end{aligned}$$

The expression $\Delta = 0$ results in a polynomial equation in x which is 16th degree for Case 4-4-A and 24th degree for Case 4-4-C. When Δ vanishes, (3.15), (3.16), and (3.17) have simultaneous solutions in the variables x , y , and z .

3.3.2 Case 4-4-B

The vanishing of the eliminant for Case 4-4-B results in an eighth degree polynomial equation in x . The procedure for obtaining this equation begins by equating $(A_{23} c_4 + B_{23} s_4)$ in (3.2) for $i = 1$ and 2, which yields the following expression independent of θ_4 :

$$pp c_3 + qq s_3 + rr = 0, \quad (3.19)$$

where

$$\begin{aligned}
pp &= p_2^{(1)} / (S_{55}^{(1)} s_{45}^{(1)}) - p_2^{(2)} / (S_{55}^{(2)} s_{45}^{(2)}), \\
qq &= q_2^{(1)} / (S_{55}^{(1)} s_{45}^{(1)}) - q_2^{(2)} / (S_{55}^{(2)} s_{45}^{(2)}), \\
rr &= r_2^{(1)} / (S_{55}^{(1)} s_{45}^{(1)}) - r_2^{(2)} / (S_{55}^{(2)} s_{45}^{(2)}).
\end{aligned}$$

Expanding s_3 and c_3 in the tan-half-angle $y = \tan(\theta_3/2)$, (3.3) and (3.19) can be expressed in the form

$$e_j y^2 + f_j y + g_j = 0, \quad (j = 1, 2), \quad (3.20)$$

where

$$\begin{aligned}
e_1 &= rr - pp, & f_1 &= 2 qq, & g_1 &= rr + pp, \\
e_2 &= r_3 - p_3, & f_2 &= 2 q_3, & g_2 &= r_3 + p_3.
\end{aligned}$$

Eliminating y from (3.20), the following equation is obtained.

$$(e_1 f_2 - e_2 f_1)(f_1 g_2 - f_2 g_1) - (e_1 g_2 - e_2 g_1)^2 = 0. \quad (3.21)$$

Equation (3.21) is an eighth degree polynomial equation in $\tan(\theta_2/2)$ since e_j and g_j are quadratic in x .

3.4 Numerical Verifications

In this section, a numerical example is presented for each of Cases 4-4-B and 4-4-C to verify the analysis. The verification procedure was as follows: first the dimensions of the top and base platforms in the mechanisms were specified. The platforms are planar. Then, a set of leg lengths were obtained by a reverse displacement analysis. Knowing the dimensions of the platforms and the leg length, the forward displacement analysis developed was then applied to determine all the 16 locations of the top platform. Finally, all the 16 solutions were verified by a reverse displacement analysis that the distances between points connects by the legs equal the corresponding leg lengths.

3.4.1 Case 4-4-B

The dimensions of the top and base platforms were defined by the following coordinates of the vertices (see Fig. 3.5) in two different reference systems for the top and base platforms.

$$\begin{array}{ll} a \ (0, 0, 0), & A \ (0, 0, 0), \\ b \ (2, 0, 0), & B \ (18, 0, 0), \end{array}$$

$$\begin{array}{ll} c (4, 4, 0), & C (14, 14, 0), \\ d (-2, 4, 0), & D (-2, 10, 0). \end{array}$$

The leg lengths were as follows:

$$\begin{array}{ll} Aa = 15.16575, & Cb = 12.77364, \\ Ba = 17.37814, & Dc = 16.22146, \\ Bb = 18.68404, & Dd = 16.78414. \end{array}$$

Expanding the eliminant (3.21), the following polynomial equation was obtained:

$$x^8 + 1.3532193x^6 - 0.2835099x^4 - 0.0230815x^2 + 0.0036245.$$

The polynomial equation has the following eight roots:

$$x = \pm 0.4453624, \pm 0.3132981, (\pm i1.2360720), \text{ and } (\pm i0.3490684).$$

The variable x is the tan-half-angle of the dihedral angle θ_2 . For each value of x , a value of y was obtained by using (3.20). With each pair of x and y , two values of z are obtained by using either equation in (3.2). Therefore, 16 solution sets of tan-half-angles x , y , and z were found and they are listed in Table 3.2. Using these results, the coordinates of the top platform were calculated. The origin of the reference system is A. (See Fig. 3.5.) B lies on the x -axis, and C and D are in the x - y plane. The coordinates of the vertices a, b, c, and d are shown in Table 3.3.

Table 3.2 Variables x , y , and z of Case 4-4-B
(Only Eight Sets of Variables are Shown Here)

<u>Solution</u>	<u>1</u>	<u>2</u>	<u>3</u>	<u>4</u>
x	0.44536	0.44536	0.31330	0.31330
y	-1.45795	-1.45795	0.48157	0.48157
z	-3.19008	-0.43657	(0.83521 - i0.53986)	(0.83521 + i0.53986)

	<u>Solution 5</u>	<u>6</u>	<u>7</u>	<u>8</u>
x	(i1.23607)	(i1.23607)	(i0.34907)	(i0.34907)
y	(i1.02848)	(i1.02848)	(-i0.74997)	(-i0.74997)
z	(i0.57590)	(-i0.90235)	(-i0.76842)	(i0.94817)

Table 3.3 Coordinates of the Vertices of the Top Platform of Case 4-4-B
(Only Half of the Sixteen Reflections Are Shown Here)

	<u>Solution 1</u>	<u>Solution 2</u>
a	(7.0000e+00, 9.0000e+00, 1.0000e+01)	(7.0000e+00, 9.0000e+00, 1.0000e+01)
b	(6.6527e+00, 1.0970e+01, 1.0000e+01)	(6.6527e+00, 1.0970e+01, 1.0000e+01)
c	(5.7557e+00, 1.2842e+01, 1.3961e+01)	(1.0245e+01, 1.3634e+01, 1.0000e+01)
d	(6.7976e+00, 6.9335e+00, 1.3961e+01)	(1.1287e+01, 7.7250e+00, 1.0000e+01)
	<u>Solution 3</u>	
a	(7.0000e+00 + i0.0000e+00, 1.1049e+01 + i0.0000e+00, 7.6765e+00 + i0.0000e+00)	
b	(5.458e+00 + i0.0000e+00, 1.0628e+01 + i0.0000e+00, 8.8784e+00 + i0.0000e+00)	
c	(6.804e+00 + i5.0015e-01, 1.0419e+01 - i2.5251e+00, 1.3861e+01 - i2.4145e-01)	
d	(1.143e+01 + i5.0015e-01, 1.1680e+01 - i2.5251e+00, 1.0255e+01 - i2.4145e-01)	
	<u>Solution 4</u>	
a	(7.0000e+00 + i0.0000e+00, 1.1049e+01 + i0.0000e+00, 7.6765e+00 + i0.0000e+00)	
b	(5.4577e+00 + i0.0000e+00, 1.0628e+01 + i0.0000e+00, 8.8784e+00 + i0.0000e+00)	
c	(6.8043e+00 - i5.0015e-01, 1.0419e+01 + i2.5251e+00, 1.3861e+01 + i2.4145e-01)	
d	(1.1431e+01 - i5.0015e-01, 1.1680e+01 + i2.5251e+00, 1.0255e+01 + i2.4145e-01)	
	<u>Solution 5</u>	
a	(7.0000e+00 - i1.1084e-29, -6.4427e+01 - i7.7192e-15, -7.8932e-15 - i6.3006e+01)	
b	(4.9485e+01 + i1.5907e-14, 2.3207e+01 + i3.8191e-14, 4.0368e-14 + i3.4363e+01)	
c	(4.2216e+02 + i1.0750e-13, 8.3031e+02 + i3.4085e-13, 3.5354e-13 + i9.2334e+02)	
d	(2.9471e+02 + i1.0408e-13, 5.6740e+02 + i2.9934e-13, 3.1470e-13 + i6.3123e+02)	
	<u>Solution 6</u>	
a	(7.0000e+00 - i1.1084e-29, -6.4427e+01 - i7.7192e-15, -7.8932e-15 - i6.3006e+01)	
b	(4.9485e+01 + i1.5907e-14, 2.3207e+01 + i3.8191e-14, 4.0368e-14 + i3.4363e+01)	
c	(-2.9193e+02 - i1.6785e-13, -6.4028e+02 - i4.3498e-13, -4.6446e-13 - i7.1180e+02)	
d	(-4.1939e+02 - i1.6447e-13, -9.0318e+02 - i4.7249e-13, -4.9674e-13 - i1.0039e+03)	
	<u>Solution 7</u>	
a	(7.0000e+00 + i0.0000e+00, 1.7187e+01 + i0.0000e+00, 0.0000e+00 + i1.0696e+01)	
b	(1.8769e+00 + i1.0205e-15, 9.6051e+00 + i2.1576e-15, 2.4175e-15 + i1.7663e+00)	
c	(-6.1992e+01 + i1.0740e-14, -1.4831e+02 + i1.8573e-14, 2.1286e-14 - i1.6852e+02)	
d	(-4.6623e+01 + i1.5410e-14, -1.2557e+02 + i3.1728e-14, 3.5136e-14 - i1.4173e+02)	
	<u>Solution 8</u>	
a	(7.0000e+00 + i0.0000e+00, 1.7187e+01 + i0.0000e+00, 0.0000e+00 + i1.0696e+01)	
b	(1.8769e+00 + i1.0205e-15, 9.6051e+00 + i2.1576e-15, 2.4175e-15 + i1.7663e+00)	
c	(1.0455e+02 - i3.2578e-14, 1.0337e+02 - i4.8187e-14, -5.6372e-14 + i1.4074e+02)	
d	(1.1992e+02 - i2.1578e-14, 1.2612e+02 - i4.1353e-14, -4.4259e-14 + i1.6753e+02)	

3.4.2 Case 4-4-C

The coordinates of the vertices of the top platform and base were chosen the same as those for Case 4-4-B and they are shown in Section 3.4.1. The leg lengths were as follows:

$$\begin{aligned} Aa &= 15.1657, & Cc &= 10.8545, \\ Bb &= 15.7907, & Cd &= 11.8770, \\ Bc &= 15.1719, & Dd &= 14.2917. \end{aligned}$$

The following polynomial was obtained through expansion of the eliminant (3.18):

$$\begin{aligned} \Delta = x^{24} + 2.4989x^{22} - 112.54x^{20} - 158.81x^{18} + 3605.8x^{16} + 1773.5x^{14} - 19278x^{12} \\ - 26782x^{10} - 6005.0x^8 + 4494.4x^6 + 1071.6x^4 - 194.97x^2 + 1.9274 = 0. \end{aligned}$$

This polynomial has the following 24 roots:

$$\begin{aligned} x = \pm 0.10257, \pm 0.34826, \pm 0.58739, \pm 2.59074, \pm 2.58299, \pm 1.80329, \\ (0.05301 \pm i2.82547), (-0.05301 \pm i2.82547), (\pm i1.16480), \\ (\pm i1.07011), (\pm i0.85835), \text{ and } (\pm i0.64173). \end{aligned}$$

Using these results, the coordinates of the top platform were calculated. The origin of the fixed system in the base is A (see Fig. 3.6), B lies on the x axis, and C and D are in the xy plane. The locations of the vertices a, b, c, and d are listed in Table 3.4.

Table 3.4 Coordinates of the Vertices of the Top Platform
(Only Half of the Twenty-four Reflections Are Shown Here)

	<u>Solution 1</u>	<u>Solution 2</u>
a	(6.7013e+00, 1.2180e+01, 6.0617e+00)	(7.0000e+00, 9.0000e+00, 1.0000e+01)
b	(7.7579e+00, 1.0494e+01, 5.8588e+00)	(8.6483e+00, 7.8672e+00, 1.0000e+01)
c	(1.0518e+01, 9.4469e+00, 9.2179e+00)	(1.2562e+01, 1.0031e+01, 1.0000e+01)
d	(7.3485e+00, 1.4505e+01, 9.8268e+00)	(7.6174e+00, 1.3429e+01, 1.0000e+01)

	<u>Solution 3</u>	<u>Solution 4</u>
a	(7.4534e+00, 7.4501e+00, 1.0906e+01)	(9.3291e+00, 9.4188e+00, 7.3657e+00)
b	(6.9456e+00, 6.2841e+00, 9.3625e+00)	(7.9506e+00, 1.0416e+01, 6.3142e+00)
c	(6.5020e+00, 8.2994e+00, 5.3949e+00)	(5.5780e+00, 8.0354e+00, 3.3638e+00)
d	(8.0254e+00, 1.1797e+01, 1.0026e+01)	(9.7136e+00, 5.0445e+00, 6.5184e+00)
	<u>Solution 5</u>	<u>Solution 6</u>
a	(9.3270e+00, 4.7539e+00, 1.0973e+01)	(9.0066e+00, 1.0437e+01, 6.3200e+00)
b	(9.9661e+00, 6.3246e+00, 1.2033e+01)	(1.0257e+01, 1.1771e+01, 7.1306e+00)
c	(1.1629e+01, 9.7642e+00, 9.7086e+00)	(1.3176e+01, 1.0206e+01, 1.0137e+01)
d	(9.7117e+00, 5.0520e+00, 6.5274e+00)	(9.4233e+00, 6.2054e+00, 7.7047e+00)
	<u>Solution 7</u>	
a	(1.0162e+01 - i1.8752e-02, 1.2697e+01 + i1.4645e-01, 2.8393e-01 - i5.8778e+00)	
b	(8.3169e+00 - i1.8676e-02, 1.4632e+01 + i1.2236e-01, 2.5759e-01 - i7.6524e+00)	
c	(4.9272e+00 - i1.6648e-02, 7.8495e+00 - i4.7564e-03, 1.1791e-01 - i1.5290e+00)	
d	(1.0463e+01 - i1.6877e-02, 2.0449e+00 + i6.7507e-02, 1.9694e-01 + i3.7949e+00)	
	<u>Solution 8</u>	
a	(1.0162e+01 + i1.8752e-02, 1.2697e+01 - i1.4645e-01, 2.8393e-01 + i5.8778e+00)	
b	(8.3169e+00 + i1.8676e-02, 1.4632e+01 - i1.2236e-01, 2.5759e-01 + i7.6524e+00)	
d	(4.9272e+00 + i1.6648e-02, 7.8495e+00 + i4.7564e-03, 1.1791e-01 + i1.5290e+00)	
c	(1.0463e+01 + i1.6877e-02, 2.0449e+00 - i6.7507e-02, 1.9694e-01 - i3.7949e+00)	
	<u>Solution 9</u>	
a	(1.8291e+01 - i1.1833e-15, 2.2895e+00 + i3.0869e-14, -3.0714e-14 - i1.0479e+01)	
b	(2.0673e+01 - i7.3262e-16, 1.5884e+01 + i1.9157e-16, -3.4142e-16 + i3.1764e+00)	
c	(2.4925e+01 - i1.5492e-16, 1.3563e+01 - i4.4262e-17, 1.2723e-15 + i1.3151e+00)	
d	(1.7780e+01 + i4.6710e-15, -2.7219e+01 + i1.3346e-15, -9.4210e-16 - i3.9652e+01)	
	<u>Solution 10</u>	
a	(3.0782e+01 + i2.0459e-15, -1.7179e+01 + i2.0459e-15, 4.9015e-14 + i3.1822e+01)	
b	(2.9407e+01 - i6.4894e-16, 1.1401e+01 - i6.4894e-16, 2.3412e-15 + i3.2790e+00)	
c	(2.4896e+01 - i1.2313e-16, 1.3555e+01 - i1.2313e-16, 1.2685e-15 + i1.0453e+00)	
d	(2.9021e+01 - i1.0210e-14, -7.2186e+01 - i1.0210e-14, -1.1313e-15 + i8.6675e+01)	
	<u>Solution 11</u>	
a	(-1.8834e+00 + i2.6779e-15, 1.5270e+01 + i2.6779e-15, -1.7035e-14 + i2.5943e+00)	
b	(-4.7455e-01 + i2.8387e-15, 2.6476e+00 + i2.8387e-15, -4.9969e-15 - i9.9484e+00)	
c	(3.8489e+00 + i1.2228e-15, 7.5414e+00 + i1.2228e-15, -2.8264e-15 - i5.1901e+00)	
d	(-3.7771e-01 - i7.1178e-15, 4.5410e+01 - i7.1178e-15, 3.3738e-15 + i3.2438e+01)	
	<u>Solution 12</u>	
a	(4.5298e+00 + i1.8262e-16, 1.5797e+01 + i1.8262e-16, 8.7347e-16 + i6.3291e+00)	
b	(-2.5963e+00 + i1.6905e-16, 8.9811e+00 + i1.6905e-16, 5.7671e-17 + i1.5985e+01)	
c	(-1.5984e+01 - i7.1781e-15, 1.8748e+00 - i7.1781e-15, -7.8805e-15 + i3.0467e+01)	
d	(5.3942e+00 + i2.7136e-15, 2.2322e+01 + i2.7136e-15, 2.5268e-15 + i1.4996e+00)	

In order to verify these results, a reverse displacement analysis was performed. All solutions, including complex ones, reproduced the correct edge lengths with at least 7 digit accuracy.

CHAPTER 4 THE ANALYSES OF THE 4-5 PLATFORMS

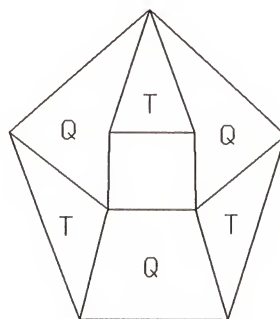
4.1 Introduction

Each of the 4-5 Platforms contains a quadrilateral top platform and a pentagonal base. The top platform is supported by six SPS serial chains (legs) that act in-parallel. The ends of the six legs join at four points at the vertices of the top platform and the other ends of the legs join at five points at the vertices of the base. No more than two legs meet at one vertex.

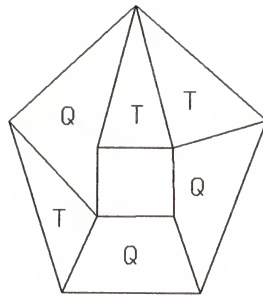
Similar to the 4-4 Platform mechanisms, the 4-5 Platforms are classified into three main cases according to the arrangements of the "triangles" and "skew-quadrilaterals" which are defined in the same way as those for the 4-4 Platforms. Figure 4.1 illustrates the top views of four cases. Each case has a different sequence of the triangles "T's" and the skew-quadrilaterals "Q's" around the top platform. For Cases 4-5-A, 4-5-B, and 4-5-C, the leg arrangements are, respectively, represented by T-Q-T-Q-T-Q, T-T-Q-T-Q-Q, and T-T-T-Q-Q-Q. These three cases have different structures which can be identified by the number of pairs of Q's adjacent to each other. The numbers of pairs of Q's adjacent to each other in Cases 4-5-A, 4-5-B, and 4-5-C are, respectively, zero, one, and two. In other words, Case 4-5-A does not contain any leg which is singly connected at the vertices of both the top and base

platforms. Case 4-5-B has one singly connected leg and Case 4-5-C has two singly connected legs. It should be noted that Case 4-4-C Platform which was analyzed in Chapter 3 contains also one singly connected leg. There are two variations of T-T-Q-T-Q-Q sequences for Case 4-5-B as shown in Figs. 4.1(b) and 4.1(c).

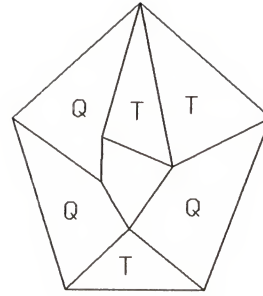
In the following sections, the formulation of the forward displacement analysis for each case is presented. A model which was established in Chapter 2 will be employed for formulating the analyses of all the cases. The elimination processes for all the cases are presented in Section 4.3. It will show that the degree of the polynomial equation obtained in the analysis for Case 4-5-A is eight, for Case 4-5-B is 24, and for 4-5-C is 32. In Section 4.4, some numerical examples will be presented to verify the results for some cases. The results will show that the maximum numbers of real assembly configurations for Cases 4-5-A, 4-5-B, and 4-5-C are, respectively, sixteen, twenty-four, and thirty-two.



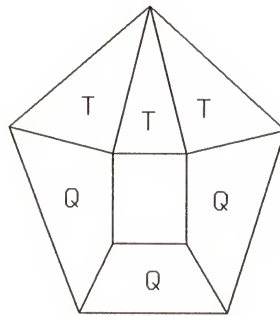
(a) Case 4-5-A



(b) Case 4-5-Ba



(c) Case 4-5-Bb



(d) Case 4-5-C

Fig. 4.1 The 4-5 Platforms (Top Views)

4.2 Formulation of the Analyses

The number of connection points of the legs in the base of the 4-5 Platforms is five. Therefore, in each case of the 4-5 mechanisms, there are three skew-quadrilaterals which are formed by two adjacent legs, an edge from the top, and an edge from the base. The closed-loop chain model presented in Section 2.3 will be employed in the analysis for all the cases. For Cases 4-5-A and 4-5-B, constructions, which are utilized for most cases of the 4-4 Platforms, will be used again. The

procedure to obtain the forward displacement analysis for all the cases of the 4-5 Platforms is the same as that for the 4-4 Platforms: it is necessary to obtain three algebraic independent equations each containing two or three variables. Then, an eliminant for these equations is derived, and from this eliminant, a polynomial in one of the variables is obtained.

4.2.1 Case 4-5-A, a T-Q-T-Q-T-Q Platform

Assuming that the top and base platforms are planar and the sides of the base AE and BC are nonparallel (see Fig. 4.2), this mechanism can be modeled by a Case 4-4-B Platform by constructions. In Sections 3.2.1 and 3.2.2, constructions were used to model Cases 4-4-Aa and 4-4-Ab Platforms by the 3-3 Platforms.

By extending the sides of the base AE and BC to obtain the intersection point F, the pentagonal base becomes a quadrilateral EFCD as shown in Fig. 4.2. The extension lines, AF and FB, the lengths of the edges of the base platform, EA and BC, and the leg lengths, Aa and Bb, are known. Then, the two "virtual" connecting leg lengths, Fa and Fb, can be uniquely determined by using the cosine law for a planar triangle. Thus a "virtual" Case 4-4-B Platform with the quadrilateral base EFCD and the quadrilateral top abcd is created.

The three variables which are used to obtain the locations of the top platform are defined as the dihedral angles θ_2 , θ_3 , and θ_4 . The dihedral angle θ_2 measures the elevation of the triangle ΔEFa relative to the base, θ_3 measures ΔEFa relative to ΔaFb , and θ_4 measures ΔaFb relative to the top platform. The Case 4-5-A Platform

is geometrically similar to the Case 4-4-B Platform. The forward analysis for the Case 4-4-B Platform can be found in Section 3.2.2.

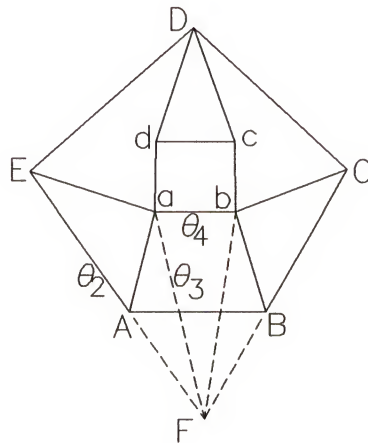


Fig. 4.2 A "Virtual" Case 4-4-B Platform of Case 4-5-A

The degree of the polynomial obtained for this case is four in x^2 , which gives eight values of θ_2 . However, as shown in Section 3.2.2, each values of θ_2 will yield two values of θ_4 and therefore, there are 16 solution sets of the angles θ_2 , θ_3 , and θ_4 . Accordingly, there are a maximum of 16 real assembly configurations for Case 4-5-A.

4.2.2 Case 4-5-B, a T-T-Q-T-Q-Q Platform

There are two variations of leg arrangements for Case 4-5-B as shown in Figs. 4.1(b) and 4.1(c). The formulations for both Cases 4-5-Ba and 4-5-Bb are the same as both of them contain two distinct skew-hexahedra which can be modeled by a closed-loop serial chain introduced in Section 2.3. The first two equations necessary for the analysis of both of these cases are obtained by using the closed-loop chain model and the third equation for both cases is obtained by construction. In terms of

mechanisms, the numbers of assembly configurations obtained from the analysis for both cases are the same.

The formulation of the first two equations for Cases 4-5-Ba and 4-5-Bb is presented in the following:

Three variables, θ_2 , θ_3 , and θ_4 are used to compute the locations of the top platform relative to the base as shown in Fig. 4.3. They are, respectively, the dihedral angles between ΔABA and the base, ΔABA and ΔaBb , ΔaBb and the top platform.

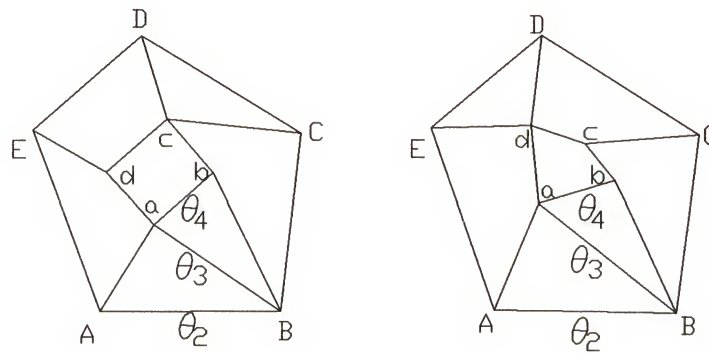


Fig. 4.3 Case 4-5-B Platform

In terms of solid geometry, each mechanism contains two skew-hexahedra which are shown in Fig. 4.4. An equation which gives the relationship among the three dihedral angles θ_2 , θ_3 , and θ_4 can be obtained for each of the two skew-hexahedra using the closed-loop chain model. These dihedral angles which will be used in the equations are defined as follows:

$$\begin{aligned}\theta_2 &= \theta_2' + 180^\circ, \\ \theta_3 &= 180^\circ + \theta_3', \\ \theta_4 &= 180^\circ + \theta_4',\end{aligned}\tag{4.1}$$

where the angles θ_2' , θ_3' , and θ_4' are designated in the skew-hexahedra as illustrated in Fig. 4.4.

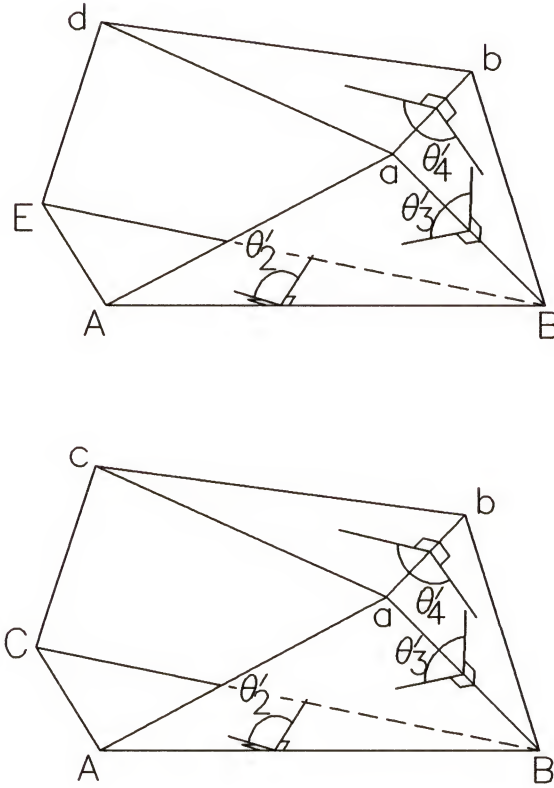


Fig. 4.4 Two Skew-Hexahedra of Cases 4-5-Ba and 4-5-Bb

As the definitions of the dihedral angles are different from those used in Section 2.3, a closed-loop chain with the joint angles (that is, the dihedral angles) defined in (4.1) is introduced. This closed-loop chain is illustrated in Fig. 4.5.

A vector loop equation for the closed loop chain can be expressed as

$$S_{11}^{(i)} \underline{S}_1^{(i)} + S_{22} \underline{S}_2 + S_{33} \underline{S}_3 - S_{44} \underline{S}_4 + S_{55}^{(i)} \underline{S}_5^{(i)} = \underline{\ell}_{ii} \underline{\ell}_i. \quad (4.2)$$

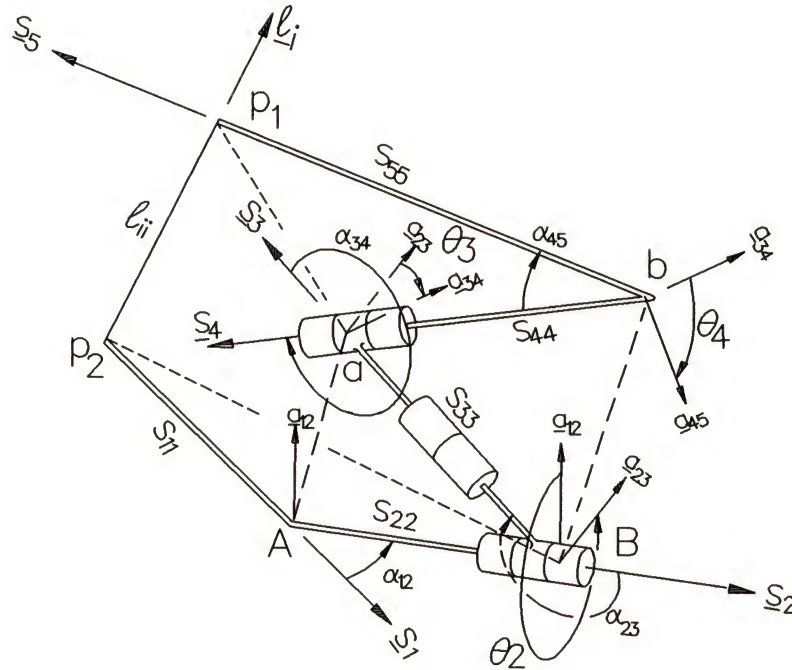


Fig. 4.5 A Closed Loop Chain

Taking self-scalar products for both sides of (4.2), and substituting the scalar products obtained from Table 2.13 in Duffy (1980), (4.2) can be expressed in the form

$$\begin{aligned}
 k^{(i)} + S_{11}^{(i)} S_{22} c_{12} + S_{11}^{(i)} S_{33} Z_2 - S_{11}^{(i)} S_{44} Z_{32} + S_{11}^{(i)} S_{55}^{(i)} Z_{432} \\
 + S_{22} S_{33} c_{23} - S_{22} S_{44} Z_3 + S_{22} S_{55}^{(i)} Z_{43} \\
 - S_{33} S_{44} c_{34} + S_{33} S_{55}^{(i)} Z_4 - S_{44} S_{55}^{(i)} c_{45} = 0,
 \end{aligned} \tag{4.3}$$

where

$$k^{(i)} = (S_{11}^{(i)2} + S_{22}^2 + S_{33}^2 + S_{44}^2 + S_{55}^{(i)2} - \ell_{ii}^2)/2. \tag{4.4}$$

The notation Z results in expressions that are linear in the sines and cosines of joint angles. Expanding c_2 , s_2 , c_4 , and s_4 in terms of the tan-half-angles $y = \tan(\theta_2/2)$ and $x = \tan(\theta_4/2)$, (4.3) can be expressed in the form

$$(a_i x^2 + b_i x + c_i) y^2 + (d_i x^2 + e_i x + f_i) y + g_i x^2 + h_i x + j_i = 0, \quad (4.5)$$

where

$$\begin{aligned} a_i &= a_{i0} c_3 + a_{i2}, & b_i &= b_{i1} s_3, & c_i &= c_{i0} c_3 + c_{i2}, \\ d_i &= d_{i1} s_3, & e_i &= e_{i0} c_3, & f_i &= f_{i1} s_3, \\ g_i &= g_{i0} c_3 + g_{i2}, & h_i &= h_{i1} s_3, & j_i &= j_{i0} c_3 + j_{i2}. \end{aligned}$$

Further, the expressions of the coefficients a_{i0} , a_{i2} , b_{i1} , c_{i0} , ..., j_{i2} are listed in Table 4.1.

These coefficients are different for the two equations ($i = 1$ and 2) because the knowns, S_{11} , S_{55} , ℓ_{11} , c_{12} , s_{12} , c_{45} , and s_{45} , in the coefficients have different definitions as follows:

For $i = 1$,

$$\begin{aligned} S_{11}^{(1)} &= EA, & S_{55}^{(1)} &= bd, & \ell_{11} &= Ed, \\ c_{12}^{(1)} &= -\cos(\angle EAB), & s_{12}^{(1)} &= (1 - c_{12}^{(1)2})^{1/2}, \\ c_{45}^{(1)} &= \cos(\angle abd), \text{ and} & s_{45}^{(1)} &= (1 - c_{45}^{(1)2})^{1/2}. \end{aligned}$$

For $i = 2$,

$$\begin{aligned} S_{11}^{(2)} &= CA, & S_{55}^{(2)} &= bc, & \ell_{22} &= Cc, \\ c_{12}^{(2)} &= -\cos(\angle CAB), & s_{12}^{(2)} &= (1 - c_{12}^{(2)2})^{1/2}, \\ c_{45}^{(2)} &= \cos(\angle abc), \text{ and} & s_{45}^{(2)} &= (1 - c_{45}^{(2)2})^{1/2}. \end{aligned}$$

The other knowns S_{22} , S_{33} , S_{44} , c_{23} , s_{23} , c_{34} , and s_{34} are the same for both $i = 1$ and 2 and they are given by

$$\begin{aligned} S_{22} &= AB, & S_{33} &= Ba, & S_{44} &= ab, \\ c_{23} &= -\cos(\angle ABa), & s_{23} &= -(1 - c_{23}^2)^{1/2}, \\ c_{34} &= \cos(\angle Bac), & s_{34} &= -(1 - c_{34}^2)^{1/2}. \end{aligned}$$

Whilst the first two equations contain all the three variables θ_2 , θ_3 , and θ_4 , the third equation contains θ_3 and θ_4 only. The derivations of the third equation for each of Cases 4-5-Ba and 4-5-Bb are presented in the following:

Case 4-5-Ba. It is assumed that AE and CD lie in a plane and are not parallel. The extension lines FD and FE in the base and the "virtual" leg Fc are added to the 4-5 Platform. (See Fig. 4.6.) The lengths of these lines can be determined by using a cosine law for a planar triangle.

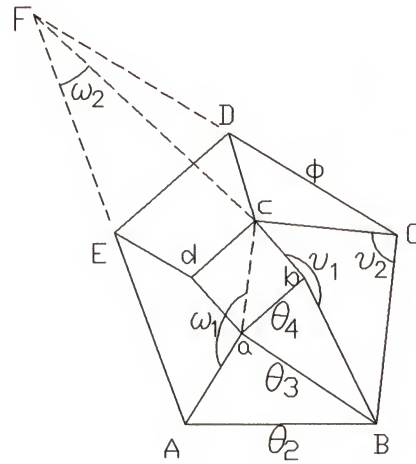


Fig. 4.6 Case 4-5-Ba Platform with Constructions

The relationship between the dihedral angles θ_3 and θ_4 can be obtained by using a model of the spherical four-bar linkage presented in Section 2.2. Consider vertex a to be a location of a spherical four-bar linkage. The four links, the output, coupler, input, and ground links are represented, respectively, by angles $\angle BaA$, $\angle caA$, $\angle cab$, and $\angle baB$. It should be noted that the coupler links, $\angle caA$ or ω_1 is a variable. The axes of the four joints are along aB, aA, ac, and ab. θ_3 denotes the output angle, and θ_4 denotes the input angle. Using (2.1), the relationship between these two

angle is given by

$$\xi_1 c_3 c_4 + \xi_2 c_3 + \xi_3 c_4 + \xi_4 s_4 s_3 + \xi_5 = -c_{12}, \quad (4.6)$$

where

$$\begin{aligned} \xi_1 &= s_{23} c_{34} s_{41}, & \xi_2 &= s_{23} s_{34} c_{41}, & \xi_3 &= s_{34} s_{41} c_{23}, \\ \xi_4 &= -s_{23} s_{41}, & \xi_5 &= -c_{23} c_{34} c_{41}. \end{aligned}$$

Further,

$$\begin{aligned} c_{12} &= \cos \omega_1, \\ c_{23} &= \cos(\angle BaA), & s_{23} &= (1 - c_{23})^{1/2}, \\ c_{34} &= \cos(\angle baB), & s_{34} &= (1 - c_{34})^{1/2}, \\ c_{41} &= \cos(\angle cab), & s_{41} &= (1 - c_{34})^{1/2}. \end{aligned}$$

Using the cosine law for the spherical triangle introduced in Section 2.4, the relationship between the angle ω_2 and the dihedral angle ϕ is given by

$$\cos \omega_2 = K_1 + K_2 \cos \phi, \quad (4.7)$$

where

$$\begin{aligned} K_1 &= \cos(\angle CFc) \cos(\angle CFE), \\ K_2 &= -\sin(\angle CFc) \sin(\angle CFE). \end{aligned}$$

The dihedral angle ϕ measures the elevation of the triangle ΔFcC relative to the base.

Applying (2.7) to the skew-quadrilateral $aAFc$, the relationship between ω_1 and ω_2 can be expressed in the form

$$\cos \omega_1 = K_3 + K_4 \cos \omega_2, \quad (4.8)$$

where

$$K_3 = \frac{Aa^2 + ac^2 - cF^2 - FA^2}{2 Aa ac} \quad \text{and} \quad K_4 = \frac{cF FA}{Aa ac}.$$

Substituting (4.8) in (4.7) gives

$$\cos \omega_1 = K_3 + K_1 K_4 + K_2 K_4 \cos \phi. \quad (4.9)$$

Now, applying the cosine law for the spherical triangle at vertex C, the relationship between v_2 and ϕ is given by

$$\cos v_2 = K_5 + K_6 \cos \phi, \quad (4.10)$$

where

$$K_5 = \cos(\angle DCc) \cos(\angle DCB),$$

$$K_6 = -\sin(\angle DCc) \sin(\angle DCB).$$

The relationship between v_1 and v_2 in the skew-quadrilateral bcCB is expressed as

$$\cos v_1 = K_7 + K_8 \cos v_2, \quad (4.11)$$

where

$$K_7 = \frac{bB^2 + bc^2 - BC^2 - cC^2}{2 bB bc} \quad \text{and} \quad K_8 = \frac{BC cC}{bB bc}.$$

Substituting (4.11) in (4.10) gives

$$\cos v_1 = K_7 + K_5 K_8 + K_6 K_8 \cos \phi. \quad (4.12)$$

The relationship between θ_4 and $\cos v_1$ can be obtained by using the cosine law for a spherical triangle and it is given by

$$\cos v_1 = K_9 + K_{10} c_4, \quad (4.13)$$

where

$$K_9 = \cos(\angle abc) \cos(\angle abB),$$

$$K_{10} = -\sin(\angle abc) \sin(\angle abB).$$

Substituting (4.13) in (4.12) and re-arranging gives

$$\cos\phi = m + nc_4, \quad (4.14)$$

where

$$m = (K_9 - K_7 - K_5K_8)/K_6/K_8,$$

$$n = K_{10}/K_6/K_8.$$

Substituting (4.14) in (4.9) gives

$$\cos\omega_1 = p + qc_4, \quad (4.15)$$

where

$$p = K_3 + K_1K_4 + K_2K_4m,$$

$$q = K_2K_4n.$$

Now, substituting right-handed side of (4.15) in (4.6) yields

$$\xi_1c_3c_4 + \xi_2c_3 + (\xi_3 + q)c_4 + \xi_4s_4s_3 + (\xi_5 + p) = 0. \quad (4.16)$$

By introducing the tan-half-angle relationships for θ_4 in (4.16):

$$c_4 = \frac{1 - x^2}{1 + x^2} \quad \text{and} \quad s_4 = \frac{2x}{1 + x^2}, \quad \text{where } x = \tan\left(\frac{\theta_4}{2}\right),$$

yields

$$g_3x^2 + h_3x + j_3 = 0, \quad (4.17)$$

where

$$g_3 = (\xi_2 - \xi_1)c_3 + (\xi_5 - \xi_3 + p - q),$$

$$h_3 = 2\xi_4s_3,$$

$$j_3 = (\xi_2 + \xi_1)c_3 + (\xi_5 + \xi_3 + p + q).$$

The coefficients of x in (4.17) depend linearly on the sines and cosines of θ_3 and the

dimensions of the platforms and the leg lengths of the mechanisms. It is interesting to note that the third equation (4.17) does not depend on leg length E_d .

Equation (4.17) together with the two equations in (4.5) are the three simultaneous equations which will be used to derived a polynomial equation in x [$x = \tan(\theta_4/2)$]. Section 4.3 presents the derivation and it shows that the polynomial is of 24th degree in x .

Table 4.1 Coefficients of Equation (4.5)

$a_{i0} = A + B + C + D + E$	$a_{i2} = F + G + H + I + J + K + L$
$b_{i1} = P + Q$	
$c_{i0} = A + B + C - D - E$	$c_{i2} = F + G + H + I - J - K - L$
$d_{i1} = M + N$	$e_{i0} = R$
	$f_{i1} = M - N$
$g_{i0} = -A + B - C - D + E$	$g_{i2} = F - G - H - I + J - K + L$
$h_{i1} = -P + Q$	
$j_{i0} = -A + B - C + D - E$	$j_{i2} = F - G - H - I - J + K - L$
$A = -c_{23}s_{12}s_{34}s_{11}s_{44}$	
$B = c_{12}s_{23}s_{34}s_{11}s_{44} + s_{23}s_{34}s_{22}s_{44} - c_{12}c_{45}s_{23}s_{34}s_{11}s_{55} - c_{45}s_{23}s_{34}s_{22}s_{55}$	
$C = c_{23}c_{45}s_{12}s_{34}s_{11}s_{55}$	$D = -c_{23}c_{34}s_{12}s_{45}s_{11}s_{55}$
$E = c_{12}c_{34}s_{23}s_{45}s_{11}s_{55} + c_{34}s_{23}s_{45}s_{22}s_{55}$	
$F = k + c_{12}s_{11}s_{22} + c_{12}c_{23}s_{11}s_{33} + c_{23}s_{22}s_{33} - c_{12}c_{23}c_{34}s_{11}s_{44} - c_{23}c_{34}s_{22}s_{44} - c_{34}s_{33}s_{44}$	
$+ c_{12}c_{23}c_{34}c_{45}s_{11}s_{55} + c_{23}c_{34}c_{45}s_{22}s_{55} + c_{34}c_{45}s_{33}s_{55} - c_{45}s_{44}s_{55}$	
$G = s_{12}s_{23}s_{11}s_{33}$	$H = -c_{34}s_{12}s_{23}s_{11}s_{44}$

$$\begin{aligned}
I &= c_{34}c_{45}s_{12}s_{23}s_{11}s_{55} & J &= c_{12}c_{23}s_{34}s_{45}s_{11}s_{55} + c_{23}s_{34}s_{45}s_{22}s_{55} \\
K &= s_{12}s_{23}s_{34}s_{45}s_{11}s_{55} & L &= s_{34}s_{45}s_{33}s_{55} \\
M &= -2s_{12}s_{34}s_{11}s_{44} + 2c_{45}s_{12}s_{34}s_{11}s_{55} & N &= -2c_{34}s_{12}s_{45}s_{11}s_{55} \\
P &= -2c_{23}s_{12}s_{45}s_{11}s_{55} & Q &= 2c_{12}s_{23}s_{45}s_{11}s_{55} + 2s_{23}s_{45}s_{22}s_{55} \\
R &= 4s_{12}s_{45}s_{11}s_{55}
\end{aligned}$$

Case 4-5-Bb. The third equation for Case 4-5-Bb is obtained by using the following construction: assuming that the top and the base platforms are both planar and the edges ab and dc in the top and the edges BC and ED in the base are not parallel, then the extension lines be , ce , CF , and DF can be found, and the "virtual" legs, eB and dF can be determined by using cosine law for a planar triangle. Figure 4.7 shows the resulting Case 4-5-Bb Platform after the construction.

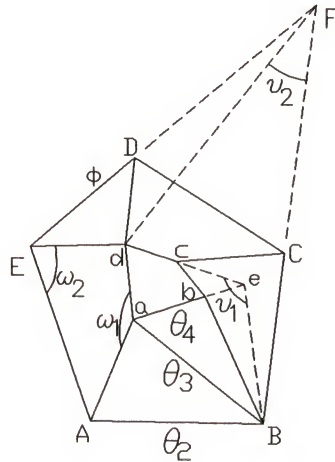


Fig. 4.7 Construction for Case 4-5-Bb Platform

Comparing the two cases shown in Figs. 4.6 and 4.7, it can be seen that both Cases 4-5-Ba and 4-5-Bb with the construction are the same geometrically. The base

of Case 4-5-Bb defined by the vertices A, B, F, E correspond, respectively, to the vertices A, B, C, F of Case 4-5-Ba. Similarly, the top platform of Case 4-5-Bb defined by the vertices a, e, d correspond, respectively, to the vertices a, b, c of Case 4-5-Ba. Finally, the legs Aa, Ba, Be, Fd, and Ed in Case 4-5-Bb correspond, respectively, to the legs Aa, Ba, Bb, Cc, and Fc in Case 4-5-Ba. (It should be noted that leg Ed in Case 4-5-Ba and leg Cc in Case 4-5-Bb are redundant in the derivations of the third equation.) Therefore, the third equation for Case 4-5-Bb can be obtained by using the same procedure as that for Case 4-5-Ba.

While the analysis for Case 4-5-Bb presented above is rather complicated, there is another approach which is much simpler and does not need to use the closed-loop chain model. By using construction as illustrated in Fig. 4.8, Case 4-5-Bb can be modeled by a Case 4-4-C Platform. Comparing the "virtual" Case 4-4-C with Case 4-4-C, the vertices F, B, C, and D in Fig. 4.8 correspond, respectively, to the vertices C, B, A, and D in Fig. 3.7. Also, the legs, Fa, Ba, Bb, Cc, Dd, and Fd in Fig. 4.8. correspond, respectively, to the legs Cc, Bc, Be, Aa, Dd, and Cd in Fig. 3.7. The legs Aa and Ed in Fig. 4.8 are redundant.

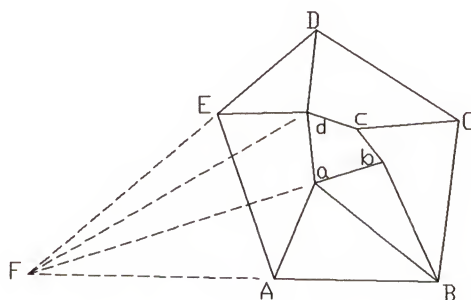


Fig. 4.8 A "Virtual" Case 4-4-C Platform of Case 4-5-Bb

4.2.3 Case 4-5-C, a T-T-T-Q-Q-Q Platform

Case 4-5-C has the feature that the top platform is connected to the base by two triangles in serial fashion. Three variables, θ_2 , θ_3 , and θ_4 are used to compute the locations of the top platform relative to the base as shown in Fig. 4.9. The variable - θ_2 is the dihedral angle which measures the elevation of the triangular face ΔABa relative to the base, θ_3 is the dihedral angle between ΔABa and ΔaBb , and θ_4 is the dihedral angle between ΔaBb

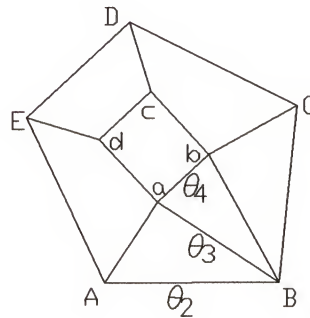


Fig. 4.9 Case 4-5-C Platform

In terms of solid geometry, the mechanism contains two skew-hexahedra which are illustrated in Fig. 2.2.

Two of the necessary three equations for the analysis contain all the three dihedral angles θ_2 , θ_3 , and θ_4 , and the third one contains θ_2 and θ_3 only. The dihedral angles are designated as shown in Fig. 4.10. All the three equations are obtained by using a serial chain which models the skew-hexahedra. The derivation of the equations is detailed in Section 2.3. Equation 2.5 which results from a vector loop equation for the closed-loop chain is again expressed as follows:

$$\begin{aligned}
k^{(i)} + S_{11}^{(i)}S_{22}c_{12} + S_{11}^{(i)}S_{33}Z_2 + S_{11}^{(i)}S_{44}Z_{32} + S_{11}^{(i)}S_{55}^{(i)}Z_{432}^{(i)} \\
+ S_{22}S_{33}c_{23} + S_{22}S_{44}Z_3 + S_{22}S_{55}^{(i)}Z_{43}^{(i)} + S_{33}S_{44}c_{34} \\
+ S_{33}S_{55}^{(i)}Z_4^{(i)} + S_{44}S_{55}^{(i)}c_{45}^{(i)} = 0,
\end{aligned} \tag{4.18}$$

where

$$k^{(i)} = (S_{11}^{(i)2} + S_{22}^2 + S_{33}^2 + S_{44}^2 + S_{55}^{(i)2} - \ell_{ii}^2)/2.$$

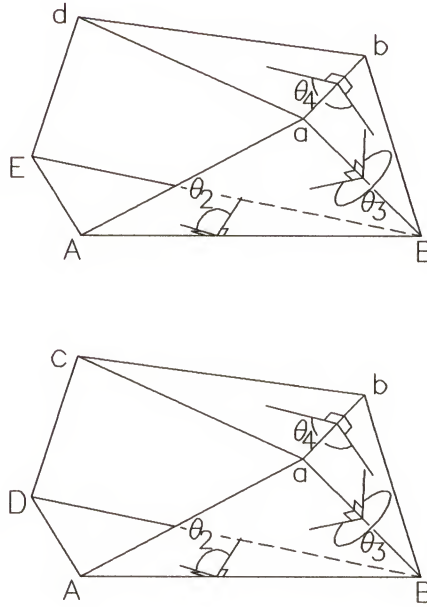


Fig. 4.10 Two Skew-Hexahedra of Case 4-5-C

Two equations, for $i = 1$ and 2 , are derived for the first and second skew-hexahedra respectively.

The sines and cosines of the joint angles or dihedral angles in (4.18) can be expressed in terms of the tan-half-angles where $x = \tan(\theta_3/2)$, $y = \tan(\theta_4/2)$, and $z = \tan(\theta_2/2)$. Introducing these tan-half-angles and re-grouping terms, (4.18) becomes

$$(a_i x^2 + b_i x + c_i) y^2 + (d_i x^2 + e_i x + f_i) y + g_i x^2 + h_i x + j_i = 0, \quad (4.19)$$

where the nine coefficients which are expressed in terms of the variable z as follows:

$$a_i = z^2(a_{i2} - a_{i0}) + a_{i0} + a_{i2},$$

$$b_i = 2b_{i1}z,$$

$$c_i = z^2(c_{i2} - c_{i0}) + c_{i0} + c_{i2},$$

$$d_i = 2d_{i1}z,$$

$$e_i = z^2(e_{i2} - e_{i0}) + e_{i0} + e_{i2},$$

$$f_i = 2f_{i1}z,$$

$$g_i = z^2(g_{i2} - g_{i0}) + g_{i0} + g_{i2},$$

$$h_i = 2h_{i1}z,$$

$$j_i = z^2(j_{i2} - j_{i0}) + j_{i0} + j_{i2}, \text{ and}$$

$i = 1$ and 2 .

Further, the expressions of the coefficients a_{i0} , a_{i2} , b_{i1} , c_{i0} , ..., j_{i2} of z are listed in Table 2.1. It should be noted that S_{11} , S_{55} , ℓ_{ii} , c_{12} , s_{12} , c_{45} , and s_{45} in the expressions of the coefficients are different for the three equations and they are distinguished by using the superscribe (i) as follows:

For $i = 1$,

$$\begin{aligned} S_{11}^{(1)} &= EA, & S_{55}^{(1)} &= bd, & \ell_{11} &= dE, \\ c_{12}^{(1)} &= -\cos(\angle EAB), & s_{12}^{(1)} &= (1 - c_{12}^{(1)2})^{1/2}, \\ c_{45}^{(1)} &= -\cos(\angle abd), \text{ and } & s_{45}^{(1)} &= (1 - c_{45}^{(1)2})^{1/2}. \end{aligned} \quad (4.20)$$

For $i = 2$,

$$S_{11}^{(2)} = DA, \quad S_{55}^{(2)} = bc, \quad \ell_{22} = cD,$$

$$\begin{aligned} c_{12}^{(2)} &= -\cos(\angle DAB), & s_{12}^{(2)} &= (1 - c_{12}^{(1)2})^{1/2}, \\ c_{45}^{(2)} &= -\cos(\angle abc), \text{ and } & s_{45}^{(2)} &= (1 - c_{45}^{(1)2})^{1/2}. \end{aligned} \quad (4.21)$$

The third equation ($i = 3$) is derived from (4.18) with $S_{55}^{(3)} = 0$. It is a function of the dihedral angles θ_2 and θ_3 only. It can be expressed in the tan-half-angles of these angles as follows,

$$g_3 x^2 + h_3 x + j_3 = 0, \quad (4.22)$$

where

$$g_3 = z^2(g_{12} - g_{10}) + g_{10} + g_{12},$$

$$h_3 = 2h_{11}z,$$

$$j_3 = z^2(j_{12} - j_{10}) + j_{10} + j_{12}.$$

Further, the expressions of the coefficients g_{10} , g_{12} , h_{11} , j_{10} , and j_{12} of z can be found in Table 2.1. The knowns, S_{11} , S_{55} , ℓ_{33} , c_{12} , and s_{12} in the coefficients are given by

$$S_{11}^{(3)} = CA, \quad S_{55}^{(3)} = 0, \quad \ell_{33} = bC,$$

$$c_{12}^{(3)} = -\cos(\angle CAB), \text{ and } s_{12}^{(3)} = (1 - c_{12}^{(3)2})^{1/2}.$$

The three variables in the three simultaneous equations in (4.19) and (4.22) are the dihedral angles in the three distinct skew-polyhedra. If the base of the In-parallel Platform is nonplanar. Then the dihedral angle θ_2 defined in one equation will not be the same as in the others. Similarly, if the top platform is nonplanar, the dihedral angle θ_4 in one equation will not be the same as in the others. Therefore, for a mechanism with nonplanar top and base platforms, the variables y and z in the three equations should be changed and the coefficients are adjusted accordingly. An example of a case with nonplanar base will be presented in Section 4.4.2.

The two equations in (4.19) together with (4.22) are the three equations which are used for deriving a polynomial equation in z by an elimination method described in the following section.

4.3 The Eliminants of the Equation Sets

Since Case 4-5-A is analyzed by using the solution for Case 4-4-B Platform, the elimination for that case can be found in Section 3.3.2 and will not be repeated here. The formulation of the forward analysis for Cases 4-5-B and 4-5-C reduces to the following equation set

$$(a_1x^2 + b_1x + c_1)y^2 + (d_1x^2 + e_1x + f_1)y + g_1x^2 + h_1x + j_1 = 0 \quad (4.23a)$$

$$(a_2x^2 + b_2x + c_2)y^2 + (d_2x^2 + e_2x + f_2)y + g_2x^2 + h_2x + j_2 = 0 \quad (4.23b)$$

$$g_3x^2 + h_3x + j_3 = 0 \quad (4.23c)$$

where for Cases 4-5-Ba and 4-5-Bb, the coefficients of x and y are linear in sines and cosines of θ_3 , and for Case 4-5-C, the coefficients are quadratic in z .

In order to solve the equation set, x and y are first algebraically eliminated by the Sylvester's dialytic method (Salmom 1885, pp. 79). The elimination of the two unknowns is presented in the following.

The two unknowns x and y can be eliminated in a single operation by generating thirteen extra equations from the three equations in (4.23) as follows:

To each of the three equations, multiply x , y , and xy to generate nine extra equations. Then, multiply the third equation (4.23c) by xy^2 , xy^3 , y^2 , and y^3 to generate another four extra equations. Therefore, together with the three original equations,

a total of sixteen equation are derived and they can be written in the matrix form:

$$M \underline{r} = \underline{0}, \quad (4.24)$$

where

$$\underline{r} = [x^3 y^3 \ x^2 y^3 \ xy^3 \ y^3 \ x^3 y^2 \ x^2 y^2 \ xy^2 \ y^2 \ x^2 y \ xy \ y \ x^2 \ x \ 1]^T,$$

and the 16×16 matrix M is given by

$$M = \begin{bmatrix} 0 & 0 & 0 & 0 & 0 & 0 & 0 & 0 & a_i & b_i & c_i & d_i & e_i & f_i & g_i & h_i & j_i \\ 0 & 0 & 0 & 0 & a_i & d_i & g_i & b_i & c_i & 0 & e_i & f_i & 0 & h_i & j_i & 0 & 0 \\ 0 & a_i & b_i & c_i & 0 & 0 & 0 & d_i & e_i & f_i & g_i & h_i & j_i & 0 & 0 & 0 & 0 \\ a_i & b_i & c_i & 0 & d_i & g_i & 0 & e_i & f_i & 0 & h_i & j_i & 0 & 0 & 0 & 0 & 0 \\ 0 & 0 & 0 & 0 & g_3 & 0 & 0 & h_3 & j_3 & 0 & 0 & 0 & 0 & 0 & 0 & 0 & 0 \\ g_3 & h_3 & j_3 & 0 & 0 & 0 & 0 & 0 & 0 & 0 & 0 & 0 & 0 & 0 & 0 & 0 & 0 \\ 0 & 0 & 0 & 0 & 0 & 0 & 0 & g_3 & h_3 & j_3 & 0 & 0 & 0 & 0 & 0 & 0 & 0 \\ 0 & g_3 & h_3 & j_3 & 0 & 0 & 0 & 0 & 0 & 0 & 0 & 0 & 0 & 0 & 0 & 0 & 0 \\ 0 & 0 & 0 & 0 & 0 & 0 & g_3 & 0 & 0 & 0 & 0 & 0 & 0 & 0 & h_3 & j_3 & 0 \\ 0 & 0 & 0 & 0 & 0 & 0 & 0 & 0 & 0 & 0 & g_3 & h_3 & j_3 & 0 & 0 & 0 & 0 \\ 0 & 0 & 0 & 0 & 0 & g_3 & 0 & 0 & 0 & 0 & h_3 & j_3 & 0 & 0 & 0 & 0 & 0 \\ 0 & 0 & 0 & 0 & 0 & 0 & 0 & 0 & 0 & 0 & 0 & 0 & 0 & g_3 & h_3 & j_3 & 0 \end{bmatrix},$$

where, $i = 1$ and 2 .

The equation set (4.24) can be satisfied if, and only if, the following condition holds:

$$\text{determinant}(M) = 0. \quad (4.25)$$

Equation (4.25) represents the condition under which the three equations (4.23) have a common solution for x and y . The left hand side of (4.25) is then the eliminant of the system of equations (4.23).

For Case 4-5-B, every entry of the 16×16 matrix M is linear either in cosine or sine of θ_3 . Hence a straight expansion of the eliminant will result in an expression in the form

$$\sum_{\substack{i=0,16 \\ j=0,16 \\ i+j \leq 16}} C_{ij} s_3^i c_3^j = 0, \quad (4.26)$$

where C_{ij} are known and which depend only on the dimensions of the mechanisms. If now the sines and cosines of θ_3 in (4.26) are substituted by the tan-half-angles $z = \tan(\theta_3/2)$, a 32nd degree polynomial equation in z will be produced. However, in a numerical example which will be presented in Section 4.4.1, (4.26) can be expressed in a 24th degree polynomial equation in z by substituting the identities

$$s_3^i \equiv (1 - c_3^2)^v s_3^u, \quad (4.27)$$

where

$$1 \leq i \leq 16,$$

v = quotient of i divided by 2, and

u = remainder of i divided by 2.

This yields

$$\sum_{\substack{i=0,1 \\ j=0,12 \\ i+j \leq 12}} C_{ij} s_3^i c_3^j = 0. \quad (4.28)$$

Specifically, C_{ij} ($i=0,1$; $j=13, 14, 15$, and 16 ; and $13 \leq i+j \leq 16$) are set to zeroes because they are negligible comparing to the other coefficients. Now, by introducing the tan-half-angle relationships for θ_3 :

$$c_3 = \frac{1 - z^2}{1 + z^2} \quad \text{and} \quad s_3 = \frac{2z}{1 + z^2}, \quad \text{where } z = \tan\left(\frac{\theta_3}{2}\right)$$

Equation (4.28) can be expressed in a polynomial equation of degree 24.

Several sets of dimensions of the mechanism have been used to test this method, it was found that (4.26) can always be reduced to a 24th degree polynomial equation by the substitutions. It is believed that by substituting the identities (4.27) in (4.26), as many as eight extraneous roots in z are eliminated. Therefore, there are 24 solutions for z and a corresponding 24 pairs of solutions for x and y .

For Case 4-5-C, the entries of the matrix M are either linear or quadratic in z . It follows that the expansion of the eliminant will be a polynomial of degree not higher than 32. In the next section, it will show that the expansion indeed results in a polynomial equation of degree 32 in z and no extraneous roots have been introduced in the elimination procedure. As the result, that there are 32 solutions for z and a corresponding 32 pairs of solutions for x and y .

When z is obtained from the polynomial equation, every entry of the matrix M has a definite numerical value. Then, the pair of variables x and y can be determined from (4.24) as follows:

Reducing the dimension of the matrix M to a 15×15 matrix by deleting the first row and the sixteenth column of matrix M , the set of 16 equations in the form of (4.24) becomes a set of 15 equations which are expressed in the form:

$$N \underline{s} = \underline{m}, \quad (4.29)$$

where

$$N = \begin{bmatrix} 0 & 0 & 0 & 0 & 0 & 0 & 0 & 0 & a_2 & b_2 & c_2 & d_2 & e_2 & f_2 & g_2 & h_2 \\ 0 & 0 & 0 & 0 & a_i & d_i & g_i & b_i & c_i & 0 & e_i & f_i & 0 & h_i & j_i \\ 0 & a_i & b_i & c_i & 0 & 0 & 0 & d_i & e_i & f_i & g_i & h_i & j_i & 0 & 0 \\ a_i & b_i & c_i & 0 & d_i & g_i & 0 & e_i & f_i & 0 & h_i & j_i & 0 & 0 & 0 \\ 0 & 0 & 0 & 0 & g_3 & 0 & 0 & h_3 & j_3 & 0 & 0 & 0 & 0 & 0 & 0 \\ g_3 & h_3 & j_3 & 0 & 0 & 0 & 0 & 0 & 0 & 0 & 0 & 0 & 0 & 0 & 0 \\ 0 & 0 & 0 & 0 & 0 & 0 & 0 & g_3 & h_3 & j_3 & 0 & 0 & 0 & 0 & 0 \\ 0 & g_3 & h_3 & j_3 & 0 & 0 & 0 & 0 & 0 & 0 & 0 & 0 & 0 & 0 & 0 \\ 0 & 0 & 0 & 0 & 0 & 0 & g_3 & 0 & 0 & 0 & 0 & 0 & 0 & h_3 & j_3 \\ 0 & 0 & 0 & 0 & 0 & 0 & 0 & 0 & 0 & 0 & g_3 & h_3 & j_3 & 0 & 0 \\ 0 & 0 & 0 & 0 & 0 & g_3 & 0 & 0 & 0 & 0 & h_3 & j_3 & 0 & 0 & 0 \\ 0 & 0 & 0 & 0 & 0 & 0 & 0 & 0 & 0 & 0 & 0 & 0 & 0 & g_3 & h_3 \end{bmatrix},$$

(i = 1 and 2),

$$\underline{s} = [x^3 y^3 \ x^2 y^3 \ xy^3 \ y^3 \ x^3 y^2 \ x^3 y \ x^3 \ x^2 y^2 \ xy^2 \ y^2 \ x^2 y \ xy \ y \ x^2 \ x]^\tau,$$

and,

$$\underline{m} = [j_2 \ 0 \ 0 \ 0 \ 0 \ 0 \ 0 \ 0 \ 0 \ 0 \ 0 \ 0 \ 0 \ 0 \ 0 \ j_3]^\tau.$$

The solutions of x and y can be obtained from \underline{s} which is given by

$$\underline{s} = N^{-1} \underline{m}. \quad (4.30)$$

4.4 Numerical Verifications

The eliminants derived for each of Cases 4-5-B and 4-5-C are determinants of square matrices of dimension 16. The entries of these matrices are symbolic.

Specifically, the eliminant of Case 4-5-B consists of entries which are functions of c_3 and s_3 , and the eliminant of Case 4-5-C consists functions of z . Therefore, the expansion of the determinants of the symbolic matrices of such large sizes is a laborious task. To facilitate the expansion, a symbolic software package called *Mathematica* (Wolfram, 1989) was employed. Also, the Laplace's Expansion method (Howard, 1966) was applied to speed up the computation. This method is described in the following section.

A 24th and 32th degree polynomial equations were obtained respectively from the eliminants for Cases 4-5-B and 4-5-C. In the following sections, a numerical example is presented for each case to verify the analysis. All the solutions were verified by the reverse displacement analysis that the distances between points connects by the legs equal the corresponding leg lengths.

4.4.1 Case 4-5-Ba

The dimensions of the top and base platforms were defined by the following coordinates of the vertices (see Fig. 4.6) in two reference systems for the top and base platforms:

a (0, 0, 0),	A (0, 0, 0),
b (2, 0, 0),	B (12, 0, 0),
c (4, 4, 0),	C (20, 10, 0),
d (-2, 4, 0),	D (10, 20, 0),
	E (0, 14, 0).

The leg lengths were as follows:

$$\begin{aligned} Aa &= 15.16575, & Cb &= 13.78405, \\ Ba &= 14.35270, & Dc &= 12.24745, \\ Bb &= 15.68439, & Dd &= 16.43168. \end{aligned}$$

With the above dimensions of the mechanisms, the coefficients of the three equations (4.23) were determined by using the formulation presented in Section (4.2.2). The coefficients are listed in Table 4.2.

Table 4.2 Coefficients of (4.23) for Case 4-5-Ba

$a_1 = 0.0347c_3 - 0.5010$	$b_1 = -0.2920s_3$	$c_1 = -0.1484c_3 - 0.6064$
$d_1 = 0.1524s_3$	$e_1 = 1.2833c_3$	$f_1 = -0.6523s_3$
$g_1 = 0.0878c_3 + 1.0000$	$h_1 = -0.7391s_3$	$j_1 = -0.3757c_3 + 1.8317$
$a_2 = -0.2336c_3 + 0.0255$	$b_2 = 0.3323s_3$	$c_2 = -0.0252c_3 + 0.2085$
$d_2 = 0.4254s_3$	$e_2 = 0.6051c_3$	$f_2 = 0.0460s_3$
$g_2 = -0.0854c_3 + 1.0000$	$h_2 = 0.1215s_3$	$j_2 = -0.0092c_3 + 1.6248$
$g_3 = 1.0000c_3 - 0.4581$	$h_3 = -1.4224s_3$	$j_3 = 0.1080c_3 - 1.8125$

The coefficients in Table 4.2 were used as the entries of the 16×16 matrix M in (4.25). By using the *Mathematica* on an IBM PS/2 Model 80, which was the fastest computer available for the software, a straight calculation of the determinant of this matrix was unsuccessful. Therefore, the Laplace's Expansion method was used to expand the determinant of the matrix into many determinants of smaller sizes so that they were able to be obtained by the *Mathematica*.

The Laplace's Expansion Theorem (Howard, 1966) is stated as follows:

Select any m rows(columns) from matrix $M_{n \times n}$ and form all the m -rowed minors of M found in these m rows(columns). Then $|M|$ is equal to the sum of the products of each of these minors and its algebraic complement, or cofactor.

The above theorem is applied for the expansion of the eliminant $|M|$ in the following procedure:

First, interchanging the rows of M and partitioning, the eliminant is expressed as

$$|M| = |P Q|, \quad (4.31)$$

where

$$P = \begin{bmatrix} a_1 & b_1 & c_1 & 0 \\ a_2 & b_2 & c_2 & 0 \\ g_3 & h_3 & j_3 & 0 \\ 0 & a_1 & b_1 & c_1 \\ 0 & a_2 & b_2 & c_2 \\ 0 & g_3 & h_3 & j_3 \\ 0 & 0 & 0 & 0 \\ 0 & 0 & 0 & 0 \\ 0 & 0 & 0 & 0 \\ 0 & 0 & 0 & 0 \\ 0 & 0 & 0 & 0 \\ 0 & 0 & 0 & 0 \\ 0 & 0 & 0 & 0 \\ 0 & 0 & 0 & 0 \\ 0 & 0 & 0 & 0 \end{bmatrix}, \quad Q = \begin{bmatrix} d_1 & g_1 & 0 & e_1 & f_1 & 0 & h_1 & j_1 & 0 & 0 & 0 & 0 \\ d_2 & g_2 & 0 & e_2 & f_2 & 0 & h_2 & j_2 & 0 & 0 & 0 & 0 \\ 0 & 0 & 0 & 0 & 0 & 0 & 0 & 0 & 0 & 0 & 0 & 0 \\ 0 & 0 & 0 & d_1 & e_1 & f_1 & g_1 & h_1 & j_1 & 0 & 0 & 0 \\ 0 & 0 & 0 & d_2 & e_2 & f_2 & g_2 & h_2 & j_2 & 0 & 0 & 0 \\ 0 & 0 & 0 & 0 & 0 & 0 & 0 & 0 & 0 & 0 & 0 & 0 \\ a_1 & d_1 & g_1 & b_1 & c_1 & 0 & e_1 & f_1 & 0 & h_1 & j_1 & 0 \\ a_2 & d_2 & g_2 & b_2 & c_2 & 0 & e_2 & f_2 & 0 & h_2 & j_2 & 0 \\ g_3 & 0 & 0 & h_3 & j_3 & 0 & 0 & 0 & 0 & 0 & 0 & 0 \\ 0 & g_3 & 0 & 0 & 0 & 0 & h_3 & j_3 & 0 & 0 & 0 & 0 \\ 0 & 0 & g_3 & 0 & 0 & 0 & 0 & 0 & 0 & h_3 & j_3 & 0 \\ 0 & 0 & 0 & a_1 & b_1 & c_1 & d_1 & e_1 & f_1 & g_1 & h_1 & j_1 \\ 0 & 0 & 0 & a_2 & b_2 & c_2 & d_2 & e_2 & f_2 & g_2 & h_2 & j_2 \\ 0 & 0 & 0 & g_3 & h_3 & j_3 & 0 & 0 & 0 & 0 & 0 & 0 \\ 0 & 0 & 0 & 0 & 0 & 0 & g_3 & h_3 & j_3 & 0 & 0 & 0 \\ 0 & 0 & 0 & 0 & 0 & 0 & 0 & 0 & 0 & g_3 & h_3 & j_3 \end{bmatrix}.$$

Then, forming all the four-rowed minors found in P of matrix M , and neglecting those which contains row of zeros, $C_4^6 = 15$ minors can be found. Of these 15 minors, nine of their cofactors contain rows of zeros. It follows that there are only six products of minors and their cofactors which are not equal to zero. The following are the six minors $|P_i|$ ($i = 1, 2, \dots, 6$ and P_i is a 4×4 matrix.) together with their corresponding cofactors $|Q_i|$ ($i = 1, 2, \dots, 6$, and Q_i is a 12×12 matrix):

$$|P_1| = |\text{row}[1, 2, 3, \text{ and } 6] \text{ of } P|,$$

$$|Q_1| = |\text{row}[4, 5, 7, \dots, \text{ and } 16] \text{ of } Q|,$$

$$|P_2| = |\text{row}[1, 3, 4, \text{ and } 6] \text{ of } P|,$$

$$|Q_2| = |\text{row}[2, 5, 7, \dots, \text{ and } 16] \text{ of } Q|,$$

$$|P_3| = |\text{row}[1, 3, 5, \text{ and } 6] \text{ of } P|,$$

$$|Q_3| = - |\text{row}[2, 4, 7, \dots, \text{ and } 16] \text{ of } Q|,$$

$$|P_4| = |\text{row}[2, 3, 4, \text{ and } 6] \text{ of } P|,$$

$$|Q_4| = - |\text{row}[1, 5, 7, \dots, \text{ and } 16] \text{ of } Q|,$$

$$|P_5| = |\text{row}[2, 3, 5, \text{ and } 6] \text{ of } P|,$$

$$|Q_5| = |\text{row}[1, 4, 7, \dots, \text{ and } 16] \text{ of } Q|,$$

$$|P_6| = |\text{row}[3, 4, 5, \text{ and } 6] \text{ of } P|,$$

$$|Q_6| = |\text{row}[1, 2, 7, \dots, \text{ and } 16] \text{ of } Q|,$$

where $|\text{row}[i, j, k, \dots \text{ and } p] \text{ of } N|$ = the determinant of a matrix which consists of row i, j, k, \dots , and p of the matrix N .

By using the Laplace's Expansion Theorem, the determinant of M is given by

$$|M| = \sum_{i=1}^6 |P_i| |Q_i|, \quad (4.32)$$

where P_i is a 4×4 matrix and Q_i is a 12×12 matrix. The determinant of each of these matrices of these sizes was able to be obtained by using the *Mathematica*.

Substituting the entries listed in Table 4.2 in (4.32), an expression in the form of (4.26) was obtained. Then, introducing the identities (4.27) in that expression and expanding yields

$$\begin{aligned} & 2.23591 \times 10^{-17} c_3^{16} - 2.77635 \times 10^{-17} c_3^{15} - 3.06255 \times 10^{-15} c_3^{14} + 6.57518 \times 10^{-14} c_3^{13} \\ & + c_3^{12} + 0.18623 c_3^{11} - 16.94912 c_3^{10} - 31.19358 c_3^9 + 117.88777 c_3^8 \\ & + 285.95239 c_3^7 - 94.30702 c_3^6 - 848.06232 c_3^5 - 854.91994 c_3^4 \\ & - 195.47726 c_3^3 + 141.26847 c_3^2 + 72.67142 c_3 - 20.27043 = 0. \end{aligned} \quad (4.33)$$

Equation (4.33) shows that the values of the coefficients of c_3^i for $13 \leq i \leq 16$ are negligible compared to the other coefficients. Setting the terms of c_3^i for $13 \leq i \leq 16$ equal to zero, and expanding c_3 in term of the tan-half-angle, $z = \tan(\theta_3/2)$, (4.33) can be expressed in the polynomial equation

$$\begin{aligned} & z^{24} - 10.96713 z^{22} - 34.74052 z^{20} - 121.42994 z^{18} - 187.44728 z^{16} \\ & - 905.84820 z^{14} - 2854.56759 z^{12} - 2359.51509 z^{10} + 2908.71337 z^8 \\ & + 3712.64283 z^6 + 517.42517 z^4 - 521.68261 z^2 - 143.58301 = 0. \end{aligned} \quad (4.34)$$

Equation (4.34) has the following 24 roots:

$$\begin{aligned} z = & \pm 0.75992, \pm 0.73447, (\pm i 0.69299), (\pm i 5.37977), (1.24272 \pm i 0.85340), \\ & (-1.24272 \pm i 0.85340), (0.84108 \pm i 1.50709), (-0.84108 \pm i 1.50709), \\ & (0.00602 \pm i 0.69688), (-0.00602 \pm i 0.69688), (0.26487 \pm i 1.28602), \text{ and} \\ & (-0.26487 \pm i 1.28602). \end{aligned}$$

For each value of z , a pair of values x and y were obtained by using (4.30). It has been verified that every solution set satisfies the equation system (4.23). Using these solutions, the locations of the top platform were determined in a reference system whose origin is at A. (See Fig. 4.6.) B lies on the x -axis, and E is in the x - y plane. Table 4.3 shows the coordinates of the vertices a, b, c, and d. For the dimensions given in this example, four real and 20 complex assembly configurations were found. It has been verified by a reverse displacement analysis that all the 24 solutions reproduced the correct edge length with at least 12 digit accuracy.

Table 4.3 Coordinates of the Vertices of the Top Platform of Case 4-5-Ba

	<u>Solution 1</u>	<u>Solution 2</u>
a	(7.0000e+00, 8.8064e+00, 1.0171e+01)	(7.0000e+00, 8.8064e+00, -1.0171e+01)
b	(6.9543e+00, 1.0806e+01, 1.0187e+01)	(6.9543e+00, 1.0806e+01, -1.0187e+01)
c	(1.0899e+01, 1.2899e+01, 9.9380e+00)	(1.0899e+01, 1.2899e+01, -9.9380e+00)
d	(1.1036e+01, 6.9004e+00, 9.8897e+00)	(1.1036e+01, 6.9004e+00, -9.8897e+00)
	<u>Solution 3</u>	<u>Solution 4</u>
a	(7.0000e+00, 9.0000e+00, 1.0000e+01)	(7.0000e+00, 9.0000e+00, -1.0000e+01)
b	(7.0000e+00, 1.1000e+01, 1.0000e+01)	(7.0000e+00, 1.1000e+01, -1.0000e+01)
c	(1.1000e+01, 1.3000e+01, 1.0000e+01)	(1.1000e+01, 1.3000e+01, -1.0000e+01)
d	(1.1000e+01, 7.0000e+00, 1.0000e+01)	(1.1000e+01, 7.0000e+00, -1.0000e+01)
	<u>Solution 5</u>	
a	(7.0000e+00 - i1.1752e-32, 1.6621e+01 - i2.3915e-15, 4.0726e-15 + i9.7600e+00)	
b	(1.0722e+01 - i4.7709e-16, 1.6969e+01 - i1.4423e-15, 3.6150e-15 + i6.6018e+00)	
c	(2.3711e+01 - i6.1600e-15, 2.5711e+01 + i8.0464e-16, 4.5689e-18 - i8.4026e+00)	
d	(1.2545e+01 - i3.2742e-15, 2.4667e+01 - i1.0797e-15, 3.1978e-15 + i1.0723e+00)	
	<u>Solution 6</u>	
a	(7.0000e+00 + i1.1752e-32, 1.6621e+01 + i2.3915e-15, 4.0726e-15 - i9.7600e+00)	
b	(1.0722e+01 + i4.7709e-16, 1.6969e+01 + i1.4423e-15, 3.6150e-15 - i6.6018e+00)	
c	(2.3711e+01 + i6.1600e-15, 2.5711e+01 - i8.0464e-16, 4.5689e-18 + i8.4026e+00)	
d	(1.2545e+01 + i3.2742e-15, 2.4667e+01 + i1.0797e-15, 3.1978e-15 - i1.0723e+00)	
	<u>Solution 7</u>	
a	(7.0000e+00 - i3.0085e-30, -2.4983e+02 + i3.0563e-14, -3.0608e-14 - i2.4947e+02)	
b	(4.9982e+00 + i1.3779e-16, -2.7198e+02 + i3.9912e-14, -3.9969e-14 - i2.7162e+02)	
c	(6.9900e+01 - i1.0871e-14, 7.1900e+01 - i1.5642e-13, 1.5502e-13 + i7.8305e+01)	
d	(7.5905e+01 - i1.9978e-14, 1.3836e+02 - i2.3238e-13, 2.3179e-13 + i1.4477e+02)	
	<u>Solution 8</u>	
a	(7.0000e+00 + i3.0085e-30, -2.4983e+02 - i3.0563e-14, -3.0608e-14 + i2.4947e+02)	
b	(4.9982e+00 - i1.3779e-16, -2.7198e+02 - i3.9912e-14, -3.9969e-14 + i2.7162e+02)	
c	(6.9900e+01 + i1.0871e-14, 7.1900e+01 + i1.5642e-13, 1.5502e-13 - i7.8305e+01)	
d	(7.5905e+01 + i1.9978e-14, 1.3836e+02 + i2.3238e-13, 2.3179e-13 - i1.4477e+02)	
	<u>Solution 9</u>	
a	(7.0000e+00 + i1.9847e-17, 1.3255e+01 + i1.5363e+00, -4.9547e+00 + i4.1102e+00)	

b (5.7830e+00 - i7.9453e-01, 1.3696e+01 + i2.0029e+00, -6.8416e+00 + i4.7315e+00)
 c (1.2356e+01 - i3.0124e+00, 1.4356e+01 - i3.0124e+00, -1.1467e+01 + i8.6383e-01)
 d (1.6007e+01 - i6.2886e-01, 1.3035e+01 - i4.4122e+00, -5.8064e+00 - i1.0002e+00)

Solution 10

a (7.0000e+00 + i0.0000e+00, 1.3255e+01 - i1.5363e+00, -4.9547e+00 - i4.1102e+00)
 b (5.7830e+00 + i7.9453e-01, 1.3696e+01 - i2.0029e+00, -6.8416e+00 - i4.7315e+00)
 c (1.2356e+01 + i3.0124e+00, 1.4356e+01 + i3.0124e+00, -1.1467e+01 - i8.6383e-01)
 d (1.6007e+01 + i6.2886e-01, 1.3035e+01 + i4.4122e+00, -5.8064e+00 + i1.0002e+00)

Solution 11

a (7.0000e+00 - i2.4715e-16, 1.3255e+01 - i1.5363e+00, 4.9547e+00 + i4.1102e+00)
 b (5.7830e+00 + i7.9453e-01, 1.3696e+01 - i2.0029e+00, 6.8416e+00 + i4.7315e+00)
 c (1.2356e+01 + i3.0124e+00, 1.4356e+01 + i3.0124e+00, 1.1467e+01 + i8.6383e-01)
 d (1.6007e+01 + i6.2886e-01, 1.3035e+01 + i4.4122e+00, 5.8064e+00 - i1.0002e+00)

Solution 12

a (7.0000e+00 + i2.4715e-16, 1.3255e+01 + i1.5363e+00, 4.9547e+00 - i4.1101e+00)
 b (5.7830e+00 - i7.9453e-01, 1.3696e+01 + i2.0029e+00, 6.8416e+00 - i4.7315e+00)
 c (1.2356e+01 - i3.0124e+00, 1.4356e+01 - i3.0124e+00, 1.1467e+01 - i8.6383e-01)
 d (1.6007e+01 - i6.2886e-01, 1.3035e+01 - i4.4122e+00, 5.8064e+00 + i1.0002e+00)

Solution 13

a (7.0000e+00 + i0.0000e+00, 8.8978e+00 - i4.3484e+00, 1.1492e+01 + i3.3667e+00)
 b (4.8586e+00 - i1.0978e+00, 1.0790e+01 - i5.5833e+00, 1.1480e+01 + i4.5646e+00)
 c (6.4656e+00 + i7.7174e-01, 8.4656e+00 + i7.7174e-01, 3.8465e+00 + i3.0233e+00)
 d (1.2890e+01 + i4.0650e+00, 2.7899e+00 + i4.4765e+00, 3.8826e+00 - i5.7043e-01)

Solution 14

a (7.0000e+00 + i2.2730e-16, 8.8978e+00 + i4.3484e+00, 1.1492e+01 - i3.3667e+00)
 b (4.8586e+00 + i1.0978e+00, 1.0790e+01 + i5.5833e+00, 1.1480e+01 - i4.5646e+00)
 c (6.4656e+00 - i7.7174e-01, 8.4655e+00 - i7.7174e-01, 3.8465e+00 - i3.0233e+00)
 d (1.2890e+01 - i4.0650e+00, 2.7899e+00 - i4.4765e+00, 3.8826e+00 + i5.7043e-01)

Solution 15

a (7.0000e+00 + i5.0753e-16, 8.8978e+00 + i4.3484e+00, -1.1492e+01 + i3.3667e+00)
 b (4.8586e+00 + i1.0978e+00, 1.0790e+01 + i5.5833e+00, -1.1480e+01 + i4.5646e+00)
 c (6.4656e+00 - i7.7174e-01, 8.4656e+00 - i7.7174e-01, -3.8465e+00 + i3.0233e+00)
 d (1.2890e+01 - i4.0650e+00, 2.7899e+00 - i4.4765e+00, -3.8826e+00 - i5.7043e-01)

Solution 16

a (7.0000e+00 + i4.9430e-16, 8.8978e+00 - i4.3484e+00, -1.1492e+01 - i3.3667e+00)
 b (4.8586e+00 - i1.0978e+00, 1.0790e+01 - i5.5833e+00, -1.1480e+01 - i4.5646e+00)
 c (6.4656e+00 + i7.7174e-01, 8.4656e+00 + i7.7174e-01, -3.8465e+00 - i3.0233e+00)
 d (1.2890e+01 + i4.0650e+00, 2.7899e+00 + i4.4765e+00, -3.8826e+00 + i5.7043e-01)

Solution 17

a (7.0000e+00 - i4.0602e-15, 1.9228e+01 - i4.7291e+01, 4.8920e+01 + i1.8587e+01)
 b (1.0779e+01 - i9.2577e-02, 1.7580e+01 - i4.1491e+01, 4.3957e+01 + i1.6591e+01)
 c (2.9080e+01 - i1.5432e+01, 3.1080e+01 - i1.5432e+01, 2.3246e+01 + i2.0023e+01)
 d (1.7743e+01 - i1.5155e+01, 3.6025e+01 - i3.2831e+01, 3.8135e+01 + i2.6013e+01)

Solution 18

a (7.0000e+00 + i1.1757e-14, 1.9228e+01 + i4.7291e+01, 4.8920e+01 - i1.8587e+01)
 b (1.0779e+01 + i9.2577e-02, 1.7580e+01 + i4.1491e+01, 4.3957e+01 - i1.6591e+01)
 c (2.9080e+01 + i1.5432e+01, 3.1080e+01 + i1.5432e+01, 2.3246e+01 - i2.0023e+01)
 d (1.7743e+01 + i1.5155e+01, 3.6025e+01 + i3.2831e+01, 3.8135e+01 - i2.6013e+01)

Solution 19

a (7.0000e+00 + i4.4837e-15, 1.9228e+01 + i4.7291e+01, -4.8920e+01 + i1.8587e+01)
 b (1.0779e+01 + i9.2577e-02, 1.7580e+01 + i4.1491e+01, -4.3957e+01 + i1.6591e+01)
 c (2.9080e+01 + i1.5432e+01, 3.1080e+01 + i1.5432e+01, -2.3246e+01 + i2.0023e+01)
 d (1.7743e+01 + i1.5155e+01, 3.6025e+01 + i3.2831e+01, -3.8135e+01 + i2.6013e+01)

Solution 20

a (7.0000e+00 - i4.4837e-15, 1.9228e+01 - i4.7291e+01, -4.8920e+01 - i1.8587e+01)
 b (1.0779e+01 - i9.2577e-02, 1.7580e+01 - i4.1491e+01, -4.3957e+01 - i1.6591e+01)
 c (2.9080e+01 - i1.5432e+01, 3.1080e+01 - i1.5432e+01, -2.3246e+01 - i2.0023e+01)
 d (1.7743e+01 - i1.5155e+01, 3.6025e+01 - i3.2831e+01, -3.8135e+01 - i2.6013e+01)

<u>Solution 21</u>			
a	(7.0000e+00 + i4.4273e-17,	1.2987e+01 + i3.1571e-01,	3.6961e+00 - i1.1093e+00)
b	(2.9845e+00 - i2.4724e+00,	1.3330e+01 - i1.7956e+00,	7.9670e-01 + i2.0652e+00)
c	(6.3156e+00 - i2.0730e-02,	8.3156e+00 - i2.0730e-02,	5.2264e-01 - i6.0959e-01)
d	(1.8362e+01 + i7.3963e+00,	7.2875e+00 + i6.3131e+00,	9.2207e+00 - i1.0133e+01)
<u>Solution 22</u>			
a	(7.0000e+00 - i1.5860e-17,	1.2987e+01 - i3.1571e-01,	3.6961e+00 + i1.1093e+00)
b	(2.9845e+00 + i2.4724e+00,	1.3330e+01 + i1.7956e+00,	7.9670e-01 - i2.0652e+00)
c	(6.3156e+00 + i2.0730e-02,	8.3156e+00 + i2.0730e-02,	5.2264e-01 + i6.0959e-01)
d	(1.8362e+01 - i7.3963e+00,	7.2875e+00 - i6.3131e+00,	9.2207e+00 + i1.0133e+01)
<u>Solution 23</u>			
a	(7.0000e+00 + i4.7581e-17,	1.2987e+01 - i3.1571e-01,	-3.6961e+00 - i1.1093e+00)
b	(2.9845e+00 + i2.4724e+00,	1.3330e+01 + i1.7956e+00,	-7.9670e-01 + i2.0652e+00)
c	(6.3156e+00 + i2.0730e-02,	8.3156e+00 + i2.0730e-02,	-5.2264e-01 - i6.0959e-01)
d	(1.8362e+01 - i7.3963e+00,	7.2875e+00 - i6.3131e+00,	-9.2207e+00 - i1.0133e+01)
<u>Solution 24</u>			
a	(7.0000e+00 - i6.3441e-17,	1.2987e+01 + i3.1571e-01,	-3.6961e+00 + i1.1093e+00)
b	(2.9845e+00 - i2.4724e+00,	1.3330e+01 - i1.7956e+00,	-7.9670e-01 - i2.0652e+00)
c	(6.3156e+00 - i2.0730e-02,	8.3156e+00 - i2.0730e-02,	-5.2264e-01 + i6.0959e-01)
d	(1.8362e+01 + i7.3963e+00,	7.2875e+00 + i6.3131e+00,	-9.2207e+00 + i1.0133e+01)

4.4.2 Case 4-5-C

The dimensions of the top and base platforms were defined by the following coordinates of the vertices (see Fig. 4.9) in two different reference systems for the top and base platforms:

a (0, 0, 0),	A (0, 0, 0),
b (2, 0, 0),	B (12, 0, 0),
c (4, 4, 0),	C (20, 10, -1),
d (-2, 4, 0),	D (10, 20, -3),
	E (0, 14, 0).

The leg lengths were as follows:

Aa = 15.16575,	Cb = 17.05872,
Ba = 14.35270,	Dc = 14.79865,

$$Bb = 15.68439, \quad Dd = 16.43168.$$

By using the formulation of the forward analysis presented in Section 4.2.3, the coefficients of the three equations (4.23) were determined using the above dimensions. The coefficients are listed in Table 4.4.

Table 4.4 Coefficients of (4.23) for Case 4-5-C

$a_1 = 1.27076z^2 - 0.65875,$	$a_2 = 3.33185z^2 + 0.57127z - 0.47663,$
$b_1 = -1.13853z,$	$b_2 = -0.01833z^2 + 0.24441z + 0.01833,$
$c_1 = 1.92645z^2 - 0.39968,$	$c_2 = 3.27782z^2 + 0.55850z - 0.44552,$
$d_1 = -1.12000z,$	$d_2 = 0.12066z^2 - 1.60890z - 0.12066,$
$e_1 = 1.29003z^2 + 0.50969,$	$e_2 = 0.71129z^2 + 0.16814z - 0.40967,$
$f_1 = 1.12000z,$	$f_2 = -0.12066z^2 + 1.60890z + 0.12066,$
$g_1 = 0.94937z^2 - 0.40700,$	$g_2 = 2.53960z^2 + 0.44777z - 0.44556,$
$h_1 = 0.26608z,$	$h_2 = -0.16966z^2 + 2.26216z + 0.16966,$
$j_1 = 0.79613z^2 - 0.46755,$	$j_2 = 2.03955z^2 + 0.32956z - 0.15755,$
$g_3 = 1.22068z^2 + 0.15209z - 0.30027,$	
$h_3 = -0.01561z^2 + 0.31236z + 0.01561,$	
$j_3 = 1.28339z^2 + 0.14121z - 0.12875.$	

The coefficients in Table 4.4 were used as the entries of the 16×16 matrix M in (4.25). Expanding the eliminant $|M|$ by using (4.32), the following polynomial equation was obtained:

$$\begin{aligned}
& z^{32} + 0.46615z^{31} + 13.18789 z^{30} + 6.15424 z^{29} + 77.07621 z^{28} \\
& + 50.80789 z^{27} + 198.95912 z^{26} + 188.29800 z^{25} + 136.94156 z^{24} \\
& + 303.84657 z^{23} - 228.42892 z^{22} - 622.99122 z^{21} + 73.71978 z^{20} \\
& + 445.22852 z^{19} + 15.29718 z^{18} - 180.40027 z^{17} - 18.39950 z^{16} \\
& + 46.92069 z^{15} + 6.43884 z^{14} - 8.13726 z^{13} - 1.26738 z^{12} \\
& + 0.93742 z^{11} + 0.15209 z^{10} - 0.069706 z^9 - 0.010887 z^8 \\
& + 0.0031998 z^7 + 4.21372e10^{-4} z^6 - 8.79984e10^{-5} z^5 \\
& - 6.76736e10^{-6} z^4 + 1.59803e10^{-5} z^3 + 4.03896e10^{-8} z^2 \\
& - 1.06452e10^{-8} z + 4.27691e10^{-10} = 0.
\end{aligned}$$

This polynomial equation has the following 32 roots:

$$\begin{aligned}
z = & -0.58555, -0.38441, 0.39388, 0.44536, \\
& (-0.83867 \pm i2.15579), (-0.58914 \pm i0.07489), (-0.52010 \pm i0.17587), \\
& (-0.46674 \pm i2.22614), (-0.42348 \pm i0.09766), (-0.25284 \pm i0.03833), \\
& (-0.18077 \pm i0.00391), (0.04690 \pm i0.03172), (0.12204 \pm i0.07796), \\
& (0.42824 \pm i0.20122), (0.51010 \pm i0.15704), (0.80819 \pm i2.11023), \\
& (0.87061 \pm i1.76248), \text{ and } (0.31794 \pm i0.08123).
\end{aligned}$$

A pair of values x and y in (4.23) were obtained by using (4.30) for each z . Using these solutions, the locations of the top platform were determined in a reference system whose origin is at A. (See Fig. 4.9.) B lies on the x axis, and E is in the xy plane. Tables 4.5 shows the coordinates of the vertices a, b, c, and d. It can be seen that for the dimensions given in this example, four real and twenty-eight complex assembly configurations were found. For conciseness, only one solution for every pair

of complex conjugate solutions is presented in Table 4.5.

It has been verified by a reverse displacement analysis that all the 32 solutions reproduced the correct edge lengths with at least 7 digit accuracy.

Table 4.5 Coordinates of the Vertices of the Top Platform of Case 4-5-C

	<u>Solution 1</u>	<u>Solution 2</u>
a	(7.0000e+00, 6.5835e+00, -1.1733e+01)	(7.0000e+00, 9.9894e+00, -9.0117e+00)
b	(7.8442e+00, 8.0439e+00, -1.2807e+01)	(5.1121e+00, 1.0580e+01, -9.3075e+00)
c	(1.2237e+01, 8.6599e+00, -1.2241e+01)	(3.9506e+00, 1.1531e+01, -1.3520e+01)
d	(9.7047e+00, 4.2787e+00, -9.0175e+00)	(9.6143e+00, 9.7603e+00, -1.2633e+01)
	<u>Solution 3</u>	<u>Solution 4</u>
a	(7.0000e+00, 9.8398e+00, 9.1749e+00)	(7.0000e+00, 9.0000e+00, 1.0000e+01)
b	(6.1126e+00, 1.1588e+01, 8.7786e+00)	(7.0000e+00, 1.1000e+01, 1.0000e+01)
c	(7.7945e+00, 1.5193e+01, 1.0821e+01)	(1.1000e+01, 1.3000e+01, 1.0000e+01)
d	(1.0457e+01, 9.9491e+00, 1.2010e+01)	(1.1000e+01, 7.0000e+00, 1.0000e+01)
	<u>Solution 5</u>	
a	(7.0000e+00 + i9.8860e-16, -1.7097e+01 - i4.4748e+00, -6.5913e+00 + i1.1607e+01)	
b	(2.7996e+01 - i3.7407e+00, -7.5336e+00 + i1.9778e+00, -7.3650e+00 - i1.0148e+01)	
c	(3.9760e+01 - i4.2892e+01, 9.8326e+00 - i9.6581e+00, -4.6537e+01 - i2.7064e+01)	
d	(-2.3230e+01 - i3.1670e+01, -1.8857e+01 - i2.9016e+01, -4.4215e+01 + i3.8201e+01)	
	<u>Solution 6</u>	
a	(7.0000e+00 + i0.0000e+00, 6.5178e+00 - i1.3138e+00, -1.1864e+01 - i7.2176e-01)	
b	(6.7387e+00 + i1.3114e+00, 9.0158e+00 - i1.1974e+00, -1.1933e+01 - i1.4829e+00)	
c	(2.0241e+00 + i2.7503e+00, 1.1421e+01 + i9.5778e-01, -1.2970e+01 - i3.0242e+00)	
d	(2.8079e+00 - i1.1840e+00, 3.9271e+00 + i6.0857e-01, -1.2766e+01 - i7.4060e-01)	
	<u>Solution 7</u>	
a	(7.0000e+00 - i2.5376e-16, 7.7905e+00 - i3.1353e+00, -1.1601e+01 - i2.1056e+00)	
b	(5.3942e+00 + i1.7710e+00, 1.0230e+01 - i1.6918e+00, -1.0549e+01 - i2.7496e+00)	
c	(2.0779e+00 - i1.5682e+00, 7.2544e+00 + i1.6360e+00, -5.8122e+00 - i2.9972e+00)	
d	(6.8952e+00 - i6.8811e+00, -6.3468e-02 - i2.6947e+00, -8.9677e+00 - i1.0650e+00)	
	<u>Solution 8</u>	
a	(7.0000e+00 - i2.5377e-16, -1.8953e+01 - i3.0571e+00, -4.2390e+00 + i1.3668e+01)	
b	(2.8589e+01 - i2.3616e+00, -7.7235e+00 + i8.7448e-01, -4.5260e+00 - i1.0148e+01)	
c	(4.0681e+01 - i2.8290e+01, 8.0760e+00 - i8.3717e+00, -3.0769e+01 - i2.7662e+01)	
d	(-2.4085e+01 - i2.1205e+01, -2.5610e+01 - i2.0167e+01, -2.9908e+01 + i4.3786e+01)	
	<u>Solution 9</u>	
a	(7.0000e+00 - i1.1365e-16, 9.4335e+00 - i1.6185e+00, -9.8504e+00 - i1.5500e+00)	
b	(7.0057e+00 + i1.5305e+00, 8.7663e+00 - i1.3854e+00, -1.2291e+01 - i1.6100e+00)	
c	(1.3919e+01 + i8.1749e+00, 1.2488e+01 - i4.0775e+00, -1.8703e+01 + i3.9907e+00)	
d	(1.3902e+01 + i3.5832e+00, 1.4490e+01 - i4.7766e+00, -1.1382e+01 + i4.1710e+00)	
	<u>Solution 10</u>	
a	(7.0000e+00 - i2.8413e-17, 1.1863e+01 - i4.6193e-01, -6.4189e+00 - i8.5374e-01)	
b	(4.0870e+00 + i1.1906e+00, 1.1541e+01 - i1.2553e+00, -7.8965e+00 - i3.0277e+00)	
c	(4.5420e+00 + i6.9766e+00, 9.9989e+00 - i3.5807e-01, -1.5089e+01 - i2.8540e+00)	
d	(1.3281e+01 + i3.4047e+00, 1.0967e+01 + i2.0220e+00, -1.0656e+01 + i3.6680e+00)	
	<u>Solution 11</u>	
a	(7.0000e+00 - i3.9650e-18, 1.2602e+01 - i3.5701e-02, -4.7104e+00 - i9.5515e-02)	
b	(3.4200e+00 - i6.3283e-01, 1.2322e+01 + i7.8514e-01, -5.4162e+00 + i2.7887e+00)	
c	(4.2614e+00 - i7.3961e+00, 7.4192e+00 + i3.0156e+00, -1.2582e+01 + i4.6843e-01)	
d	(1.5001e+01 - i5.4976e+00, 8.2594e+00 + i5.5310e-01, -1.0465e+01 - i8.1843e+00)	

Solution 12

a	(7.0000e+00 + i3.1381e-18,	1.3421e+01 + i7.9872e-02,	1.2630e+00 - i8.4878e-01)
b	(3.0027e+00 - i7.6493e-01,	1.3412e+01 + i1.7846e-01,	2.1398e+00 - i4.3348e+00)
c	(6.9441e+00 - i3.9208e+00,	7.8874e+00 + i1.7857e+00,	6.0904e+00 + i1.0613e+00)
d	(1.8936e+01 - i1.6260e+00,	7.9158e+00 + i1.4899e+00,	3.4598e+00 + i1.1519e+01)

Solution 13

a	(7.0000e+00 - i5.8480e-17,	1.3209e+01 + i5.0298e-01,	3.2932e+00 - i2.0174e+00)
b	(3.6071e+00 - i1.7193e+00,	1.3245e+01 + i8.8289e-01,	5.3039e+00 - i4.9253e+00)
c	(6.5481e+00 - i7.7038e+00,	1.5201e+01 - i1.1536e+00,	1.2776e+01 - i2.0366e+00)
d	(1.6727e+01 - i2.5460e+00,	1.5094e+01 - i2.2933e+00,	6.7438e+00 + i6.6869e+00)

Solution 14

a	(7.0000e+00 + i6.0795e-16,	9.5658e+00 + i3.4713e+00,	1.0557e+01 - i3.1456e+00)
b	(5.2873e+00 - i2.3027e+00,	1.2229e+01 + i1.4551e+00,	8.5901e+00 - i3.8709e+00)
c	(2.9123e+00 + i5.4496e-01,	8.5247e+00 - i1.9271e+00,	3.9302e+00 - i2.6336e+00)
d	(8.0504e+00 + i7.4530e+00,	5.3458e-01 + i4.1218e+00,	9.8294e+00 - i4.5760e-01)

Solution 15

a	(7.0000e+00 - i1.3350e-16,	7.9639e+00 + i2.7773e+00,	1.1361e+01 - i1.9468e+00)
b	(6.3585e+00 - i2.6696e+00,	1.1532e+01 + i1.7857e+00,	1.0186e+01 - i3.5001e+00)
c	(6.9328e-01 - i5.4371e+00,	1.5345e+01 - i2.3915e+00,	9.9848e+00 - i4.7542e+00)
d	(2.6178e+00 + i2.5717e+00,	4.6418e+00 + i5.8341e-01,	1.3510e+01 - i9.4191e-02)

Solution 16

a	(7.0000e+00 + i5.6046e-16,	-1.7322e+01 + i4.7129e+00,	6.8187e+00 + i1.1973e+01)
b	(2.9236e+01 + i2.4016e+00,	-7.2152e+00 - i3.0223e+00,	5.7407e+00 - i1.1009e+01)
c	(5.8498e+01 + i2.9182e+01,	+1.9162e+01 - i3.4729e+00,	2.7312e+01 - i4.6786e+01)
d	(-8.2117e+00 + i2.1977e+01,	-1.1159e+01 + i1.9733e+01,	3.0546e+01 + i2.2161e+01)

Solution 17

a	(7.0000e+00 + i4.0168e-16,	-1.6682e+01 + i7.3491e+00,	1.0141e+01 + i1.2089e+01)
b	(2.7761e+01 + i2.9594e+00,	-5.8510e+00 - i3.2327e+00,	7.5775e+00 - i8.6516e+00)
c	(5.0892e+01 + i4.2729e+01,	2.4749e+01 + i7.1230e-01,	4.0985e+01 - i3.9802e+01)
d	(-1.1390e+01 + i3.3851e+01,	-7.7458e+00 + i3.2457e+01,	4.8677e+01 + i2.2421e+01)

Solution 18

a	(7.0000e+00 + i1.2027e-16,	1.1076e+01 + i1.1577e+00,	7.8931e+00 - i1.6246e+00)
b	(7.0630e+00 - i1.3297e+00,	1.0980e+01 + i9.0377e-01,	1.0306e+01 - i1.5999e+00)
c	(1.9470e+01 - i7.6439e+00,	1.6174e+01 + i9.6669e+00,	1.4484e+01 + i6.2553e+00)
d	(1.9281e+01 - i3.6548e+00,	1.6462e+01 + i1.0429e+01,	7.2466e+00 + i6.1815e+00)

CHAPTER 5

A SURVEY OF OTHER CLASSES OF IN-PARALLEL PLATFORMS

5.1 Introduction

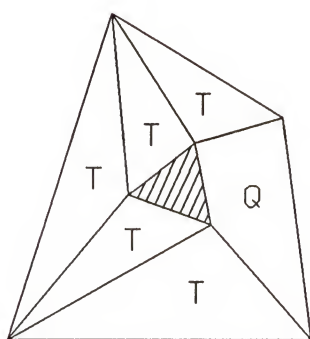
This study deals with the In-parallel Platform mechanisms whose six legs meet either singly or pair-wise at the vertices of the top and base platforms. In Chapters 3 and 4, the displacement analysis of all the cases of the 4-4 and 4-5 Platforms, in which the six legs connected at four or five distinct points in the top and base platforms, were performed successfully. However, some other classes of the In-parallel Platforms with different numbers of connection points are also worth investigating. Apart from the 4-4 and 4-5 Platforms, there are eight classes, namely the 3-3, 3-4, 3-5, 3-6, 4-6, 5-5, 5-6, and 6-6 Platforms. The 3-3 and 3-6 Platforms have been analyzed by some researchers as mentioned in Section 3.1. In the following sections, the 3-4, 3-5, 4-6, 5-5, 5-6, and 6-6 Platforms are investigated.

All the In-parallel Platforms which have three connection points in the top platforms can be easily analyzed by using constructions if the bases of the Platforms are nonplanar. Griffis and Duffy (1989) modeled a 3-6 Platform by a 3-3 Platform using construction. When the number of connection points is more than four, the number of the skew-quadrilaterals of the skew-octahedron embedded in the

mechanisms increases. It follows that the numbers of unknowns and the nonlinear equations used in the analysis increase. As a result, the analysis of those mechanisms is much more complicated and in most cases impossible. Nevertheless, for some cases which have certain kinds of sequences of the triangles and skew-quadrilaterals around the top platforms, their displacement analysis problems can be solved by using constructions and a model introduced in Chapter 2.

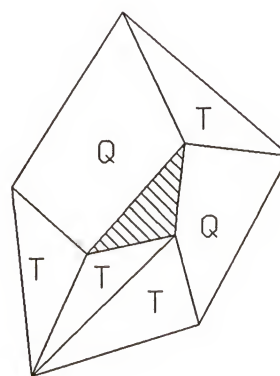
5.2 The 3-4 and 3-5 Platforms

There is only one kind of leg arrangement for each of the 3-4 and 3-5 Platforms. Their leg arrangements are, respectively, represented by T-T-T-T-T-Q and T-T-T-Q-T-Q as illustrated in Fig. 5.1.



(a)

Fig. 5.1 (a) The 3-4 Platform



(b)

(b) The 3-5 Platform

Since there are many triangles embedded within the mechanisms, many dihedral angles (or variables) are available for formulating the analysis. It is believed that there are more than one way to analyze these mechanisms. [Indeed the 3-6

Platform, which is more general than the 3-4 and 3-5 Platforms, was analyzed in several papers (see Section 1.2) using different approaches]. Here constructions are used to analyze the 3-4 and 3-5 Platforms for the purpose of simplicity.

Figure 5.2 shows the 3-4 and 3-5 Platforms with constructions. Assuming that the bases of the Platforms are planar and the base edges AB , CD are not parallel. Also for the 3-5 Platform, CD and AE are not parallel. The lengths of the edges of the bases can be extended to form triangular bases. The extension lines, the lengths of the six legs, and the length of the bases are known. Then the "virtual" connecting leg lengths, Fb , Fc , Ga , and Gc can be uniquely determined. Thus, a "virtual" 3-3 Platform is created for each of the 3-4 and 3-5 Platforms. It follows that the 3-4 and 3-5 Platforms are geometrically similar to the 3-3 Platform. The maximum number of assembly configurations of the Platforms is 16.

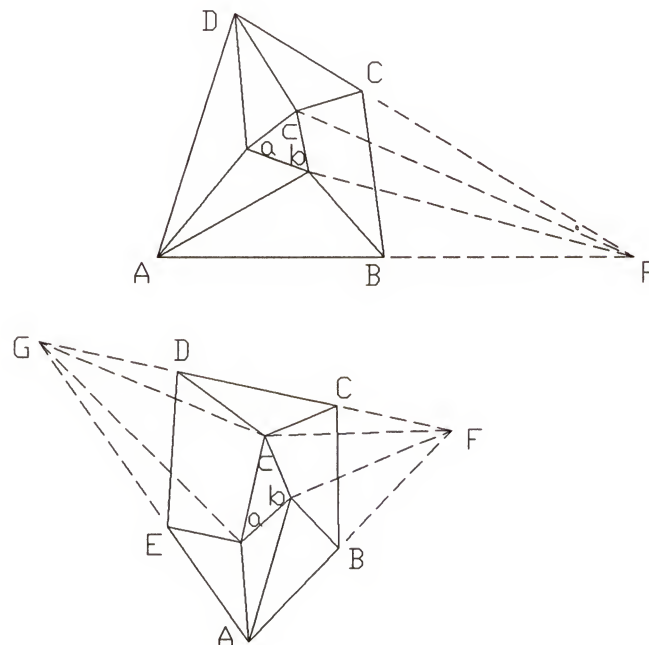
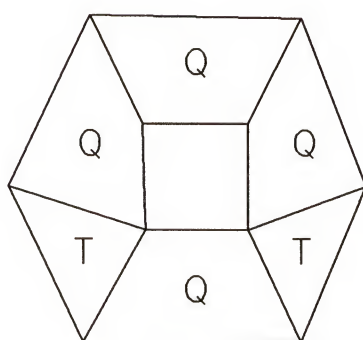


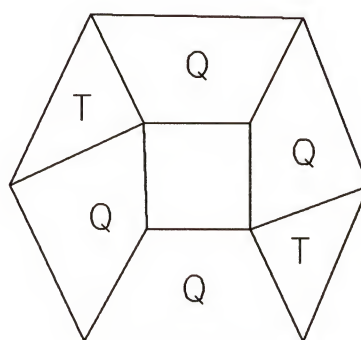
Fig 5.2 Constructions for the 3-4 and 3-5 Platforms

5.3 The 4-6 Platforms

Similar to the 4-4 Platforms, the 4-6 Platforms are classified into two cases according to the arrangements of the "triangle" and "skew-quadrilaterals" around the top platform. Figure 5.3 illustrated the top views of the two cases of the 4-6 Platforms. Each case has a different sequence of the triangles T and skew-quadrilaterals Q around the top platform. For Cases 4-6-A and 4-6-B, the leg arrangements are represented by T-Q-T-Q-Q-Q and T-Q-Q-T-Q-Q. Both of the cases contain two legs which are singly connected at the vertices of both the top and base platforms.



(a) Case 4-6-A



(b) Case 4-6-B

Fig. 5.3 The Two Cases of 4-6 Platforms (Top Views)

5.3.1 Case 4-6-A, a T-Q-T-Q-Q-Q Platform

Construction can be used to model a Case 4-6-A Platform by a Case 4-5-C Platform provided that the two base edges of the triangles lie in a plane and are not

parallel. A "virtual" Case 4-5-C Platform of Case 4-6-A is shown in Fig. 5.4.

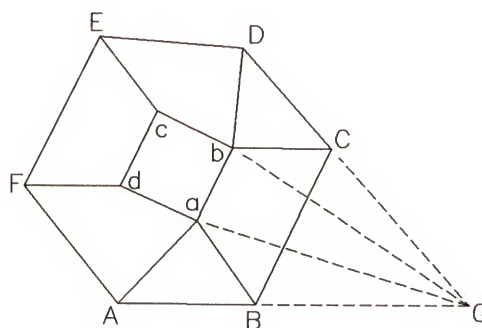


Fig. 5.4 A "Virtual" Case 4-5-C Platform of Case 4-6-A

The two base edges AF and BC are extended to meet at point G so that the hexagonal base becomes a pentagonal base with vertices G, C, D, E, and F. The "virtual" leg lengths Ga and Gb can be uniquely determined by using the cosines law for the triangles $\triangle AGa$ and $\triangle BGb$. Neglecting the two redundant legs Aa and Bb, it can be seen that the "virtual" Case 4-5-C Platform consists of a quadrilateral top abcd, a pentagonal base GCDEF, and six legs, Ga, Gb, Cb, Dc, Ed, and Fa. (Compare Figs. 5.4 with 4.9.)

The displacement analysis of Case 4-5-C Platform was presented in Section 4.2.3. By using the results of that analysis, it can be deduced that the displacement analysis of Case 4-6-A Platform will result in a 32 degree polynomial in a tan-half-angle of the dihedral angle between two faces of the skew-octahedron embedded within the mechanism. Accordingly, there are a maximum of thirty-two real assembly configurations for Case 4-6-A Platform. Therefore, this Case 4-6-A Platform is geometrically similar to the Case 4-5-C Platform.

where

$$a_i = z^2(a_{i2} - a_{i0}) + a_{i0} + a_{i2},$$

$$b_i = 2b_{i1}z,$$

$$c_i = z^2(c_{i2} - c_{i0}) + c_{i0} + c_{i2},$$

$$d_i = 2d_{i1}z,$$

$$e_i = z^2(e_{i2} - e_{i0}) + e_{i0} + e_{i2},$$

$$f_i = 2f_{i1}z,$$

$$g_i = z^2(g_{i2} - g_{i0}) + g_{i0} + g_{i2},$$

$$h_i = 2h_{i1}z,$$

$$j_i = z^2(j_{i2} - j_{i0}) + j_{i0} + j_{i2}, \text{ and}$$

$i = 1, 2, \text{ and } 3.$

Further, the variables x , y , and z are tan-half-angles of θ_3 , θ_4 , and θ_2 . The expressions of the coefficients a_{i0} , a_{i2} , b_{i1} , c_{i0} , ..., j_{i2} of z are listed in Table 2.1. The constants S_{11} , S_{55} , ℓ_{ii} , c_{12} , s_{12} , c_{45} , and s_{45} in the expressions of the coefficients are different for the three equations.

For $i = 1$,

$$S_{11} = FA, \quad S_{55} = cd, \quad \ell_{11} = dF,$$

$$c_{12} = -\cos(\angle FAG), \quad s_{12} = (1 - c_{12}^2)^{1/2},$$

$$c_{45} = -\cos(\angle acd), \text{ and } s_{45} = (1 - c_{45}^2)^{1/2}.$$

For $i = 2$,

$$S_{11} = CA, \quad S_{55} = bc, \quad \ell_{22} = bC,$$

$$c_{12} = -\cos(\angle CAG), \quad s_{12} = (1 - c_{12}^2)^{1/2},$$

$$c_{45} = -\cos(\angle bca), \text{ and } s_{45} = (1 - c_{45}^2)^{1/2}.$$

For $i = 3$,

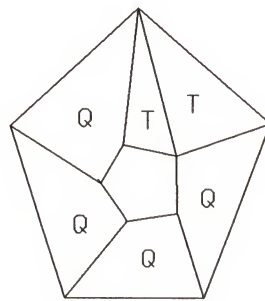
$$\begin{aligned} S_{11} &= EA, & S_{55} &= 0, & \ell_{33} &= cE, \\ c_{12} &= -\cos(\angle EAG), & s_{12} &= (1 - c_{12}^2)^{1/2}. \end{aligned}$$

The three equations in (5.1) were used for deriving a polynomial equation in z by the elimination method presented in Section 4.3. The expansion of the eliminant (4.25) resulted in a polynomial equation of degree 32 in z . It follows that there are 32 solutions for z and a corresponding 32 pairs of solutions for x and y . All the solutions were verified by a reverse displacement analysis and it was confirmed that no extraneous roots were introduced. Therefore, there are a maximum of 32 assembly configurations for Case 4-6-B.

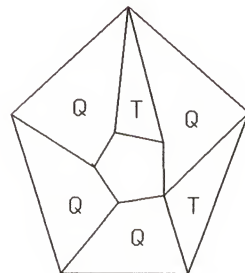
5.4 The 5-5 Platforms

The 5-5 Platforms are classified into three cases according to their leg arrangements. The leg arrangements of the three cases are, respectively, represented by T-T-Q-Q-Q-Q, T-Q-T-Q-Q-Q, and T-Q-Q-T-Q-Q. The top views of the three cases are illustrated in Fig. 5.6. Among these three cases, Case 5-5-A has a feature which is distinct from the other two cases. It can be seen that there are four consecutive Q's around the top platform. It follows that Case 5-5-A contains three legs which have their own connection points at the vertices of both the top and base platforms. This feature is very important because it is the only In-parallel Platform in this study that

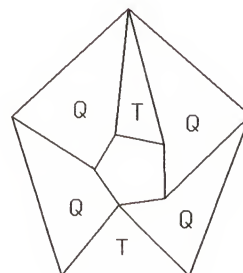
has three singly connected legs. Fortunately, this case can be analyzed since it has two triangles T that are adjacent to each other. As a result, the skew-octahedron embedded in the mechanisms contains three skew-hexahedra which can be modeled by the serial chain introduced in Chapter 2. This case will be analyzed in this section. It should be mentioned here that this case was also analyzed by Innocenti and Parenti-Castelli (1990). The other two cases, Cases 5-5-B and 5-5-C, do not have any of the features which allow the use of models and constructions. Their displacement analyses problems were not solved.



(a) Case 5-5-A



(b) Case 5-5-B



(c) Case 5-5-C

Fig. 5.6 The Three Cases of 5-5 Platforms (Top Views)

The displacement analysis of Case 5-5-A is presented in the following:

As mentioned earlier, Case 5-5-A has the feature that the top platform is connected to the base by two triangles in serial fashion. Three variables, θ_2 , θ_3 , and θ_4 , are the dihedral angles which are used to determine the locations of the top platform. (See Fig. 5.7.) In terms of solid geometry, the skew-octahedron embedded in the mechanisms contains three distinct skew-hexahedra which are illustrated in Fig. 5.8. The dihedral angles are designated as shown in Fig. 5.8. It should be noted that the three dihedral angles, θ_2 's, which measure the elevation of triangular faces of the three skew-hexahedra relative to the base, are not equal if the base of the skew-octahedron is not planar. Similarly, the three dihedral angles, θ_4 's, between triangular faces of the three skew-hexahedra relative to the top platform are different if the top platform is not planar.

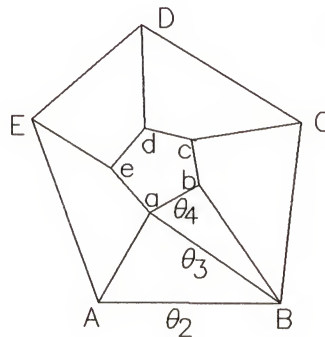


Fig. 5.8 Case 5-5-A Platform

By using the serial chain model introduced in Section 2.3, the relationship between the three dihedral angles in each of the three skew-hexahedra can be obtained. It follows that three equations can be obtained and each of which contain

all the three variables θ_2 , θ_3 , and θ_4 .

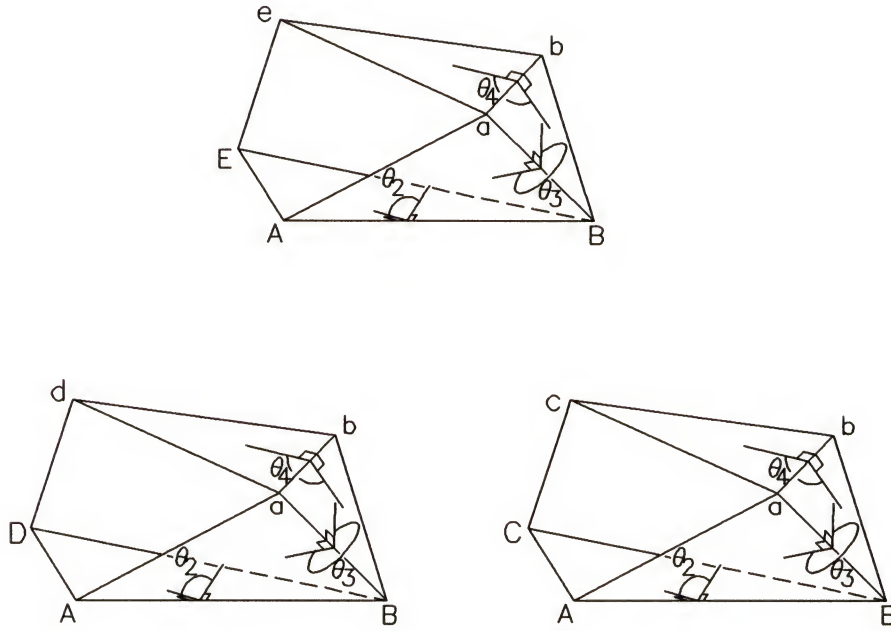


Fig. 5.8 Three Skew-Hexahedra of Case 5-5-A

The three equations ($i = 1, 2$, and 3), which are in the form of (2.6), are expressed again as follows,

$$(a_i x^2 + b_i x + c_i)y^2 + (d_i x^2 + e_i x + f_i)y + g_i x^2 + h_i x + j_i = 0, \quad (5.2)$$

where

$$\begin{aligned} a_i &= a_{i0} c_2 + a_{i2}, & b_i &= b_{i1} s_2, & c_i &= c_{i0} c_2 + c_{i2}, \\ d_i &= d_{i1} s_2, & e_i &= e_{i0} c_2 + e_{i2}, & f_i &= f_{i1} s_2, \\ g_i &= g_{i0} c_2 + g_{i2}, & h_i &= h_{i1} s_2, & j_i &= j_{i0} c_2 + j_{i2}. \end{aligned}$$

and x and y are, respectively, the tan-half-angles of θ_3 and θ_4 . Further, the expressions of the coefficients a_{i0} , a_{i2} , b_{i1} , c_{i0} , ..., j_{i2} are listed in Table 2.1. These coefficients are different for the three equations because the knowns, S_{11} , S_{55} , ℓ_{ii} , c_{12} ,

s_{12} , c_{45} , and s_{45} in the coefficients have different definitions as follows,

For $i = 1$,

$$\begin{aligned} S_{11} &= EA, & S_{55} &= be, & \ell_{11} &= Ee, \\ c_{12} &= -\cos(\angle EAB), & s_{12} &= (1 - c_{12}^2)^{1/2}, \\ c_{45} &= -\cos(\angle eba), \text{ and} & s_{45} &= (1 - c_{45}^2)^{1/2}. \end{aligned}$$

For $i = 2$,

$$\begin{aligned} S_{11} &= DA, & S_{55} &= bd, & \ell_{22} &= Dd, \\ c_{12} &= -\cos(\angle DAB), & s_{12} &= (1 - c_{12}^2)^{1/2}, \\ c_{45} &= -\cos(\angle dba), \text{ and} & s_{45} &= (1 - c_{45}^2)^{1/2}. \end{aligned}$$

For $i = 3$,

$$\begin{aligned} S_{11} &= CA, & S_{55} &= bc, & \ell_{33} &= Cc, \\ c_{12} &= -\cos(\angle CAB), & s_{12} &= (1 - c_{12}^2)^{1/2}, \\ c_{45} &= -\cos(\angle cba), \text{ and} & s_{45} &= (1 - c_{45}^2)^{1/2}. \end{aligned}$$

The other knowns, S_{22} , S_{33} , S_{44} , c_{23} , s_{23} , c_{34} , and s_{34} , are the same for all the three equations ($i = 1, 2$, and 3) and they are given by,

$$\begin{aligned} S_{22} &= AB, & S_{33} &= Ba, & S_{44} &= ab, \\ c_{23} &= -\cos(\angle ABa), \text{ and} & s_{23} &= -(1 - c_{23}^2)^{1/2}. \end{aligned}$$

The equation set (5.2) can be solved by an elimination process similar to that for Case 4-5-C presented in Section 4.3. The two unknowns, x and y , can be algebraically eliminated in a single operation by devising twenty-one extra equations as follows:

To each of the three equations, multiply x , y , xy , y^2 , y^2x , y^3 , and y^3x to generate

twenty-one equations. Therefore, together with the original equations, a total of twenty-four equations are obtained and they can be expressed as

$$M \underline{r} = \underline{0}, \quad (5.3)$$

where

$$\underline{r} = [x^3y^5 \ x^2y^5 \ xy^5 \ y^5 \ x^3y^4 \ x^2y^4 \ xy^4 \ y^4 \ x^3y^3 \ x^2y^3 \ xy^3 \ y^3 \\ x^3y^2 \ x^2y^2 \ xy^2 \ y^2 \ x^2y \ xy \ y \ x^2 \ x \ 1]^T,$$

and the 24×24 matrix M is given by

$$M = \begin{bmatrix} 0 & 0 & 0 & 0 & 0 & 0 & 0 & 0 & 0 & 0 & 0 & 0 & 0 & 0 & 0 & a_i & b_i & c_i & d_i & e_i & f_i & g_i & h_i & j_i \\ 0 & 0 & 0 & 0 & 0 & 0 & 0 & 0 & 0 & 0 & 0 & 0 & 0 & a_i & d_i & g_i & b_i & c_i & 0 & e_i & f_i & 0 & h_i & j_i & 0 \\ 0 & 0 & 0 & 0 & 0 & 0 & 0 & 0 & 0 & a_i & b_i & c_i & 0 & 0 & 0 & d_i & e_i & f_i & g_i & h_i & j_i & 0 & 0 & 0 & 0 \\ 0 & 0 & 0 & 0 & 0 & 0 & 0 & 0 & a_i & b_i & c_i & 0 & d_i & g_i & 0 & e_i & f_i & 0 & h_i & j_i & 0 & 0 & 0 & 0 & 0 \\ 0 & 0 & 0 & 0 & 0 & a_i & b_i & c_i & 0 & d_i & e_i & f_i & 0 & 0 & 0 & g_i & h_i & j_i & 0 & 0 & 0 & 0 & 0 & 0 & 0 \\ 0 & 0 & 0 & 0 & a_i & b_i & c_i & 0 & d_i & e_i & f_i & 0 & g_i & 0 & 0 & h_i & j_i & 0 & 0 & 0 & 0 & 0 & 0 & 0 & 0 \\ 0 & a_i & b_i & c_i & 0 & d_i & e_i & f_i & 0 & g_i & h_i & j_i & 0 & 0 & 0 & 0 & 0 & 0 & 0 & 0 & 0 & 0 & 0 & 0 & 0 \\ a_i & b_i & c_i & 0 & d_i & e_i & f_i & 0 & g_i & h_i & j_i & 0 & 0 & 0 & 0 & 0 & 0 & 0 & 0 & 0 & 0 & 0 & 0 & 0 & 0 \end{bmatrix}$$

where $i = 1, 2$, and 3 .

For the equation set (5.3) to have nontrivial solutions,

$$\text{determinant}(M) = 0. \quad (5.4)$$

Equation (5.4) is the condition under which the three equations (5.2) have a common solution for x and y . The eliminant of the equation set is then $\text{determinant}(M)$ which will be written as $|M|$.

Every entry of the 24×24 matrix M is linear in cosines or sines of θ_2 . It follows that a straight expansion of the eliminant would result in a expression in the form

$$\sum_{\substack{i=0,24 \\ j=0,24 \\ i+j \leq 24}} C_{ij} s_2^i c_2^j = 0, \quad (5.5)$$

where the coefficients C_{ij} depend on the dimensions of the mechanisms only.

Now, by substituting the identities

$$s_2^i \equiv (1 - c_2^2)^v s_2^u, \quad (5.6)$$

where

$$1 \leq i \leq 16,$$

v = quotient of i divided by 2, and

u = remainder of i divided by 2.

Equation (5.4) can be expressed as

$$\sum_{\substack{i=0,1 \\ j=0,20 \\ i+j \leq 20}} C_{ij} s_2^i c_2^j = 0. \quad (5.7)$$

Specifically, C_{ij} (for $i = 0,1$; $j = 21, 22, 23$, and 24 ; and $21 \leq i + j \leq 24$) are set to zeroes because, as presented in the following numerical example, they are extremely small comparing to the other coefficients. Now, expanding s_2 and c_2 in terms of the tan-half-angle $z = \tan(\theta_2/2)$, (5.7) becomes a polynomial equation of degree 40 in z . Therefore, for a particular set of the dimensions of the mechanism, there are forty solutions for z and a corresponding forty pairs of solutions for x and y .

A numerical example is given in the following to verify the analysis.

The dimensions of the top and base platforms were defined by the following coordinates of the vertices (see Fig. 5.7) in some arbitrary chosen reference systems.

$$a (0, 0, 0),$$

$$A (0, 0, 0),$$

$$b (2, 0, 3),$$

$$B (12, 0, -8),$$

$$\begin{array}{ll}
c \ (8, 7, -5), & C \ (20, 15, 9), \\
d \ (4, 11, 2), & D \ (10, 13, -15), \\
e \ (-2, 3, -7), & E \ (-8, 21, -10).
\end{array}$$

The leg lengths were given by

$$\begin{array}{ll}
Aa = 14.43087, & Cc = 10.71928, \\
Ba = 20.79062, & Dd = 28.48897, \\
Bb = 19.36236, & Ee = 34.97020.
\end{array}$$

With the above dimensions of the mechanisms, the coefficients in the equation set (5.2) were determined. These coefficients were used as the entries of the 24×24 matrix M in (5.4). By using the Laplace's Expansion method introduced in Section 4.4, the eliminant $|M|$ was expanded into 924 pairs of minors and cofactors, and each of which was the determinants of 12×12 matrices. The determinant of matrix of this size was able to be obtained by using the *Mathematica*. The summation of the 924 pairs of determinants was in the form of (5.5). Substituting the identities (5.6) in (5.5) and expanding, the following equation was obtained

$$\begin{aligned}
& 6.2 \times 10^{-11} c_2^{24} + 3.5 \times 10^{-11} c_2^{23} s_2 + 1.8 \times 10^{-10} c_2^{23} + 2.2 \times 10^{-9} c_2^{22} \\
& - 1.3 \times 10^{-10} c_2^{21} s_2 - 1.0 \times 10^{-9} c_2^{21} + 4.1 \times 10^{-9} c_2^{20} s_2 \\
& + c_2^{20} - 2.9 c_2^{19} s_2 - 7.6 c_2^{19} - 0.4 c_2^{18} s_2 + 42.0 c_2^{18} - 9.3 c_2^{17} s_2 \\
& - 133.4 c_2^{17} + 82.2 c_2^{16} s_2 - 195.5 c_2^{16} - 846.7 c_2^{15} s_2 + 2926.1 c_2^{15} \\
& - 1621.6 c_2^{14} s_2 + 9440.4 c_2^{14} + 6419.9 c_2^{13} s_2 - 9192.7 c_2^{13} \\
& + 34220.3 c_2^{12} s_2 - 95273.2 c_2^{12} + 3786.5 c_2^{11} s_2 - 36708.5 c_2^{11} \\
& - 1.9 \times 10^5 c_2^{10} s_2 + 3.5 \times 10^5 c_2^{10} - 97312.9 c_2^9 s_2 + 1.6 \times 10^5 c_2^9
\end{aligned}$$

$$\begin{aligned}
& + 4.2 \times 10^5 c_2^8 s_2 - 6.3 \times 10^5 + 97956.3 c_2^7 s_2 - 31720.7 c_2^7 - 4.8 \times 10^5 c_2^6 s_2 \\
& + 6.5 \times 10^5 c_2^6 + 1.8 \times 10^5 c_2^5 s_2 - 2.9 \times 10^5 c_2^5 + 4.0 \times 10^5 c_2^4 s_2 - 5.3 \times 10^5 c_2^4 \\
& - 2.2 \times 10^5 c_2^3 s_2 + 2.4 \times 10^5 c_2^3 - 2.6 \times 10^5 c_2^2 s_2 + 2.6 \times 10^5 c_2^2 \\
& + 30663.2 c_2 s_2 - 30662.5 c_2 - 1504.2 s_2 + 1504.2 = 0.
\end{aligned}$$

Neglecting the coefficients of $s_2^i c_2^j$ for $i = 0, 1, j = 21, 22, \dots, 24$, and $21 \leq i + j \leq 24$ in (5.7), and introducing the tan-half-angle $z = \tan(\theta_2/2)$ gives

$$\begin{aligned}
& z^{40} - 7.0z^{39} + 32.9z^{38} - 111.8z^{37} + 315.6z^{36} - 772.3z^{35} + 1740.8z^{34} \\
& - 3734.3z^{33} + 7743.2z^{32} - 15451.9z^{31} + 29037.5z^{30} - 50194.1z^{29} \\
& + 78147.9z^{28} - 107789.1z^{27} + 129123.0z^{26} - 129649.6z^{25} + 99745.5z^{24} \\
& - 38991.2z^{23} - 40589.9z^{22} + 117579.2z^{21} - 169474.1z^{20} + 182449.0z^{19} \\
& - 156983.8z^{18} + 106306.5z^{17} - 48847.9z^{16} - 39.0z^{15} + 32553.9z^{14} \\
& - 48231.1z^{13} + 50845.0z^{12} - 45265.9z^{11} + 35668.4z^{10} - 25156.4z^9 \\
& + 15816.9z^8 - 8771.8z^7 + 4235.1z^6 - 1751.6z^5 + 609.6z^4 - 173.5z^3 \\
& + 39.1z^2 - 6.3z + 0.7 = 0.
\end{aligned} \tag{5.7}$$

This polynomial equation has the following 40 roots:

$$\begin{aligned}
z = & 0.91893, 1.28951, (-1.58300 \pm i1.23531), (-0.94442 \pm i0.04436), \\
& (-0.51204 \pm i0.52790), (-0.34429 \pm i1.16614), (-0.32935 \pm i1.72850), \\
& (-0.15135 \pm i1.05909), (-0.12815 \pm i0.86348), (0.03876 \pm i0.39556), \\
& (0.11733 \pm i0.63920), (0.17828 \pm i0.43789), (0.21976 \pm i0.64108), \\
& (0.41931 \pm i1.99215), (0.52770 \pm i0.45971), (0.62888 \pm i0.74189), \\
& (0.66799 \pm i1.15571), (0.66939 \pm i0.79044), (0.74574 \pm i0.54064), \\
& (0.94728 \pm i0.08923), \text{ and } (1.22741 \pm i1.47725).
\end{aligned}$$

Each solution for z gives a pair of solutions for x and y . It follows that there are forty solution sets for the equation set (5.2). With the solutions for x , y , and z , the coordinates of the vertices of the top platform were determined in a reference system whose origin is at A (see Fig. 5.7). B lies on the x -axis, and E is in the xy plane. With the given dimensions, two real and thirty-eight complex assembly configurations were found. The coordinates of the vertices a, b, c, d, and e are listed in Table 5.1. For conciseness, only one solution for each pair of complex conjugate solutions is listed. It can be seen that there is no reflection of the configuration through the base platform due to the fact that the base is nonplanar. All the forty solutions, including the complex ones, have been verified that the correct leg lengths with at least four digit accuracy were reproduced.

Table 5.1 Coordinates of the Vertices of the Top Platform of Case 5-5-A

	<u>Solution 1</u>	<u>Solution 2</u>
a	(6.0000e+00, 8.5000e+00, 1.0000e+01)	(7.1933e+00, 4.1838e+00, 1.1790e+01)
b	(5.6527e+00, 1.0470e+01, 7.0000e+00)	(4.4893e+00, 3.5633e+00, 9.4870e+00)
c	(1.1504e+01, 1.7594e+01, 1.5000e+01)	(9.9177e+00, 1.3772e+01, 5.5732e+00)
d	(1.6138e+01, 1.4349e+01, 8.0000e+00)	(1.0964e+01, 6.2627e+00, 7.2366e-01)
e	(9.3017e+00, 7.0513e+00, 1.7000e+01)	(1.3950e+01, 7.7139e+00, 1.3761e+01)
	<u>Solution 3</u>	
a	(-2.8317e+00 + i4.3554e+00, -1.5992e+01 - i2.0980e+00, -3.2476e+00 + i6.5331e+00)	
b	(-2.0095e+00 + i8.5519e+00, -1.4259e+01 - i3.7911e+00, 2.2119e+00 + i6.4386e+00)	
c	(9.1525e+00 + i1.5580e+01, -2.6551e+00 - i1.0550e+01, 2.2150e+00 + i2.5448e+00)	
d	(-5.7732e+00 + i2.2156e+01, 3.2760e+00 - i2.6467e+00, 7.3938e+00 + i1.2447e+01)	
e	(-2.5674e+00 + i4.0051e-01, -1.4150e+01 - i3.3240e-01, -1.2043e+01 + i6.7840e+00)	
	<u>Solution 4</u>	
a	(-7.5276e+00 + i1.7650e-01, -6.7917e+00 - i5.9678e-01, -1.0291e+01 + i2.6474e-01)	
b	(-6.9428e+00 - i4.4690e-03, -3.2116e+00 - i5.3457e-01, -1.0557e+01 + i7.0443e-01)	
c	(1.0994e-01 - i1.2508e+01, -5.8158e+00 + i1.7810e+00, 4.3283e+00 + i1.6177e+01)	
d	(1.5559e+01 + i1.2862e+00, -4.3503e+00 + i2.0162e+00, -1.1907e+01 + i2.0077e+01)	
e	(-1.6852e+00 - i1.8369e+00, -1.3740e+01 + i1.2943e-01, -7.0259e+00 + i5.4122e+00)	
	<u>Solution 5</u>	
a	(-1.1359e+01 + i9.3419e-01, -2.4579e+00 - i1.3461e+01, -1.6038e+01 + i1.4013e+00)	
b	(-1.1160e+01 - i8.2640e-01, 4.9963e+00 - i1.8619e+01, -2.1772e+01 - i5.3648e+00)	
c	(-4.0163e-01 - i2.3799e+00, 1.2165e+01 + i1.2763e+01, 1.0039e+01 - i1.1912e+01)	
d	(2.3227e+00 - i4.5677e-01, 3.6628e+00 - i1.2820e+00, -6.1363e+00 - i4.2050e+00)	
e	(-7.5905e+00 + i3.7533e+00, -1.4241e+01 + i4.3809e+00, 2.6515e+00 + i1.2081e+01)	

Solution 6

- a $(-1.0052e+01 + i2.0337e+01, -3.8961e+01 - i1.6269e+01, -1.4077e+01 + i3.0506e+01)$
 b $(-9.8219e+00 + i3.4835e+01, -4.8441e+01 - i1.0427e+01, -5.7720e-01 + i3.4362e+01)$
 c $(5.4473e+01 - i4.5121e-01, 9.9008e-01 + i2.8242e+01, -6.4325e+00 - i2.6647e+01)$
 d $(1.7141e+01 - i9.4800e+00, 1.1535e+00 - i1.6725e+00, -2.0721e+01 - i3.3998e+00)$
 e $(6.3868e+00 - i1.8523e+01, -5.2625e+00 - i1.7435e+01, -4.1774e+01 + i6.0234e+00)$

Solution 7

- a $(3.1044e+00 + i1.2220e+01, -2.6103e+01 + i5.4254e+00, 5.6566e+00 + i1.8330e+01)$
 b $(4.4267e+01 + i2.2676e+01, -6.8400e+00 + i9.2471e+00, 1.6782e+01 - i2.6972e+01)$
 c $(5.1670e+01 + i3.5595e+01, -1.6658e+01 + i1.4811e+01, 3.1062e+01 - i2.9844e+01)$
 d $(1.0507e+02 - i5.0494e+01, 9.1299e+00 - i2.3504e+01, -6.3463e+01 - i8.8930e+01)$
 e $(-5.8580e+01 - i1.4046e+01, -5.9448e+01 - i4.8741e+00, -2.2530e+01 + i8.7995e+01)$

Solution 8

- a $(-2.8455e+01 + i4.2269e+01, -7.7151e+01 - i4.9844e+01, -4.1682e+01 + i6.3403e+01)$
 b $(-3.0557e+01 + i5.2335e+01, -9.5408e+01 - i5.9270e+01, -5.1579e+01 + i7.8653e+01)$
 c $(-4.2232e-02 - i3.8533e+01, 1.8820e+01 + i8.8389e+01, 1.0456e+02 - i1.1615e+01)$
 d $(-6.7043e+01 - i2.3267e+01, 6.1570e+01 - i3.1699e+01, -3.4590e+00 - i6.8613e+01)$
 e $(-2.3917e+01 - i4.5549e+00, 4.6791e-01 + i3.4068e-01, 1.4006e+01 - i2.7290e+00)$

Solution 9

- a $(-3.9937e+01 - i7.9412e+00, 1.4607e+01 - i6.9749e+01, -5.8905e+01 - i1.1912e+01)$
 b $(-5.4861e+01 - i1.4903e+01, 2.3253e+01 - i8.4743e+01, -6.3459e+01 - i1.7565e+01)$
 c $(2.1065e+01 - i6.9159e+01, 7.3238e+01 - i6.4663e+00, -3.1846e+01 - i1.1023e+01)$
 d $(1.5888e+01 - i1.9221e+01, 2.4954e+01 - i1.6097e+01, -5.2159e+01 - i8.5963e-01)$
 e $(1.1672e+01 - i7.3129e+00, 9.7947e+00 - i1.7850e+01, -4.2945e+01 + i1.7047e+00)$

Solution 10

- a $(-5.2668e+00 - i6.7251e+00, 1.7746e+01 - i5.9184e+00, -6.9002e+00 - i1.0088e+01)$
 b $(-2.5269e+01 - i1.6311e+01, 1.3398e+01 - i1.6066e+01, 5.4630e+00 - i2.9166e+01)$
 c $(1.0184e+01 - i2.1807e+01, 4.0375e+01 - i5.7963e+00, 3.4716e+00 + i1.2114e+01)$
 d $(-3.2819e+01 + i1.3278e+01, 1.1263e+01 - i5.1633e+00, -2.7906e+01 - i3.6558e+01)$
 e $(3.5748e+01 + i1.3210e+01, 3.0469e+01 + i1.5467e+01, -3.3744e+01 + i3.0507e+01)$

Solution 11

- a $(-3.3702e+00 - i1.6191e+01, 3.2475e+01 - i4.7130e+00, -4.0553e+00 - i2.4287e+01)$
 b $(-9.2498e+00 - i1.2216e+01, 3.0274e+01 - i8.8269e+00, -8.2761e+00 - i2.7678e+01)$
 c $(1.1906e+02 + i3.1512e+01, 3.7488e+00 + i1.0671e+02, -5.0880e+01 + i3.2078e+01)$
 d $(4.8415e+01 + i1.0003e+02, -6.2212e+01 + i5.2624e+01, -7.7223e+01 - i1.6230e+01)$
 e $(4.1074e+01 + i1.8958e+00, 1.7608e+01 + i3.4623e+01, -1.5223e+01 - i4.6739e+00)$

Solution 12

- a $(-1.7811e+00 - i8.1442e+00, 2.0512e+01 - i1.7027e+00, -1.6716e+00 - i1.2216e+01)$
 b $(-1.6189e+01 - i1.4497e+01, 1.8172e+01 - i3.4901e+00, 5.0649e+00 - i2.6425e+01)$
 c $(1.5116e+01 - i6.7457e+00, 1.1141e+01 - i4.4127e-01, -2.4462e+00 + i3.0274e+00)$
 d $(8.6580e+00 - i4.4849e+01, 1.6023e+01 - i5.4630e+00, 3.6602e+01 - i2.6462e+00)$
 e $(3.3304e+01 + i1.3323e-01, 2.2877e+01 + i1.7506e+00, -1.0400e+01 + i2.1993e+01)$

Solution 13

- a $(1.8195e+00 - i1.4581e+01, 2.9918e+01 + i3.6132e+00, 3.7293e+00 - i2.1872e+01)$
 b $(6.3713e+00 - i1.4352e+01, 2.7921e+01 + i6.2655e+00, 5.3203e+00 - i1.9198e+01)$
 c $(1.2753e+02 + i2.9662e+01, 2.1887e+01 + i1.0153e+02, -5.2141e+01 + i6.3605e+01)$
 d $(1.2399e+02 - i6.3302e+01, 8.5240e+01 + i8.1198e+01, 2.0555e+01 + i7.6798e+01)$
 e $(3.5260e+01 - i1.3203e+01, 4.0485e+01 + i2.8988e+01, -8.4133e+00 + i4.0050e+00)$

Solution 14

- a $(8.6667e+00 + i6.7765e+00, -1.5774e+01 + i1.2745e+01, 1.4000e+01 + i1.0165e+01)$
 b $(1.4370e+01 - i3.9397e+00, -1.9667e+01 + i3.2646e+00, 8.3155e-01 + i8.3271e+00)$
 c $(1.9498e+01 + i6.2942e+00, 1.6430e+00 + i2.6596e+00, 3.4248e+00 - i6.9391e+00)$
 d $(4.4695e+01 + i7.1934e+00, 1.0362e+01 - i9.3109e+00, -2.3239e-01 - i2.9282e+01)$
 e $(4.1146e+00 + i2.9183e+01, -3.3329e-01 + i2.7380e+01, 3.7392e+01 + i4.8650e+00)$

Solution 15

- a $(5.0633e+00 - i5.2663e+00, 1.5384e+01 + i6.1467e+00, 8.5949e+00 - i7.8994e+00)$
 b $(-9.5855e-01 - i6.8222e+00, 1.3334e+01 + i9.0800e+00, 9.4068e+00 - i1.2034e+01)$
 c $(1.7173e+01 - i1.1754e+01, 2.0380e+01 - i8.8204e+00, 2.6164e+01 + i8.2874e-01)$
 d $(6.8338e+00 + i3.2349e-01, 3.0177e+01 + i2.8742e+00, 1.3459e+01 + i1.8106e-02)$
 e $(2.0368e+01 - i2.5048e+00, 2.2822e+01 - i3.4823e+00, 1.1134e+01 + i3.6624e+00)$

	<u>Solution 16</u>	
a	(9.8193e+00 - i5.2367e+00, 1.2381e+01 + i1.4132e+01, 1.5729e+01 - i7.8550e+00)	
b	(8.4865e+00 - i1.0552e+01, 5.9042e+00 + i1.6818e+01, 1.9327e+01 - i4.9903e+00)	
c	(6.5411e+01 - i1.5845e+01, 3.5417e+00 - i4.5733e+01, -1.0181e+01 - i1.0192e+01)	
d	(5.4025e+01 + i1.4840e+01, 3.6433e+01 - i2.9129e+01, 5.4690e+00 - i2.2765e+01)	
e	(3.0193e+01 + i6.6647e+00, 2.7645e+01 - i9.7982e+00, 1.4937e+00 - i1.6482e+01)	
	<u>Solution 17</u>	
a	(1.3912e+01 - i1.9629e-01, 4.2588e-01 + i2.1530e+01, 2.1867e+01 - i2.9443e-01)	
b	(1.0445e+01 - i1.5174e+00, -2.8636e+00 + i2.3046e+01, 2.2036e+01 + i2.1186e+00)	
c	(-7.2231e+00 + i2.1228e+01, 1.4871e+01 + i2.8701e+01, 4.0462e+01 + i1.8485e+01)	
d	(-1.7899e+01 + i1.3106e+00, 4.5497e+00 + i3.5670e+01, 2.1471e+01 + i2.5894e+01)	
e	(1.2317e+01 + i7.1003e+00, 1.0819e+01 + i2.1843e+01, 2.5199e+01 + i2.2197e+00)	
	<u>Solution 18</u>	
a	(1.0441e+01 - i4.4515e+00, 1.0523e+01 + i1.4990e+01, 1.6661e+01 - i6.6773e+00)	
b	(1.2143e+01 - i3.7046e+00, 1.2658e+01 + i1.2872e+01, 1.3269e+01 - i7.6354e+00)	
c	(-9.6207e+00 + i5.8219e+01, 6.9623e+01 + i3.7624e+01, 4.2965e+01 - i9.7366e+00)	
d	(3.8458e+01 + i5.3429e+01, 6.9041e+01 - i7.9617e+00, 3.0764e+01 - i2.6432e+01)	
e	(6.8923e+00 + i1.4970e+01, 2.6411e+01 + i2.0660e+01, 3.1100e+01 - i8.1441e+00)	
	<u>Solution 19</u>	
a	(7.4063e+00 - i3.4787e+00, 1.0721e+01 + i8.2972e+00, 1.2109e+01 - i5.2180e+00)	
b	(2.4467e+00 - i3.3079e+00, 1.0236e+01 + i1.1009e+01, 1.1174e+01 - i7.5257e+00)	
c	(1.5252e+01 + i1.0280e+01, 1.9329e+01 - i1.8743e+00, -5.1095e+00 - i4.0342e+00)	
d	(1.4407e+01 - i8.3967e-02, 5.5560e+00 - i8.4192e-02, -1.0459e+00 - i1.2096e-01)	
e	(2.0385e+01 - i5.7629e-01, 1.2720e+01 - i6.4157e-01, 8.7010e+00 + i5.9065e-01)	
	<u>Solution 20</u>	
a	(6.1880e+00 - i4.2237e-01, 8.1290e+00 + i1.1229e+00, 1.0282e+01 - i6.3356e-01)	
b	(6.7011e+00 - i2.4814e+00, 1.1062e+01 + i7.1553e-01, 7.2656e+00 - i1.3798e+00)	
c	(1.7059e+01 - i2.1109e+00, 3.5888e+00 + i2.3045e+00, 5.2308e+00 - i5.3295e+00)	
d	(8.8788e+00 - i5.7724e+00, 4.0389e+00 - i4.0732e-01, -1.9017e+00 - i1.3014e+00)	
e	(7.6905e+00 + i2.7761e+00, 4.8172e-01 + i1.9925e+00, 1.3820e+01 - i1.1237e-01)	
	<u>Solution 21</u>	
a	(9.4244e+00 + i1.8245e+00, -5.2199e+00 + i1.1230e+01, 1.5137e+01 + i2.7368e+00)	
b	(1.3405e+01 + i1.9393e-02, -2.1859e+00 + i1.3876e+01, 1.5713e+01 + i1.2779e+00)	
c	(7.4122e+00 - i9.1383e+00, 4.9540e+00 + i9.5137e+00, 2.7386e+00 + i3.1075e+00)	
d	(4.6236e+00 - i1.0615e+01, 1.0698e+01 + i7.8846e+00, 9.4963e+00 + i3.8830e+00)	
e	(-1.2833e-02 + i1.5993e+00, -7.2241e+00 + i4.8593e+00, 1.0618e+01 + i6.0325e+00)	

5.5 The 5-6 and 6-6 Platforms

Figures 5.9 and 5.10 illustrate the top views of the 5-6 and 6-6 Platforms. A 6-6 Platform is shown in three-dimension in Fig. 1.2. The 5-6 Platform contains four legs which are connected singly at the vertices of both the top and base platforms. There is only one kind of leg arrangement for the Platform. The 6-6 Platform is the most general form of all the In-parallel Platforms in this study. Of course, all the legs of the 6-6 Platform are singly connected legs. The forward displacement analysis of

both of these Platforms could not be achieved by using any of the methods presented in this study.

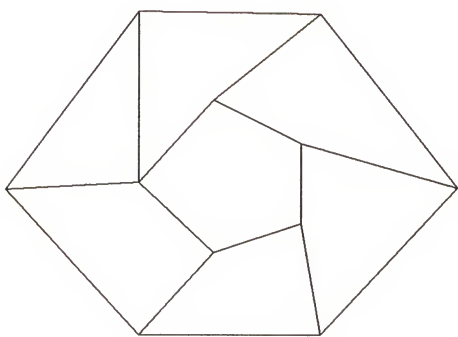


Fig. 5.9 The 5-6 Platform

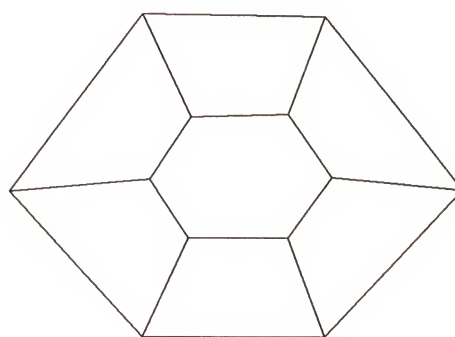


Fig. 5.10 The 6-6 Platform

CHAPTER 6

SUMMARY AND DISCUSSION

The In-parallel Platforms in this study consist of a top platform connected to a base by six spherical jointed-ended legs. The legs are connected either singly or pair-wise at the vertices of the top and base platforms. With these features, a total of nineteen forms of this Platform can be produced. The closed-form forward displacement analysis problems for most forms were solved successfully and the results are summarized in Table 6.1.

Many cases were analyzed by using constructions so that a complicated case could be modeled by a simpler one. The results of these cases from the analyses were the same and the cases were geometrically similar. For example, all the cases which have three pairs of concentric spherical joints in the top platforms could be modeled by a 3-3 Platform, and the numbers of degree of the polynomials and the numbers of assembly configurations for all the cases were sixteen.

In this study, the platforms of many cases were planar and nonparallel. However, it is believed that the removal of the constraints would not increase the degree of solution. In fact, a generalized Case 4-4-C which has nonplanar top platform and base was analyzed by Selfridge (1991). The degree of the solution was twenty-four and it was the same as that of the case with the constraints.

The two kinds of formulations for the forward analysis of Case 4-5-Bb presented in Section 4.2.2 resulted in two different equation sets. Both of these equation sets consisted of three equations in three variables. The first set, which was obtained by using the closed loop chain, consisted of two equations in three variables, and one equation in two variables. The second set, which was obtained by using a "virtual" Case 4-4-C Platform, consisted of two equations in two variables, and one equation in three variables. It was shown in Section 4.3 that the elimination of two variables from three equations in the form of the first set resulted in a thirty-second degree polynomial. In a numerical example presented in Section 4.4, a substitution of a identity in the polynomial reduced the degree to twenty-fourth for Case 4-5-Ba. On the other hand, the elimination of three equations in the form of the second equation set resulted in a twenty-fourth degree polynomial, as shown in Section 3.3.1. Obviously, the second formulation is a better one because numerical examples used in the elimination cannot give a proof of the result.

There is no proof in this study that the formulation of the analysis for Case 4-5-Ba indeed results in a twenty-fourth degree polynomial equation. Nevertheless, there are some reasons to believe that the solution for Case 4-5-Ba is generally true. Several numerical examples were carried out and it was found that the equation set could always be reduced to a twenty-fourth degree polynomial. Also, Cases 4-5-Bb, which has a similar leg arrangement to Case 4-5-Ba, was proved to have a twenty-fourth degree polynomial by a different formulation. The fact that there are two kinds of formulations for Case 4-5-Bb gives hope that Case 4-5-Ba can also be solved

by another method. Further work is needed on Case 4-5-Ba to obtain a different formulation for three equations in which two equations contain two variables and one contains three variables. From such an equation set, it is then possible to have a solid proof that the analysis of Case 4-5-Ba will result in a twenty-fourth degree polynomial equation.

It should be mentioned here that the result for Case 5-5-A is also conjectural. In this study and in Innocenti and Parenti-Castelli (1990), the results for this case were obtained by numerical examples. Further work is needed to obtain a different formulation so that the result can be solidly proved.

The problem for the most general case, whose legs connected singly at six vertices in both the top and bases platforms, remains unsolved. (See Fig. 5.10.) Also, the forward analyses of three other cases, Cases 5-5-B, 5-5-C, and 5-6, which have only one concentric spherical joint in either the top or base platforms were not achieved. Nevertheless, the analysis of the simpler cases are believed to be very conducive to solving the problem of the most general case.

The formulations of the various problems may well provide some insight into the solution for the general 6-6 Platform. Also, the results shown in Table 6.1 are quite interesting because for the Platforms analyzed, there is a relationship between the numbers of assembly configurations and the ways that the legs are arranged. Specifically, some cases contain some legs which are singly connected at the vertices of both the top and base platforms. The following relationships can be drawn from the Table: for those Platforms that do not contain any singly connected legs, the

numbers of assembly configurations are always sixteen. There are eight such Platforms. When there is one singly connected leg in a Platform, the number of assembly configurations increases by eight. Cases 4-4-C, 4-5-Ba, and 4-5-Bb are the only In-parallel Platforms which contain one singly connected leg. Their numbers of assembly configurations are twenty-four. When the number of singly connected leg in a Platform increases to two, the number of assembly configurations again increases by eight. The number of assembly configurations are thirty-two for Cases 4-5-C, 4-6-A, and 4-6-B, which are three of the five cases that have two singly connected legs. Finally, for the only case which has three singly connected legs, viz. Case 5-5-A, the number of assembly configuration is forty, assuming that this result is corrected. The above relationship suggests that the number of singly connected legs is linearly to the numbers of assembly configurations. Further, this relationship is independent to the numbers of vertices of the platforms. If this relationship is also valid for those Platforms which contain higher numbers of vertices, for example, Cases 5-6 and 6-6, then the numbers of assembly configurations for these two cases are respectively forty-eight and sixty-four.

Table 6.1 Results of The Forward Displacement Analyses of The In-Parallel Platforms

Cases	Leg Arrangements	Degree of Polynomials	Number of Assembly configurations	Number of Singly Connected legs	Remarks
3-3	T-T-T-T-T-T	16	16	0	
3-4	T-T-T-T-T-Q	16	16	0	modeled by 3-3
3-5	T-T-T-Q-T-Q	16	16	0	modeled by 3-3
3-6	T-Q-T-Q-T-Q	16	16	0	modeled by 3-3
4-4-Aa	T-T-Q-T-T-Q	16	16	0	modeled by 3-3
4-4-Ab					
4-4-B	T-T-T-Q-T-Q	8	16	0	planar top
4-4-C	T-T-T-T-Q-Q	24	24	1	planar top & base
4-5-A	T-Q-T-Q-T-Q	8	16	0	modeled by 4-4-B
4-5-Ba	T-T-Q-T-Q-Q	24	24	1	conjectured
4-5-Bb					planar top & base
4-5-C	T-T-T-Q-Q-Q	32	32	2	
4-6-A	T-Q-T-Q-Q-Q	32	32	2	modeled by 4-5-C
4-6-B	T-Q-Q-T-Q-Q	32	32	2	planar base
5-5-A	T-T-Q-Q-Q-Q	40	40	3	conjectured
5-5-B	T-Q-T-Q-Q-Q	?	?	2	
5-5-C	T-Q-Q-T-Q-Q	?	?	2	
5-6	T-Q-Q-Q-Q-Q	?	?	4	
6-6	Q-Q-Q-Q-Q-Q	?	?	6	

REFERENCES

- Behi, F., 1988, "Kinematic Analysis for a Six-Degree-of-Freedom 3-PRPS Parallel Mechanism," *IEEE Journal of Robotics and Automation*, Vol. 4, No.5. pp. 561-565.
- Charentus, S., and Renaud, M., 1989, "Modelling and Control of a Modular, Redundant Robot Manipulator," First International Symposium on Experimental Robotics, Montreal, Canada, 19-21 June.
- Cox, D. J., 1981, "The Dynamic Modeling and Command Signal Formulation for Parallel Multi-Parameter Robotic Devices," Master's Thesis, University of Florida, Gainesville, FL.
- Dieudonne, J., Parrish, R., and Bardusch, R., 1972, "An Actuator Extension Transformation for a Motion Simulator and an Inverse Transformation Applying Newton-Raphson's Method," NASA Technical Note TN D-7067, Langley Research Center, Hampton, VA, November.
- Duffy, J., 1980, *Analysis of Mechanisms and Robot Manipulators*, John Wiley and Sons, New York.
- Earl, C. F., and Rooney, J., 1983, "Some Kinematic Structures for Robot Manipulator Design," *ASME Journal of Mechanisms, Transmissions, and Automation in Design*, Vol. 105, pp. 15-22.
- Fichter, E. F., 1984, "Kinematics of a Parallel Connection Manipulator," Design Eng. Tech. Conf., Cambridge, Mass., ASME Paper 84-DET-45.
- Fichter, E. F., 1986, "A Stewart Platform-Based Manipulator: General Theory and Practical Construction," *Int. Journal of Robotics Research*, Vol. 5, No. 2, pp. 157-182.
- Fichter, E. F., and McDowell, E. D., 1980, "A Novel Design for a Robot Arm," *Proc. Int. Comput. Technol.* ASME, New York, pp. 250-256.
- Gilmartin, M., and Duffy, J., 1972, "Type and Mobility Analysis of the Spherical

- Four-Link Mechanisms," in *Mechanisms*, Applied Mechanisms Conference Proceedings, Institute of Mechanical Engineers, London, pp. 90-97.
- Gosselin, C., 1990, "Determination of the Workspace of 6-DOF Parallel Manipulators," *ASME Journal of Mechanical Design*, Vol. 112, September, pp.331-336.
- Griffis, M., and Duffy, J., 1989, "A Forward Displacement Analysis of a Class of Stewart Platforms," *Journal of Robotic Systems*, John Wiley, 6(6) pp. 703-720.
- Griffis, M., and Duffy, J., 1990, "Kinestatic Control: A Novel Theory for Simultaneously Regulating Force and Displacement," Proceedings of the 21st ASME Mechanisms Conference, Chicago IL, September 16-19.
- Hara, A., Sugimoto, K., 1989, "Synthesis of Parallel Micromanipulators," *ASME Journal of Mechanisms, Transmissions, and Automation in Design*, Vol. 111, March, pp. 34-39.
- Howard, E., 1966, *Elementary Matrix Theory*, Dover Publications, New York.
- Hunt, K. H., 1978, *Kinematic Geometry of Mechanism*, Oxford University Press, London.
- Hunt, K. H., 1983, "Structural Kinematics of In-Parallel-Actuated Robot-Arms," *ASME Journal of Mechanisms, Transmissions, and Automation in Design*, Vol. 105, pp. 705-712.
- Hunt, K. H., and Primrose, E. J. F., 1991, "Assembly Configurations of Some In-Parallel-Actuated Manipulators," Department of Mechanical Engineering, Monash University, Clayton, Victoria 3168, Australia. (Private Communication.)
- Innocenti, C., and Parenti-Castelli, V., 1989, "Direct Position Analysis of the Stewart Platform Mechanism," *Mechanism and Machine Theory*, Vol. 25, No. 6, pp. 611-621.
- Innocenti, C., and Parenti-Castelli, V., 1990, "Closed-Form Direct Position Analysis of a 5-5 Parallel Mechanism," Dipartimento di Ingegneria delle costruzioni meccaniche, nucleari, aeronautiche e di Metallurgia - Università di Bologna, Italy.
- Kerr, D. R., 1988, "Analysis, Properties, and Design of a Stewart-Platform Transducer," *Trends and Developments in Mechanisms, Machines, and Robotics -- 1988*, Vol. 3, pp. 139-146.

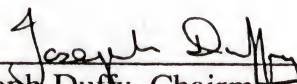
- Lin, W., Griffis, M., and Duffy, J., 1990, "Forward Displacement Analyses of the 4-4 Stewart Platforms," Proceedings of the 21st ASME Mechanisms Conference, Chicago IL, September 16-19.
- Mohamed, M. G., 1983, "Instantaneous Kinematics and Joint Displacement Analysis of Fully-Parallel Robotic Devices," Ph.D. Dissertation, University of Florida, Gainesville, FL.
- Mohamed, M. G., and Duffy, J., 1985, "A Direct Determination of the Instantaneous Kinematics of Fully Parallel Robot Manipulators," *ASME Journal of Mechanisms, Transmissions, and Automation in Design*, Vol. 107, pp. 226-229.
- Murthy, V., and Waldron, K. J., 1990, "Position Kinematics of the Generalized Lobster Arm and its Series-Parallel Dual," Proceeding of the 21th ASME Mechanisms Conference, Chicago, IL, September 16-19, 1990
- Nanua, P., and Waldron, K. J., 1989, "Direct Kinematic Solution of a Stewart Platform," IEEE Proceedings of Int. Conf. on Robotics and Automation, Scottsdale, Arizona, May 14-19, pp. 431-437.
- Nanua, P., Waldron, K. J., and Murthy, V., 1990, "Direct Kinematic Solution of a Stewart Platform," *IEEE Transaction on Robotics and Automation*, 6(4), pp. 438-444.
- Parenti-Castelli, V., and Innocenti, C., and 1990, "Forward Displacement Analysis of Parallel Mechanisms: Closed Form Solution of PRR-3S and PPR-3S Structures," Proceedings of the 21st ASME Mechanisms Conference, Chicago IL, September 16-19.
- Premack, T., Strempek, F., Solis, L., Brodd, S., Cutler, E., and Purves, L., 1984, "Design and Implementation of a Compliant Robot with Force Feedback and Strategy Planning Software," NASA Technical Memorandum 86111, Goddard Space Flight Center, Greenbelt, MD, May.
- Reinholz, C., and Gokhale, D., 1987, "Design and Analysis of Variable Geometry Truss Robots," Proceedings of the 9th Annual Applied Mechanisms Conference.
- Salmon, G., 1885, *Introductory to the Modern Higher Algebra*, Hodges, Figgis, and Co., Dublin.
- Selfridge, R. G., 1991, "Analysis of Stewart Platforms," Department of Computer and Information Science, University of Florida, Gainesville, FL. (Private Communication.)

- Stewart, D., 1965, "A Platform with Six Degrees of Freedom," *Proceedings of Institute of Mechanical Engineers*, London, Vol. 180, Pt. 1, No. 15, pp. 371-386.
- Sugimoto, K., 1987, "Kinematic and Dynamic Analysis of Parallel Manipulators by Means of Motor Algebra," *ASME Journal of Mechanisms, Transmissions, and Automation in Design*, Vol. 109, pp.3-7.
- Weng, T. C., 1988, "Kinematics of Parallel Manipulators with Ground-Mounted Actuators," Ph.D. Dissertation, University of Florida, Gainesville, FL, December.
- Wolfram, 1989. *Mathematica*, Version 1.2, Wolfram Research, Inc., 100 Trade Center Drive, Champaign, IL 61820-7237.
- Yang, D. C. H., and Lee, T. W., 1984, "Feasibility Study of a Platform Type of Robotic Manipulators from a Kinematic Viewpoint," *ASME Journal of Mechanisms, Transmissions, and Automation in Design*, Vol. 106, pp. 191-198.
- Yangsheng X., Paul, P. R., 1988, "Orthogonal Jacobian Mechanisms and Compliance of Robot Manipulators," First International Meeting Advances in Robot Kinematics, Ljubljana, Yugoslavia, September 19-21, pp.26-35.

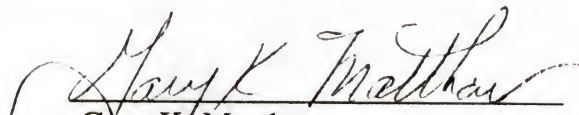
BIOGRAPHICAL SKETCH

Wei Lin was born on December 8, 1961, in Nanjing, China. After finishing high school in Hong Kong, he enrolled at the University College London in England, and graduated with a University of London B.Sc. (Eng) degree in mechanical engineering in June 1985. In August of that year, he entered the Mechanical Engineering Department at the University of Florida and received a M.S. degree in April, 1988.

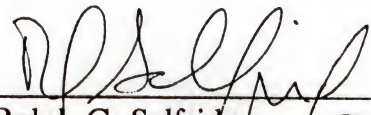
I certify that I have read this study and that in my opinion it conforms to acceptable standards of scholarly presentation and is fully adequate, in scope and quality, as a dissertation for the degree of Doctor of Philosophy.


Joseph Duffy, Chairman
Graduate Research Professor of
Mechanical Engineering


I certify that I have read this study and that in my opinion it conforms to acceptable standards of scholarly presentation and is fully adequate, in scope and quality, as a dissertation for the degree of Doctor of Philosophy.


Gary K. Matthew
Associate Professor of
Mechanical Engineering

I certify that I have read this study and that in my opinion it conforms to acceptable standards of scholarly presentation and is fully adequate, in scope and quality, as a dissertation for the degree of Doctor of Philosophy.


Ralph G. Selfridge
Professor of Computer and
Information Sciences

I certify that I have read this study and that in my opinion it conforms to acceptable standards of scholarly presentation and is fully adequate, in scope and quality, as a dissertation for the degree of Doctor of Philosophy.


Carl D. Crane, III
Assistant Professor of
Mechanical Engineering

I certify that I have read this study and that in my opinion it conforms to acceptable standards of scholarly presentation and is fully adequate, in scope and quality, as a dissertation for the degree of Doctor of Philosophy.



Neil L. White
Professor of Mathematics

This dissertation was submitted to the Graduate Faculty of the College of Engineering and to the Graduate School and was accepted as partial fulfillment of the requirements for the degree of Doctor of Philosophy.

May 1992



Winfred M. Phillips
Dean, College of Engineering

Madelyn M. Lockhart
Dean, Graduate School